Biomaterials Science: Studies on Novel Biodegradable Polymeric Materials and Tissue Engineering as Cardiac Implants

A THESIS PRESENTED BY

Finosh G T

TO

SREE CHITRA TIRUNAL INSTITUTE FOR MEDICAL
SCIENCES AND TECHNOLOGY
THIRUVANANTHAPURAM
INDIA

IN PARTIAL FULFILMENT OF THE REQUIREMENTS
FOR THE AWARD OF
DOCTOR OF PHILOSOPHY

2014

DECLARATION

I, Finosh G T, hereby certify that I had personally carried out the work depicted in the thesis entitled, ***"Biomaterials Science: Studies on Novel Biodegradable Polymeric Materials and Tissue Engineering as Cardiac Implants",*** except where due acknowledgment has been made in the text. No part of the thesis has been submitted for the award of any other degree or diploma prior to this date.

Thiruvananthapuram
23-06-2014

Finosh G T
Reg No: PhD/2011/13
Roll No: 6248

SREE CHITRA TIRUNAL INSTITUTE FOR MEDICAL SCIENCES & TECHNOLOGY, TRIVANDRUM

Thiruvananthapuram – 695011, INDIA
(An Institute of National Importance under Govt. of India)
Phone-(91)0471-2520248 Fax-(91)0471-2341814
Email: jayabalan@sctimst.ac.in Web site – www.sctimst.ac.in

CERTIFICATE

This is to certify that **Mr. Finosh G T**, in the Polymer Division of this institute has fulfilled the requirements prescribed for the Ph. D. degree of the Sree Chitra Tirunal Institute for Medical Sciences and Technology, Thiruvananthapuram. The thesis entitled, ***"Biomaterials Science: Studies on Novel Biodegradable Polymeric Materials and Tissue Engineering as Cardiac Implants"*** was carried out under my direct supervision. No part of the thesis was submitted for the award of any degree or diploma prior to this date.

* Clearance was obtained from the Institutional Ethics Committee/ Institutional Animal Ethics Committee for carrying out the study.

Thiruvananthapuram
23-06-2014

Dr. M Jayabalan PhD, DSc, FABMS
(Research Supervisor)

Scientist G & Head
Polymer Division
BMT wing, SCTIMST,
Thiruvananthapuram

The thesis entitled

"Biomaterials Science: Studies on Novel Biodegradable Polymeric Materials and Tissue Engineering as Cardiac Implants".

Submitted by

Finosh G T

for the degree of

Doctor of Philosophy

Of

**SREE CHITRA TIRUNAL INSTITUTE
FOR MEDICAL SCIENCES AND TECHNOLOGY,
THIRUVANANTHAPURAM - 695011**

is evaluated and approved by

…… ……..

Dr. M Jayabalan. PhD. DSc. Examiner
(Research Supervisor)

Dedicated To

My Family, Teachers & Friends.....

ACKNOWLEDGEMENT

I would like to express my heartfelt gratitude and respect to my supervisor Dr. M Jayabalan, Scientist G and Head, Polymer Science Division-BMT wing, SCTIMST. His guidance, lively discussions, critical evaluations and encouragement helped in nurturing my passion for science throughout the course of study. I thank him for the entire support offered during my Ph.D programme.

I am grateful to the former and present Director of SCTIMST and the present Head and the previous Heads, BMT Wing for all support provided during the course of my work.

I thank members of the doctoral advisory committee, Dr. Anoopkumar T, (Scientist F, Molecular Medicine) and Dr. Roy Joseph, (Scientist F, Polymer Processing Lab) for their timely suggestions and critical comments.

I am thankful to Dr. Sundar Jayasingh, Deputy Registrar, Dr. Prabha D. Nair, Associate Dean for PhD affairs, Dean, and all members of academic division and Director's office for their administrative support.

Contents

I thank DR. K G Raghu, Principal Scientist, NIIST for his valuable suggestions during the early phases of my studies.

I thank all my friends from our laboratory, Dr. Sunita, Dr. Sivaram, Ms. Remya, Mr. Vineeth Mr. Madhav, Dr. Dawlee S, Mr. Sumesh S and Ms. Joshy for their help.

I am thankful to Dr. K Sreenivasan of LPA, Mr. Rowsen Moses, Mr. Hari Dr. Radhakumari, Dr. H K Varma, Mr. Nishad K V, Dr. Roy Joseph, Dr. Ramesh, Dr. Kumari, Ms. Deepa, Dr. Lissy K K, Mr. Jaseer Muhamed, Dr. Anilkumar T V and Dr. Anilkumar P R for their for their assistance during the evaluations.

Thanks to the staff of various administrative departments and library of the Institute and fellow students in the campus for their lively companionship.

I am thankful to DST, KSCSTE and CICS for fellowships and travel grant.

I am thankful to my parents, family, friends and teachers for their, blessings, prayers, support and encouragements.

I thank Mr. Rajesh Ramachandran and Smitha C, Directors, Biogenix Research Center, TVPM for extending their constant support and motivation.

I further thank many who directly or indirectly helped me to prepare this thesis.

My immense gratefulness to the Lord Almighty for showering immeasurable blessings with ever loving family, caring supervisor, supporting friends, and so on for the completion of this endeavour.

Finosh G T

List of Figures

List of tables

Synopsis

Treatment of patients for end-stage cardiac failure and post ischemic complications of cardiac tissue is a challenge. Heart transplantation forms a better option for the management of myocardial infarction (MI) as the conventional treatments fail to restore normal cardiac function. Nevertheless, the lack of donors, compatibility between the donor and recipient and immune suppression-associated intricacy are challenging**.** These difficulties have led to regenerative therapy and tissue engineering. Tissue engineering enables the creation of fabricated implantable biological substitutes known as neo-organs to restore, maintain or improve tissue. At the target site, biomaterial scaffolds act as microniche, guide the tissue development in the biodegradable matrix through three-dimensional cell growth, and rejuvenate the damaged cardiac tissue. However, development of tissue engineered myocardial patch implant for repairing myocardial tissues that serve a predominantly biomechanical function is a major challenge.

For tissue engineering of myocardial tissue, the morphology, surface chemistry, biomechanics, degradation profile and bioactivity of the scaffold largely influence the cell adhesion, growth, colonization, and extracellular matrix (ECM) synthesis etc. in the three-dimensional scaffold material. The biochemical and physiological functions of a tissue is regulated by the coordinated interactions between the cells and their native

ECM. Therefore, development of biomaterial based scaffold systems mimicking ECM is more relevant and essential for the improved three-dimensional cell growth.

Among the various types of biomaterials employed as matrices for three-dimensional cell growth, the hydrogels are more advantageous due to their high water holding capacity, potent mass transport abilities, excellent soft tissue like consistency and other ECM like properties. Among the naturally available materials, seaweed-derived polysaccharide alginates are considered as more promising biocompatible material. However due to its hydrophilic nature, the alginate hydrogels do not promote cell adhesion and infiltration; protein adsorption and mammalian cell interaction is also prevented. The alginates, derived from non-mammalian sources do not produce appropriate extracellular microenvironment for the development of extracellular matrix. Also due to mechanical instability in the presence of monovalent cations, the hydrogels of alginates is not an ideal choice for tissue engineering. Several synthetic polymer hydrogels have also been employed for tissue engineering. Of these, the biodegradable polyester-based polymer hydrogels with required biomechanical properties during regeneration of tissue are preferable for cardiac tissue engineering. Though biodegradable crosslinked polymer hydrogels offer biomechanical stability for intended duration, these hydrogels do not promote adequate cell adhesion, spreading, migration and extracellular matrix production in the absence of any cell-responsive elements.

The biosynthetic hybrid hydrogels comprising biological and synthetic polymer units have emerged as promising hydrogel for cardiac tissue engineering owing to their structural, physiochemical, mechanical and biological functionalities and their

controlled degradation profile. With this background we aimed to develop biosynthetic hybrid hydrogels with improved physical, mechanical and biological properties using graft comacromers of alginate and unsaturated biodegradable polyester, poly(propylene fumarate) (PPF)/ poly(mannitol fumarate-co-sebacate) (PMFS) for developing viable myocardial patch implants for the management of MI. The major objectives of the investigation were development of biosynthetic monomodal and bimodal network hydrogels based on poly(propylene fumarate)-co-alginate and poly(mannitol fumarate-co-sebacate)-co-alginate comacromers, assessment of their potential to promote long-term cell growth under normal and hydrodynamic conditions, survival and growth of fibroblast and cardiomyoblast cells, differentiation of MSCs to cardiac lineage, inherent scavenging characteristics for reactive oxygen species (ROS) and to identify candidate hydrogel for the development of a tissue engineered myocardial patch.

The thesis consists of six chapters. Chapter-1 deals with the introduction and background of the investigation. This part describes the cause and management of myocardial infarction (MI), tissue engineering and polymeric scaffolds for the cardiac tissue engineering. The relevance and need of hydrogels for cardiac tissue engineering are also presented.

Chapter 2 deals with the literature review on hydrogels for cardiac tissue engineering. The review covers the emergence, recent advancements and limitations of cardiac tissue engineering with reference to hydrogels. The objectives and scope of the present research work is also projected in this chapter.

Chapter 3 deals with the materials and methodology. It consists of four sections. Section-1 describes the synthesis of biosynthetic monomodal and bimodal network hydrogels. Unsaturated polyesters, hydroxyl terminated-poly (propylene fumarate) (HT-PPF) and poly (mannitol fumarate-co-sebacate) (PMFS) macromers were synthesized. Alginate was then graft copolymerized with PPF and PMFS to form PPF-Alginate (HPAS) and PMFA-Alginate (PMFSA) graft comacromer respectively. The biosynthetic monomodal and bimodal network hydrogels were prepared from these graft comacromers by crosslinking the alginate segment with calcium ions and the unsaturation of the polyester segment with vinyl monomer. A panel of different hydrogels were synthesized from HPAS graft comacromer and vinyl crosslinkers methyl methacrylate (MMA), N,N' methylene bisacrylamide (NMBA), 2-hydroxy ethyl methacrylate (HEMA), n-butyl methacrylate (BMA), acrylic acid (AA) and polyethylene glycol diacrylate (PEGDA). Similarly PMFSA graft comacromer was crosslinked with divinyl crosslinkers PEGDA, NMBA and diethylene glycol dimethacrylate (DEGDMA) to form hydrogels. Section-2 describes the various characterizations employed for the hydrogels. The physiochemical characterizations involve the determination of surface functional groups by ATR-IR spectroscopy, the water holding capacity and water content, surface hydrophilicity by dynamic water contact angle measurements and surface pore morphology and pore length by ESEM analysis. The mechanical properties of the hydrogels were assessed by tensile and fatigue tests. The nature of water in the hydrogels was investigated by differential scanning calorimetry (DSC). The *in vitro* biostability was investigated by aging the

hydrogels in PBS at physiological conditions. Section-3 presents the evaluations of hemocompatibility, cytocompatibility and cell-material interactions and genocompatibility. Hemocompatibility was assessed by hemolysis, RBC aggregation, platelet adhesion and plasma protein adsorption. Cytocompatibility was studied by MTT assay, direct contact assay and live dead assay. Comet assay was used for the evaluation of genocompatibility of the hydrogels. Section-4 deals with the evaluations of biological responses of the hydrogels with reference to cardiac tissue engineering. Studies on long-term cell viability and infiltration of fibroblast, effect of unidirectional porosity on cell growth, inherent scavenging effects of ROS, growth of cardiomyoblast cells under hydrodynamic conditions using the dynamic rotary cell culture system (RCCS), coculture of fibroblasts and cardiomyoblasts, cell cycle analysis of cardiomyoblast cells grown on contact with hydrogels and the differentiation potential of bone marrow mesenchymal stem cells (MSC) to cardiac lineage are presented.

Chapters 4 and 5 deals results and discussion respectively. These chapters are divided into different sections. Section-1 deals with the chemistry of the synthesis of different hydrogels from HPAS and PMFSA graft comacromers. The condensation reactions involved in the synthesis of graft comacromers and crosslinking reactions of alginate and fumarate units involved in the preparation of hydrogels are discussed. In Section-2 the physiochemical and mechanical characteristics of hydrogels are presented. The ATR-IR spectral analysis showed the presence of alginate and polyester units on the surface. Both HPAS and PMFSA -based hydrogels inherited appreciable water content and amphiphilicity. These hydrogels hold non-freezing bound water (structured water)

in the interstitial structures of the hydrogel. The non-freezing bound water content of HPAS and PMFSA-based hydrogels was found to be in a range of 40-65% and that of the HPAS-PEGDA system was around 15-30%. But the freezing water content varied considerably among all the hydrogel which will be due to the nature of vinyl cross linkers used. The average pore length of HPAS-based hydrogels were found to be around 30-60µm and that of PMFSA-based hydrogels were 5-20µm. Biodegradation was observed in PBS at physiological conditions. The mechanical properties of the water-swelled hydrogels showed tensile values higher than the reported values of native cardiac tissue. Section-3 deals with the hemocompatibility, cytocompatibility and cell-material interactions and genocompatibility of hydrogels.The hemolysis of hydrogels were within the acceptable limit of 5%. On exposure to the present hydrogels, RBCs were able to maintain their normal morphology; no aggregation was observed under phase contrast microscope. The absence of thrombocytes indicates hemocompatibility. Protein adsorption on the hydrogel was more than 25%. SDS-PAGE analysis showed albumin as major protein adsorbed on the hydrogels. MTT assay of L929 fibroblasts grown on hydrogel extracts showed cell viability greater than 85%. The cell culture by direct contact with these hydrogels revealed no considerable change in the cell morphology. The presence of mostly green nucleus of the cells grown on all the hydrogels (live/dead assay) revealed the non-apoptotic nature of the cells. These studies signified the cytocompatibility of the hydrogels. The comet assay revealed that these hydrogels maintain the genetic integrity of the cells with DNA content more than 99% in the head region and less than 1% in tail region. Section-4 deals with the studies on

specific biological responses of the hydrogels with reference to cardiac tissue engineering. The long-term viability and infiltration assay with these hydrogels revealed more than 50% viability even after a period of 3 weeks. The enhanced and long-term cellular growth is attributed to the cell responsive features of structured water present in these hydrogels. The unidirectional pores in these hydrogels also facilitate long-term viability of fibroblasts by providing proper contact guidance and effective trafficking of nutrients. The hydrogels possessed inherent capability to scavenge ROS which is attributed to the presence of freezing free and non-freezing bound water in the hydrogel and calcium-induced conformational changes in the surface membrane of cells by the hydrogels. The present hydrogels also maintain the viability of cardiomyoblast (H9c2) cells greater than 50% after 10 days of culture under hydrodynamic conditions. The survival of fibroblasts and cardiomyoblasts together revealed the presence of favourable microniche in the PMFSA-based hydrogels for the growth of different cells. The cell cycle analysis of PMFSA-based hydrogels revealed constantly progressing cells through all the phases of the cell cycle. The studies on bone marrow mesenchymal stem cells (MSC) with PMFSA-PEGDA and PMFSA-DEGDMA hydrogels support the differentiation to cardiac lineage. Gene expression analysis of cardiac specific biomarkers, GATA-4, NKX-2.5, MEF-2, Troponin C and Troponin-C confirms the differentiation of MSCs to cardiac lineage.

The Chapter 6 deals with summary, conclusion and future prospects of the study. The most promising biosynthetic hydrogels and the potential scope for the tissue engineering of myocardial patch implant are emphasized.

Chapter 1
INTRODUCTION

7 Introduction

Cardiovascular diseases (CVD) continue to remain as a major global health threat. This is evident from the drastic increase in the CVD diagnostic trade during the recent years. According to a recent report, United States of America occupies the first place as cardiovascular disease diagnostics trade (Finosh and Jayabalan, 2012). Europe occupies the second place, followed by Japan. American Heart Association statistics reported that on every 34 seconds one American would have a coronary event and a

death/min due to the same. This accounts for around 1 of every 6 deaths in United States (Go et al., 2013). Moreover, the report also points that the CVD death rate is expected to rise in China by nearly 73% by 2030. In India also, myocardial infarction (MI) is the main cause of mortality. According to a projection by WHO and ICMR, India will be the heart attack capital in 2020 (Finosh and Jayabalan, 2012).

Treatment of patients for end-stage cardiac failure and post ischemic complications of cardiac tissue is a challenge. Cardiac transplantation has been attempted for the treatment of end-stage cardiac failure. Because of a dearth of transplantable hearts many of the patients suffer and die. Cardiac patients with class III NYHA (New York Heart Association) heart failure caused by dilated cardiomyopathy or ischemic heart disease who deteorate despite maximal medical therapy, still have some cardiac reserve and have fair chances of survival. Current treatment modalities using thrombolytic agents, statins, beta-blockers, ACE inhibitors and drugs like aspirin proved effective in controlling post infarcted complications (Wielgosz, 1995). Surgical approaches to treat pre and post infarcted heart have also appreciated. However, these approaches are not able to replace the lost myocardium like that of the normal heart.

7.1 End stage cardiac failure and post ischemic complications

Myocardial infarction usually caused by a blood clot or atherosclerotic block that limits the blood flowing to a part of heart muscle. If main coronary artery (blood vessel supplying heart) is blocked, a large part of the heart muscle is affected. The severity mainly depends on the part of the heart to be supplied by coronary artery that got blocked. This will result in reduction in blood supply to the heart, which is to be

supplied by this artery. If the block sustains, the affected part of heart, muscle will be at risk of dying. If a part of the heart muscle has died, it is replaced by scar tissue over the next few weeks but not by the normal cardiac tissue. The major risk factors for artherogenesis include smoking, obesity, hypercholesterolemia, and hypertension (Jefferson and Topol, 2005). The adverse effects of atherosclerotic block pave the way to MI and post infarct complications are many.

Since aerobic metabolism is the essential source of energy for myocardium, MI causes reduction in high-energy phosphates concentration leading to contractile dysfunction (Ely and Berne, 1992). The increase in ATP catabolic products in the myocardium because of ischemia activates anaerobic glycolysis leading to accumulation of lactate. The lactate production creates an osmotic imbalance to the myocardial cells and cause disturbances in the sarcolemma (Young et al., 1997) (Barsotti et al., 1994). The sustained ischemia will also trigger lysosomal membrane leakage resulting in the loss of membrane integrity. The damaged cell membranes form unregulated passage for divalent cations including Calcium (Ca^{2+}). The disturbances in Ca^{2+} homeostasis will also cumulate water accumulation and osmotic imbalance (Nirmala and Puvanakrishnan, 1996).

Myocytes apoptosis forms one of the major reasons for the death of cardiomyocytes and associated cells after infarction. As the cardiomyocytes are terminally differentiated, they lack dividing capacity and so the apoptotic loss of cardiomyocytes cannot be replenished by native beating cells. Abbate *et al* reported that 2 h after coronary artery occlusion around 2.8 million cells undergo apoptosis in

experimental rats, which was increased to 6.6 million at 4.5 h. At the same time necrotic cell death was accounted to be around 1.1 million cells at a time of 24 h. The apoptotic cell death was found to spread towards the surviving portion of myocardium adjacent to the injury and persisted for 1-2 days (Abbate et al., 2003).

The active role of reactive oxygen species (ROS) in the propagation of myocardial infarction (MI) and ischemia is well proven which is evident from the increase in their concentration at and around the infarct site. Following MI the contractile element of heart, the cardiomyocytes, were also found to have a higher ROS that will ultimately lead to hypertrophy and apoptosis (Kinugawa et al., 2000). ROS from the ischemic cells undergoes oxidative stress that will alter the normal biochemistry and physiology of the myocardium and results in the disturbances in Ca^{2+} homeostasis (Bahorun T, Soobrattee MA, Ramma VL, Aruoma OI, 2006)**.** However, little information is available about the actual mechanisms of ROS induced cardiomyocyte apoptosis. Still some reports point that different ROS can open different apoptotic pathways. For instance, H_2O_2 and O_2^- are able to induce p53 expression in cardiomyocytes, which can directly provoke apoptosis through the activation of Bax gene. Ischemia and reperfusion will also induce an ROS mediated apoptosis in the failing myocardium (von Harsdorf et al., 1999).

Myocardial infarction has devastating consequences in the early phase such as cardiac rupture, and in the chronic phase, chronic heart failure, for which the risk is mainly determined by infarct size. Larger infarct size induces gross morphological, histological and molecular changes (cardiac remodeling) of cardiomyocytes and ECM of the infarcted as well as non-infarcted regions, which may further leads to cardiac

arrhythmias, heart failure and mortality (White et al., 1987). After the onset of the infarction, the existing cardiac tissue leads to reperfusion injury and scar tissue formation initiates an inherent repair program.

7.2 Management of myocardial infarction

The conventional medical management of myocardial infarction includes drugs like statins, beta-blockers, nitroglycerin and calcium antagonists, coronary artery bypass grafting (CABG), implants like stents etc. The stem cell therapies offer promising opportunities in management of myocardial infarction (Perin, 2006). However, these approaches are very risky, challenging and do not satisfy the clinical arena (Hoover-Plow and Gong, 2012). Heart transplantation forms a better option. Still the lack of donors, compatibility between the donor and recipient and immune suppression associated intricacies are challenging (Zammaretti and Jaconi, 2004). These difficulties provoked the thoughts of health care professionals, physicians and scientists to cultivate a fresh treatment modality by overcoming these disputes of customary therapies without much loss to the myocardium.

Regenerative therapy and tissue engineering has emerged from the midst of these challenges and offered promising hope to millions of CVD patients throughout the sphere. Our recent review carefully delineates the requirements, progress, challenges and various approaches and aspects of cardiac tissue engineering and regeneration (Finosh and Jayabalan, 2012). After an acute infarction, the therapy or primary percutaneous coronary intervention (PCI) is commonly employed to reduce the infarct size and its propagation to the adjacent normal cells.

7.3 Tissue engineering

The term “Tissue Engineering” was introduced in 1987 by US National Science Foundation (NSF) in Washington, D.C. The definition for tissue engineering was introduced in the NSF organized conference on tissue engineering in Lake Tahoe, California - “Application of principles and methods of engineering and life sciences toward fundamental understanding of structure–function relationship in normal and pathological mammalian tissues to restore, maintain, or improve functions” (Langer and Vacanti, 1993).

Tissue engineering enables the creation of fabricated implantable biological substitutes known as neo-organs to restore, maintain or improve tissue (Papadaki et al., 2001). The three-dimensional scaffolds guide the tissue development in the matrix. Tissue engineering is more advantageous over cell transplantation since a functional three-dimensional tissue can be developed. The scaffold initially acts as an adhesive and physical support for the cells (Zimmermann et al., 2004). The entire functional living tissue is transplanted into the wound site, where further remodeling can occur. At the same time, the artificial polymeric material breaks down, leaving only a completely natural final product in the body, a neo-organ. Thus, the damaged cardiac tissue can be rejuvenated with newly grown tissue engineered implant, which will alleviate post ischemic complications. The general procedure adopted for cardiac tissue engineering is given in Figure-1.

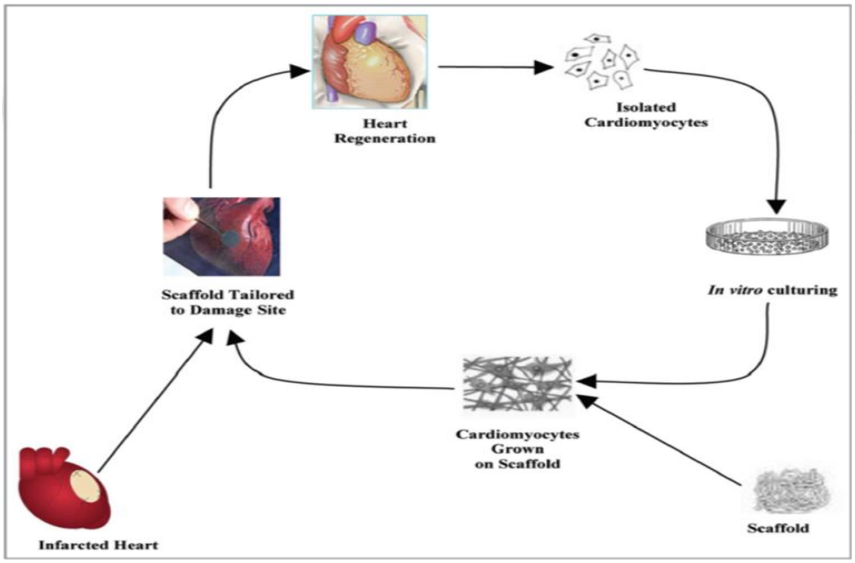

Figure-1. General procedure for tissue engineering.

7.3.1 Cardiac tissue engineering

The heart is a complex myogenic muscular organ whose function is very vital to the survival of the organism. The heart is composed of myocytes and fibroblasts arranged tightly with support from the ECM. The cells are highly metabolically active and so require a continuous supply of oxygen and nutrients. The cardiomyocytes form an electrochemical syncytium that makes the conduction and transmission of the impulses easier in response to the ionic balances across the membrane. This results in the fatigueless rhythmic contraction and relaxation of the myocardium (Vunjak-Novakovic et al., 2010) (Severs, 2000)**.**

Cardiomyocytes meet most of their requirements from their surroundings by diffusion to and from the general circulation. However, for the proper functioning and thriving of most of the cells like cardiomyocytes, a platform for support is crucial. The ECM in the actual situation provides this support. In the cardiac tissue engineering

approach, the patient receives a functional living tissue fabricated using living cardiomyocytes and associated cells that are incorporated into the three-dimensional scaffolds of biodegradable polymeric material in cell culture. Therefore, the main objective of cardiac tissue engineering is to provide an *ex-vivo* micro niche for the cells to grow, develop, retain their phenotype and perform their specific function. In short the cardiomyocytes and associated cells of heart tissue are seeded on tissue friendly materials *in vitro*. Under proper conditions, these will organize to form an engineered construct. Such a construct can be applicable for the treatment of end stage cardiac complications (Curtis and Russell, 2009). Organizing cardiomyocytes into a functional tissue capable of generating contractile force (2-4 KPa) and propagating electrical signals (~25 cm/s) is essential to generate an engineered heart tissue (EHT). Such engineered heart tissue must have functional and morphological properties similar to that of native myocardium and remain viable after implantation.

Cardiac tissue engineering is based on the premise that suitable matrices transmit appropriate signals for cardiac progenitor's cells to proliferate and form new cardiac tissue. Various techniques have been developed for the engineering of beating 3 D cardiac tissues. Many authors report much advantageous variations from classical methods, which guarantee long-term effects due to biocompatibility and biodegradability of the biomaterial.

7.3.2 Role of biomaterials as scaffold for cardiac tissue engineering

Regeneration of soft tissues like myocardium under *in vitro* condition needs an appropriate scaffold in the form of a soft and pliable material. The 3 D polymeric

scaffolds have roles in several aspects of tissue engineering- as a platform for the regeneration of remaining healthy tissues, formation of tissue from seeded cells; modulate tissue ingrowths from the surroundings and thereby satisfy the physiological and metabolic need of the regenerating tissue. Recent advances in biomaterials science and bioengineering have resulted in a multitude of scaffold options.

Natural and synthetic materials are explored as scaffold material to grow the cardiomyocytes and associated cells. To allow the development of myocardial tissue, the scaffold should be compatible to cell growth. The scaffold should be produced into three-dimensional porous structures that are dimensionally stable under physiological conditions. Furthermore, the mechanical properties of the scaffolding material should be adequate to provide the correct micro-stress-environment for the cells to develop the required phenotype and adaptation. Therefore, the scaffold should be flexible enough to allow the contraction of the growing tissue and to withstand the back up pressure of the surrounding myocardium after implantation.

Biodegradable polymeric materials form an attractive choice because of the ease of preparation with required microstructure, biomechano-electrical properties and degradation profile. Biodegradable polymers can be designed to degrade *in vivo* in a controlled manner over a predetermined period. The advantages of biodegradable materials are (i) they do not have to be removed after use by secondary surgery because degradation products formed can be excreted from the body via natural pathways and (ii) progressive loss of degradable implant material will lead to regeneration of heart

tissue. The commonly used natural and synthetic biomaterials for soft tissue engineering applications are listed in Table 1.

Table 1. Polymeric scaffolds materials used in tissue engineering

Synthetic scaffolds materials	**Natural scaffold materials**
Poly lactic acid	Fibrin glue
Poly glycolic acid	Gelatin
Hydroxyethyl methacrylate (HEMA)	Collagen
Methyl methacrylate (MMA)	Alginate
Poly propylene fumarate (PPF)	Chitosan
Poly(dioxanone)	Hyaluronoc acid
Poly(trimethylene carbonate) copolymers	Mussel proteins
Poly(e-caprolactone)	Elastin

The scaffold should be interconnected with a porous (50-200 microns) network to enable the migration of nutrients, accommodation of large number of cells inside the pores and their organization into a functioning tissue and removal of waste materials, which are all essential for initiation of vascularization. The major issue to be addressed is the oxygen diffusion beyond ~200 μm thickness as there will be a high oxygen demand by cardiomyocytes (Radisic et al., 2006). The advent of bioreactor system that incorporate electrical or mechanical stimulation offers promising opportunities for cardiomyocyte viability on EHT ((Barash et al., 2010)**,** (Brown et al., 2008). The essential qualities of a cardiac tissue-engineering scaffold are displayed in Figure 2. The scaffold should be

able to release the growth factors, biosignals and other bioactive components in a regulated fashion (Leor and Cohen, 2004).

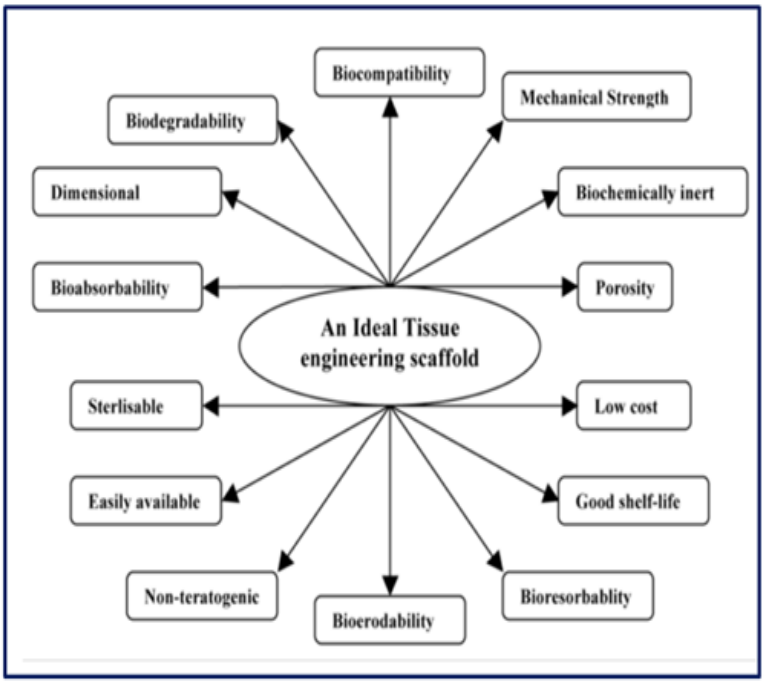

Figure-2. Characteristics of ideal cardiac tissue engineering scaffolds

7.3.3 Cell – biomaterial interaction

An ideal tissue engineering scaffold should provide a suitable substrate for transplanted cells to adhere. This will favor the localization of the cells *in vivo*, and serves as a stage for the formation of new tissue masses by the integration of transplanted cells and the corresponding host cells in the niche (Hanjaya-Putra et al., 2011). Within the adhesion molecules, a defined spectrum of bioactive molecules, such as ligands for adhesion receptors, functional parts of natural growth factors, cytoskeletal elements, hormones and enzymes or synthetic regulators of cell exist. These are incorporated in defined concentrations and spatial distribution against a bioinert matrix.

It would inspire the cells to orchestrate the host response towards the transplanted cells to initiate vascularization, to prevent anoikis and to improve their survival and proper functioning in the host environment (Nerem, 2007).

7.3.4 Response of stem cells to cardiac scaffolds

In recent years, stem cell technologies are gaining pace in the management and regenerative therapy of heart failure. Research on cell-based regenerative therapy has focused on identifying an ideal cellular source. The optimal cell source to create an engineered myocardial patch should be easy to harvest, proliferate under controlled conditions, non-immunogenic and should have the ability to differentiate into mature, functional cardiomyocytes. In principle, the natural electrophysiological, structural, and mechanical properties of cardiomyocytes make them the ideal donor cell type. However, in practice cardiomyocytes are difficult to obtain and are sensitive to ischemic insults. The *in vitro* maintenance is formidable and is allogenic.

7.3.5 Polymeric hydrogels as cardiac extracellular matrix mimic

The tissue engineering approach for developing suitable microniche scaffoldings for 3 D cardiac cell growths has been evolved due to the increasing clinical demand for tissue/organ for repair and replacement (Mano et al., 2007). This strategy mainly focuses on the cellular responses over the key biomimitic characteristics of the scaffolds in terms of chemical, mechanical, physical and topographical cues (Drury and Mooney, 2003). The biochemical and physiological functions of a tissue is regulated by the coordinated interactions between the cells and their native 3 D extracellular matrix

(ECM). The understanding about the nature, composition and orientation of the ECM has opened opportunities for the *ex-vivo* synthesis and development of biomaterial based scaffold systems mimicking ECM for improved 3 D cell culture (Kloxin et al., 2010). Among the various types of biomaterials employed as matrices for 3 D cell growth, the hydrogels subsets are more advantageous due to their high water holding capacity, potent mass transport abilities, excellent soft tissue like consistency and other promising ECM like properties (Alge et al., 2013), (Bryant and Anseth, 2003). The 3D microenvironment provided by the hydrogels is also advantageous over 2D culture for the *in vitro* design of organ parts because it has been reported that the 2D cultures are not the exact replica of the *in vivo* cell growth. The cells in 2D failed to express certain tissue specific genes at comparable levels as *in vivo* (Baker et al., 2009), (Geckil et al., 2010).

Hydrogels can be prepared by techniques like self-assembly, non-covalent interactions with ionic species, covalent crosslinking via chemical reaction, thermal transitions and so on. These hydrogels find application in cardiac tissue engineering as scaffolds, thickening and stabilizing agent, delivery vehicles for cells and signaling factors (Nelson et al., 2011), (Shapira et al., 2008). Both natural and synthetic polymers have been utilized for the fabrication of scaffolds suitable for cardiac tissue engineering (CTE). Natural polymeric biomaterials exhibit excellent biocompatibility, non-immunogenic and can enhance cell adhesion and proliferation. However, they are poor in mechanical properties and undergo uncontrolled and fast degradation in biological fluids. Synthetic polymers have tunable properties to

overcome the drawbacks elicited by the natural polymers. But the risk of inflammation and toxicity of the degradation and leaching products offers challenges in using such materials in CTE (Boffito et al., 2014).

Cardiac tissue engineering is beneficial not only to the patients needing heart transplants but also for whom requiring smaller structures, such as patch of muscle, valves or even vessels. For the successful regeneration of cardiac tissue, biomechanically favourable and biodegradable scaffold materials are essential to promote and retain appropriate numbers of cells to maintain the specific biological functions and differentiate to the correct phenotype. Therefore, it is highly relevant to develop biomechanically favourable scaffold materials using biodegradable hybrid polymers for cardiac tissue engineering.

Chapter 2
REVIEW OF LITERATURE

8 Review of Literature

8.1 Biomaterials in cardiac tissue engineering

The heart–lung machine was one of the first approaches to overcome heart disease, which was initially used by Miller and colleagues in Philadelphia, USA (Zammaretti and Jaconi, 2004). This was followed by mitral valve replacement from cadavers or fascia lata to surgically create the valve. In 1969, Kwan-Gett and co-workers first introduced the artificial heart. Eventually studies on gene delivery, cell transplantation and 3 D culture has been emerged which opened out more opportunities to engineer heart.

During the early half of 20th century itself, researchers attempted to assemble the whole heart or a part of it *in vitro* (Lewis MR., 1920). In the late 1950s, Moscona cultivated freshly isolated cells from fetal chicken heart and obtained an aggregate of cells, which resemble the intact heart tissue (Moscona, 1959). Similar explorations showed that the isolated cells from immature hearts retain the potency to reform heart-like tissues under favorable cell culture conditions (McDonald et al., 1972). This approach was also applicable to most tissues other than heart. Years later, free floating monolayer sheets that generate exogenous matrix free cardiac tissue constructs were developed (Shimizu et al., 2002). Simpson and colleagues observed that neonatal rat cardiac myocytes could associate themselves to adopt a tissue-like organization (Simpson et al., 1994).

In late 1980s, Vandenburgh, Terracio, and their co-workers introduced computer-controlled instrumentation to study the mechanical stimulation on heart (Terracio et al., 1988), (Vandenburgh et al., 1988) and demonstrated cell orientation and differentiation. Based on the studies from embryonic fibroblasts researchers developed an improved *in vitro* heart model. This model enabled the measurement of contractile force and genetic, pharmacological, and mechanical properties (Kolodney and Elson, 1993).

The introduction of material sciences to the principles of tissue engineering by the researchers from MIT, Cambridge paved new ways in cardiac tissue engineering. They used polyglycolic acid as a scaffold in bioreactor cultures (Carrier et al., 1999). Li *et al.* cultured fetal rat ventricular cells onto gelatin scaffolds *in vitro* and tailored them to infarcted rat hearts. They obtained spontaneous contractile activity. However, they displayed poor sarcomere development. The presence of many unknown cells was another demerit (Li et al., 1999). Leor (the first to report cardiomyocytes tissue engineering) and colleagues succeeded in generating vascularization in alginate scaffolds seeded with fetal cardiac cells. But these cells failed to integrate with the host myocardium (Leor et al., 2000). Vunjak-Novakovic and team combined preformed collagen foam with neonatal rat heart cells suspended in Matrigel. With electrical stimulation for extended times they could generate cardiac muscle constructs with improved morphology, contractile function, and molecular marker content (Radisic et al., 2004).

Zimmermann put forward the essential criteria for an ideal cardiac tissue construct (Zimmermann et al., 2004). It should possess functional and morphological similarities with the native heart muscle, promote viability after implantation, and provide mechanical, electrical, and functional integration with the host tissue. It should support and enhance systolic and diastolic function of the failing myocardium by contributing to contractility, electrophysiology, vascularization and robust mechanical properties (Zimmermann et al., 2004). Such an ideal construct does not exist and the scientific community is still striving to find a stable solution for this issue. Still several researchers were able to develop biomaterials scaffold with tunable properties for cardiac applications. Dar *et al.* developed high density cardiac construct using porous alginate scaffolds (Dar et al., 2002). Bursac *et al.* employed bioreactors for culturing neonatal rat ventricular myocytes on polymeric scaffolds and were able to construct 3 D multilayer cardiac tissue like constructs with appreciable electrophysiological properties (Bursac et al., 2003). In an alternate approach Shimizu *et al.* succeeded in developing viable beating tissue construct using temperature responsive polymer, PIPAAm [poly(N-isopro-pylacrylamide)] (Shimizu et al., 2002).

Organ printing, reported by Mironov *et al.*, opened new opportunities to cardiac tissue engineering especially for the development of single cell layers and cell aggregates (Mironov et al., 2003). The development of bioreactors helped to cultivate multilayered 3D structures of cardiac tissue. Such cells were superior to all the aspect when compared with that of 2 D static culture (Carrier et al., 1999). Bioreactors combined with mechanical signals could improve the uniform distribution and

proliferation of cardiac cells, which facilitated formation, and organization of ECM (Akhyari et al., 2002). Most bioreactors fail in supplying enough nutrients and oxygen to growing cardiac tissue. The human heart muscle is about 1 cm thick and the growth in the bioreactor stops around 100 μm or less than 10 cell layers thick. Beyond this distance, the cells will not get fresh medium and oxygen. The development of bioreactors favoring perfusion with respect to mechanical stimuli is needed to solve these issues (Dohmen et al., 2002).

2.1.1. Biomaterial scaffolds

Several cardiomyocyte 3 D *in vitro* culture systems entered the scene with synthetic polymers components as the underlying matrix. Li and associates have shown that cardiac cells can attach to scaffolds to form contractile cell polymer constructs. They constructed a viable cardiac graft that contracted spontaneously in culture conditions (Li et al., 2000). Bursac and co-workers, made electrophysiologic studies and comparison of the constructs in a cell-polymer bioreactor model system with native cardiac tissue (Bursac et al., 1999). A research team led by Eschenhagen successfully induced a long-term stretch to cultured cardiomyocytes. These studies were able to focus on the important features of cardiac diseases (such as myocardial hypertrophy) associated with heart failure (Eschenhagen et al., 1997).

Our group synthesized the carboxyl terminated-poly(propylene fumarate)-co-ethylene glycol)-acrylamide and polyethylene glycol terminated poly(propylene fumarate)/acrylamide hydrogel scaffolds for cardiac tissue engineering applications. These hydrogels favors adhesion and proliferation of cardiac fibroblast cells of new born

rat (Wistar) due to the formation of synergistic hydrophilic–hydrophobic surface-by-surface reorganization (Kallukalam et al., 2009). Some investigators have attempted to seed and grow cardiomyocytes in a three-dimensional scaffold material to develop an implant for implantation onto the scar tissue. Kofidis *et al.* and Zhao *et al.* have used a commercially available collagen scaffold and studied the growth of cardiomyocytes to develop a contractile bioartificial myocardial tissue (Kofidis et al., 2002), (Zhao et al., 2013). Gonen-Wadmany *et al.* studied the cellular organization of cardiomyocytes within a three-dimensional hydrogel scaffold (Gonen-Wadmany et al., 2004). Naito *et al.* studied the growth of fetal rat cardiac cells in thermo responsive artificial extra cellular matrix, poly (N-isopropyl acrylamide)-grafted gelatin (PNIPAM-gelatin) scaffold (Naito et al., 2004). Sakai *et al.* have studied the growth of cardiomyocytes *in vitro* in gelatin sponge and observed potent inflammatory reaction after 4 weeks of implantation due to dissolution of the sponge (Sakai et al., 2001). McDevitt *et al.* examined spatially organized cardiomyocyte cultures on biodegradable, elastomeric polyurethane films patterned by micro contact printing of laminin lanes (McDevitt and Palecek, 2008).

The electro spinning of polymers has gained attraction of various tissue engineering researchers as they remarkably mimic the size and scale of the natural extracellular matrix. This technique also enables the fabrication of structures with sub-micron pores and nano-topography, which have been reported to be optimal in structures for extracellular matrix-like scaffolds in CTE. Ishii *et al.* cultured primary cardiomyocytes from neonatal rats onto biodegradable electro spun nano fibrous poly (ε-

caprolactone) meshes with an average fiber diameter of 250 nm, using the cell-layering technique (Ishii et al., 2005). Employing this technique, they constructed a 3D cardiac construct with strongly beating cardiomyocytes well attached to the scaffold meshes. In addition, they could establish morphological and electrical communications in constructs with up to five layers of mesh.

2.1.2.Cell-material interaction and cellular performance

Several research groups have generated scaffold materials having better adhesive properties composed of natural polymers such as collagen. Promising results in the development of collagen-based matrix seeded with beating cardiomyocytes having improved adhesive property, morphology and contractile function, were developed. Zimmermann et al studied these patches extensively in animal models. The patch could survive with beating cells for eight weeks after engraftment on the heart of immune suppressed rats (Zimmermann et al., 2004). Similar approaches and results were obtained using alginate, a negatively charged polysaccharide from seaweed, based scaffolds by Cohen *et al.* They observed an intense neo vascularization when compared with control group (Dar et al., 2002).

A wide variety of naturally derived or synthetic polymers, to which adhesion is regulated by adsorbed proteins, are currently being used as cell vehicles due to their intrinsic cell binding capabilities (Mano et al., 2007). Synthetic peptides mediating adhesion can also be presented to cells as self-assembling hydrogels coupled with their side chains to polymer backbones, or as components of synthetic proteins consisting cell interactive domains. The utility of cell adhesion approaches should be highly specific;

otherwise, it can dramatically alter the cell response and enhance or diminish processes such as proliferation or differentiation. Besides the chemistry of the cell-material interface and its mechanics are also recognized to play a key role in the cell response. The stiffness of the adhesion substrate *in vitro* can control the differentiation of adult tissue-derived progenitor populations. However, the features of the types of cell population (primitive or committed cell populations) are unobvious (Hsiong *et al*; 2007).

Controlling the adhesive cues presented to transplanted cells has impact on their survival and the formation of new tissue structures or regeneration of damaged tissues. Introduction of hydrogels into the injured site presents specific adhesive molecules of desirable patterns for promoting the formation of complex tissue-specific structures ((Hill et al., 2006). Local angiogenesis in implantable matrices also can be improved by accelerating the homing of progenitor cells via covalent fixation of adhesion molecules that interact with the cell membrane protein. The molecule L-selectin, was proposed recently to be an excellent candidate for improving local angiogenesis (Suuronen et al., 2009). The attachment of mesenchymal cells to artificial scaffolds can be achieved by the modification of the scaffold with adhesion molecules or association with growth factors (Shi et al., 2008).

8.2 Role of stem cells for regeneration of cardiac tissue

On considering potential cells, options include embryonic stem cells and multipotent postnatal cells. Embryonic stem cells can be harvested from the inner cell mass of the blastocyst. These are well known for their pluripotency and unlimited capacity for self-renewal (Klimanskaya et al., 2008). The pluripotency of embryonic

stem cells makes them an attractive cellular source. Nevertheless, the susceptibility of these cells for teratoma formation warns for understanding the mechanisms to control the tumorigenic properties (Lees et al., 2007). Furthermore, the political and the ethical issues dealing the use of embryonic stem cells also pose substantial challenges (Weissman, 2006). Many researchers succeeded in the isolation of postnatal multipotent stem cells from various tissue sources for cardiac differentiation, which are displayed in Table 2.

The existence of resident stem cells in the myocardium is a clear indication of natural regeneration capacity. Beltrami *et al.* reported the presence of Lin(-) c-kit(POS) cells in the myocardium which own the basic features of the stem cells like self-renewal, multipotency and proliferation capacity. These cells were proved effective in the angiogenesis and in the formation of differentiated myocardium at the ischemic injury site (Beltrami et al., 2003). Another group of researchers demonstrated the Sca-1-positive (Sca-1+) cells from adult murine hearts have stem cell like characteristics. These cells expressed cardiac specific transcription factors, contractile proteins, shown sarcomeric arrangements and were able to beat spontaneously (Matsuura et al., 2004). However, their mechanism of activation and signaling cascade for differentiation and their application in cardiac tissue engineering remains to be elucidated.

Forte G. *et al.* have cultured human cardiac progenitors obtained from the auricles of patients as scaffold free engineered tissues fabricated using temperature-responsive surfaces. After engineered tissues were leant on visceral pericardium, a

number of cells migrated into the murine myocardium and in the vascular walls, where they integrated in the respective textures. The study demonstrated the suitability of engineered tissues to deliver stem cells to the myocardium (Forte et al., 2011). Branco *et al.* reported small preclinical studies and suggested that such delivery of BMCs reach the infarct site (Branco et al., 2009).

Yu Suk Choi *et al.* attempted to differentiate human adipose derived stem cells in rat model using a tissue engineering chamber. They assigned an *in vivo* bioreactor system by implanting an arteriovenous loop by interposing a femoral vein graft between the femoral artery and the femoral vein at the groin region of nude rat. The loop was connected to a polycarbonate chamber, which in turn was anchored to the inguinal ligament. Onto this tissue engineering chamber they co-cultured human adipose derived stem cells and rat cardiomyocytes which led to the effective differentiation of human adipose derived stem cells to functional cardiomyocytes (Choi et al., 2010). Placenta and umbilical cord forms one of the excellent sources of multi potent stem cells. The presence of comparatively longer telomeric DNA and higher telomerase activity of these cells is favorable as a precursor for cardiac tissue regeneration. They possess sufficient passage rate and express several markers of mesenchymal stem cells (MSCs) (Pojda et al., 2005).

8.3 Engineered Heart Tissue (EHT)

Eschenhagen and Zimmermann pioneered to generate an EHT by seeding a mix of collagen I, Matrigel and neonatal rat cardiomyocytes into lattices or circular molds.

Cyclic mechanical stimulation and the reconstitution of liquid mixture led the development of spontaneously and synchronously contracting solid EHTs after one to two weeks of cultivation. By this approach, they demonstrated the importance of physical stimuli in improving morphological, functional and mechanical properties of the EHT (Zimmermann et al., 2004). In another study they found out that their EHT exhibited better electrical coupling with the native tissue and improved diastolic and systolic function in a rat MI model (Zimmermann et al., 2004). The introduction of supra threshold electrical field stimulation helped to induce synchronous contractions of cardiomyocytes in porous scaffolds to form elongated, viable, parallel aligned cells (Tandon et al., 2009). Studies by Zimmermann *et al.* on Fischer 344 rat models revealed the *in vivo* survival of EHT by maintaining the contractility and morphological integration with the host myocardium even after a period of 8 weeks (Zimmermann et al., 2006).

A notable development in the field of EHT ensures the formation of cardiomyocyte monolayers without using scaffolds. This monolayer sheets of cardiomyocytes were obtained by seeding cardiac cells on poly(N-isopropylacrylamide)-grafted polystyrene dishes and then lowering the temperature to 20°C. The transplanted monolayer sheets onto infarcted rat hearts showed successful engraftment and improved the overall cardiac performance (Miyagawa et al., 2005). The same approach can be used for assessing Sca-1-positive resident cardiac progenitor cells (CPCs) and embryonic stem cell (ESC) derived SSEA-1-positive cardiac progenitors where both the cells possess the potential to differentiate into cells of cardiac lineage (Bel et al., 2010).

Donato *et al.* used Dacron (polyethylene terephthalate) patch for the immediate improvement in ejection fraction with sustained benefit and minimal morbidity. These patches were also beneficial for the restoration of the normal ellipsoidal shape of the left ventricle from its decompensated, globular form (Di Donato et al., 2001). Gaudette *et al.* used FDA-approved extracellular matrix (ECM) from porcine urinary bladder and outperformed the benefits seen with Dacron in a canine full thickness right ventricular defect model (Kochupura et al., 2005). Decellularized hydrogel matrix from porcine heart were also reported to enhance maturation of human embryonic stem cell (hESC)-derived cardiomyocytes and this approach opens the way to engineering of the entire organ (DeQuach et al., 2010). The EHT constructed using autologous skeletal myoblasts cell sheets is under clinical trial in Japan with successful treatment of a patient with dilated cardiomyopathy (Sawa, 2010).

For the proper pumping function, it is necessary to have variation in myofiber orientation along the depth of the ventricular wall. There are several reports focusing on the design of EHT with an aligned structure for cardiomyocyte growth. Nanopatterning of PEG hydrogels, rotary spinning of polymer nanofibers, or stamping of ECM protein lanes on thin poly(dimethylsiloxane) (PDMS) films etc. are some of the approaches to provide anisotropic cues for elongation of cardiomyocytes (Kim et al., 2009), (Badrossamay et al., 2010). Bian *et al.* fabricated PDMS molds that contained arrays of mesoscopic posts to guide compaction of cardiomyocyte-seeded hydrogels. This approach caused the enhancement of nutrients diffusion due to the introduction of pores and guidance of three dimensional cell alignments due to spatial patterning of

mechanical tension (Bian and Bursac, 2009). In general small topographical cues can affect several properties in cardiomyocytes including cell attachment, biomechanical stresses, structural remodeling, cell hypertrophy, ion channel remodeling, atrial natriuretic peptide release and binucleation and so on (Chung et al., 2011). EHT can be used as an *in vitro* model to study integration and differentiation potential of stem and progenitor cells in a cardiac environment. R1 Flk1+/PDGFRα+ cardiac progenitor cells can be able to differentiate into cardiomyocytes and integrate into EHT. Moreover EHT was instrumental in enabling identification of residual undifferentiated cell activity in ESC derived populations (Song et al., 2010), (Takahashi et al., 2007).

8.4 Hydrogels in cardiac tissue engineering

Hydrogels are porous structures and the porosity permits local angiogenesis and the fluid flux which is very crucial for neo-organogenesis (Gerecht et al., 2007). While dealing with the hydrogels for tissue engineering applications, the porosity signifies mostly for maintenance of viability of the cells seeded on to it. The porosity will also aids in channeling and trafficking the nutrients and the metabolic wastes in the form of solutes and gases to and from the growing cells even in the absence of functional blood capillaries and also pave way to vasculature formation, cell penetration and communication (Elbert, 2011). The porosity of the tissue engineering hydrogels has the potential to direct the tissue formation and function by effectively guiding the cells towards inner networks by a process called contact guidance (Provenzano et al., 2008). There are reports supporting the use of hydrogel materials for cardiac tissue engineering applications as these biomaterials can provide mechanical support to the diseased

myocardium until the native myocardial ECM is restored (Zimmermann and Eschenhagen, 2003).

The injectable and *in situ* polymerizing hydrogels made from alginate, fibrin and polyethylene glycol (PEG) were reported to have greater responses to chemical, thermal, or optical triggers. Moreover such hydrogels could address the leakage and clearance mediated cell loss (Martens et al., 2009). Tous *et al.* reported the success of acellular hydrogels for cardiac repair which induced neovascularization, stem cell recruitment and prevention of apoptosis (Tous et al., 2011)**.** Shin *et al.* recently reported the development of functional beating cardiac patch using carbon nanotube (CNT)-incorporated photo-cross-linkable gelatin methacrylate (GelMA) hydrogels. This GelMa hydrogels exhibited excellent mechanical integrity and advanced electrophysiological functions and spontaneous synchronous beating (Shin et al., 2013).

Immunogenicity, chronic and acute inflammation, mechanical mismatch with the host tissue, uniform cell distribution, multi cell culture and long-term cell viability are major challenges faced by hydrogel scaffold based tissue engineering (Khademhosseini and Langer, 2007). These difficulties led many groups to develop self-assembly approaches of tissue engineering. The increased understanding of developmental and morphogenetic processes has added more paces to this approach. The individual cells were reported to have the potential to organize into multicellular subunits especially in the form of spheroids, sheets or cylinders. These individual subunits can be further arranged to larger tissue structures even without the use of exogenous scaffolds (Norotte et al., 2009), (Mironov et al., 2009).

8.4.1 Biological polymers as hydrogels

Collagen, the major component of cardiac ECM, provides most of the mechanical strength to heart. Among several types, type I collagen is widely distributed throughout different organisms and tissues. The biocompatibility of type I collagen makes it useful for various tissue engineering applications including CTE (Yang et al., 2001). The slow gelation time of this gel was an issue when used for cardiac tissue engineering, as the encapsulated cells and factors may be flushed away before the gel is formed. However, the decellularized pericardial matrix containing abundant collagen exhibited hydrogel properties and better cellular responses for CTE as reported by Mirsadraee *et al.* (Mirsadraee et al., 2006). The residual cellular particles retaining the decellularized matrix will provoke immunological responses and so complete removal of cells and cellular debris is needed before cell seeding.

The coagulation protein fibrin in the form of hydrogel has been used for cardiac tissue engineering applications due to its non-toxic nature and biodegradation. Birla *et al.* introduced a novel strategy to engineer cardiac tissue by fabricating hollow fibrin gel tubes and populating them with neonatal cardiomyocytes. This cell loaded gel was then implanted to the femoral artery of adult rats and after 3 weeks mature cardiac tissue with dense capillary networks exhibiting all normal cardiac functions was formed (Tao et al., 2014). Several other researchers used fibrin gel for cardiomyocyte embedding and found retention of morphology and contractility and expression of cardiac specific genes even after several months of initial seeding (Huang et al., 2012).

The introduction of Matrigel (an ECM-mimicking hydrogel produced by mouse Engelbreth-Holm-Swarm tumors) composing of basement membrane proteins and growth factors revolutionized the hydrogel approach of cardiac tissue engineering. The very close resemblance with native ECM and the ability to faster vascularization had added extra credits to this hydrogel biomaterial (Anderl et al., 2009). Moreover, the viscous Matrigel can increase the cell retention in the infarcted area. Matrigel hydrogel matrix has been reported to evoke a better response to human mesenchymal stromal cells (MSCs) for cardiac differentiation under ischemic and apoptotic environment (Copland et al., 2008). Combinatorial applications of Matrigel with other natural materials were also reported to be effective for cell proliferation and angiogenesis *in vivo.* Kong *et al.* reported that the combined administration of Matrigel with fibrin gel made cardiomyocytes to maintain their normal function throughout the entire experiment time (Kong et al., 2013). Similar results were reported by Giraud *et al.* using Matrigel/collagen hydrogel and H9c2 cardiomyoblasts in acute rat MI model (El-Sherbiny and Yacoub, 2013).

8.4.2 Synthetic polymers as hydrogels

Synthetic polymer based hydrogels has also been used for cardiac tissue engineering due to their versatility in controlling physical and biochemical properties, stiffness, water content and cell adhesion. They are easy to cast and handle and are cost-effective compared to the natural polymers. However, their biocompatibility and possible inflammatory reactions are challenging issues.

Poly (ethylene glycol) (PEG), a water-soluble polymer synthesized by the ring-opening polymerization of ethylene oxide, is biocompatible and has been approved by the FDA. PEG is widely used as scaffold for various tissue engineering applications due to its anti-fouling properties and low risk of inflammation. The conjugation of cell adhesive peptides or proteins and incorporating growth factors can be employed to increase the cell adhesion on PEG based hydrogels (Li and Guan, 2011). Jongpaiboonkit *et al.* showed that Arg-Gly-Asp (RGD) peptide modification largely increased the viability of encapsulated cardiomyocytes while using PEG hydrogel for 3D cardiomyocyte culture (Jongpaiboonkit et al., 2008). PEG can be co-polymerized with other polymers to get improved properties for cardiac tissue engineering (Wang et al., 2010a).

Owing to the peptide bond mimicking amide structure, polyacrylamide hydrogels also form good candidates for cardiac tissue engineering. The thermal sol-gel transition properties make polyacrylamide hydrogels different from other synthetic ones. At lower temperature, aqueous polyacrylamide solution exists in liquid form and solidifies to form a gel at body temperature. This property has been utilized to design injectable cardiac tissue engineering hydrogels that can be delivered *in vivo.* This can be injected in liquid form using a needle which will turn into solid gels upon contact with the warm tissue (Ratner et al., 2012). Poly (N-isopropylacrylamide) (PNIPAAm) is a typical thermosensitive polymer with a thermal transition temperature (LCST) of 32 °C. Exploiting this property, Okano *et al.* generated cell sheets for cardiac tissue engineering by culturing neonatal cardiomyocytes on PNIPAAm coated tissue culture

plates. The culture plate was cooled after attaining full confluence to form a monolayer cell sheet. The cardiomyocyte monolayer sheets so formed were stacked together and implanted into the infarcted myocardium and the recovery of heart function was observed 4 weeks after implantation (Miyagawa et al., 2005). Guan *et al.* developed a family of protein conjugated PNIPAAm hydrogels acrylic acid, acrylic N-succinimide ester and HEMA-poly(trimethylene carbonate) and also functionalized them with growth factor and antioxidants (Wang et al., 2010a), ((Wang et al., 2010b). A similar result was also reported by Fujimoto *et al.* (Fujimoto et al., 2007).

8.4.3 Biosynthetic hydrogels

The biosynthetic hybrid hydrogels have emerged as promising materials for three dimensional tissue growths owing to their structural, physiochemical, mechanical and biological functionalities and their controlled degradation profile. Several combinations of biosynthetic hydrogels like glycidyl methacrylate and hyaluronic acid (Leach and Schmidt, 2005)**,** poly(ethylene glycol)–fibrinogen conjugates (Frisman et al., 2012), poly(ethylene glycol) and heparin (Welzel et al., 2011), several combinations of poly vinyl alcohol, gluteraldehyde, chitosan and dextran, polyethylene glycol–chitosan, poly acrylic acid–alginate, chitin–PLGA, PAA–chitosan, PMAA–alginate have been reported for various biomedical applications like tissue engineering (Cascone et al., 2004), drug delivery (Gayet and Fortier, 1995), gene delivery (Loh and Li, 2007) and other biomedical applications.

The outstanding properties of alginate in terms of biocompatibility, biodegradability, non-immunogenicity, nonthrombogenity and chelating power pave

way to use it in versatile biomedical applications, especially for cardiac tissue engineering. It is an FDA approved polymer too (Balakrishnan and Jayakrishnan, 2005). The chelation with divalent ions offers a simple way to form alginate hydrogels (Sun and Tan, 2013). However, the alginate-based hydrogels are mechanically weak leading to structural and morphological deformities of the scaffolds. So it fails to be a functional template for tissue regeneration (Jin Lee and Kim, 2012). This mechanical instability hinders the use of alginate hydrogels for long-term and load bearing applications like cardiac tissue engineering. These demerits of alginate can be resolved by co-polymerizing/grafting it with synthetic polyesters.

Synthetic polyesters have displayed better response for tissue engineering applications due to their controlled degradation and sustenance of mechanical properties (Wang et al., 2010a). But the use of these biodegradable polyesters in soft tissue engineering is limited due to elastic deformation, acidic degradation products, absence of cell recognition signals and so on (Serrano et al., 2010).

Synthetic unsaturated polyester, poly(propylene fumarate) (PPF) gained importance due to its mechanical stability and bioresorption profile. In the biological environment, PPF undergo enzymatic degradation to form the TCA cycle intermediate, fumaric acid, which can enter TCA cycle. The other degradation product, 1,2-propanediol is commonly used as a diluent in pharmaceutical products. PPF-based biodegradable composites and hydrogels were investigated for orthopedic and tissue engineering applications (Jayabalan et al., 2009). Sebacic acid, the C10 dicarboxylic acid, is a natural metabolite formed by β-oxidation of long chain carboxylic acids and ω-

oxidation of medium and short chain fatty acids. Since sebacic acid undergo cellular metabolism to form the TCA intermediate succinate, its use in cardiac tissue engineering hydrogels offers a safer application (Sailakshmi et al., 2013). Mannitol is the sugar alcohol formed from the hexose sugar mannose and is commonly used as food ingredients (Mäkinen and Hämäläinen, 1985). Mannitol can enter glycolytic pathway by the formation mannose by mannitol dehydrogenase enzyme, which can then form either glucose or fructose. Fumaric acid, the TCA intermediate, based polyesters were already proven to be biocompatible and non-toxic for tissue engineering applications (Jayabalan et al., 2000).

Therefore, development of biofunctionally active biosynthetic hybrid hydrogel scaffolds involving 1,2-propanediol , maleic anhydride, mannitol, sebacic acid and sodium alginate for cardiac tissue engineering applications is highly relevant.

8.5 Objectives of the present study

Regeneration of soft tissues like myocardium under *in vitro* condition needs an appropriate scaffold matrix in the form of a soft and pliable material such as hydrogel. The macromolecular structure of the hydrogel resembles that of the extracellular matrix (ECM). The swelling characteristics of hydrogel enable tissue-like elastic properties and high permeability of water. The hydrogel scaffolds, both from natural origin and synthetic, possess several demerits, which hinder their long-term application as cardiac tissue engineering scaffolds.

The drawbacks in the use of hydrogels for cardiac tissue engineering are the inability to replicate the mechanical and viscoelastic characteristics of native myocardium. Mostly the hydrogel-based tissues are mechanically weaker than their native tissue as these hydrogels do not form exactly the complex architecture of the native tissue. The mechanical strength of the hydrogel can be improved by mechanically stimulating the seeded cells, leading to remodeling within the construct. However, this approach is too tedious and time consuming. Moreover, the successful responses were reported to be minimal. However, these drawbacks can be overcome with chemically crosslinked hybrid biosynthetic hydrogel scaffolds. Such hydrogels provide promising biomaterials for tissue engineering applications due to favourable physicochemical, mechanical properties and biocompatibility.

The infiltration and long-term viability and functioning of cells on the interstices is a prerequisite for the biological response of cardiac tissue engineering hydrogel. During the course of time, most of the cells grown on the scaffolds fail to perform the desired function. This is due to the unavailability of nutrients to the cells on the hydrogel from the surrounding medium, even though extensive porous network is present. The undesired cell crowding and the inappropriate deposition of ECM components results in the closing of pores during long-term cell growth and thereby adversely affect the trafficking of biomolecules towards the interior of the hydrogel. The influence of physiochemical and mechanical properties on the cell infiltration and their migration towards the inner unoccupied networks of hydrogels, in the absence of specific signaling molecules, are still unexplored.

With hydrogels intended for cardiac tissue engineering applications, inter connecting pores contributes mostly to the maintenance of viability of the cells seeded on to it. The porosity and pore size relates inversely with the stability and directly with the degradation of the hydrogels. The porosity of a hydrogel favors tissue formation and function by guiding the cells towards inner networks by a process called contact guidance. For proper contact guidance, these hydrogels should possess oriented morphologies that will direct the cells towards the pore direction. The porosity is also essential for cell distribution and interconnection. The maximum thickness for a viable hydrogel, which lacks a functional capillary network for tissue genesis, was reported to be around 150 - 200 µm. For the growth of cardiomyocytes, 50 µm size pores are sufficient. Beyond this limit, the seeded cells fail to survive due to insufficient oxygen diffusion and nutrient transport towards the inner rooms of the hydrogel. If the pore size is too small, the cells cannot migrate and form a confluent layer. If too large, the ligands for cell attachment will be diluted which may affect the cell spreading. Conventional fabrication techniques like solvent casting/particulate leaching and freeze-drying are inadequate to have a control over the pore orientation and interconnectivity. The orientation of the pore morphology and architecture of hydrogels to a particular direction can enhance the biological performances due to the effective channeling of metabolites and wastes. Such novel fabrication strategies and cardiac hydrogels with modified morphologies are the need of the hour.

The prevention of uncontrolled ROS production and propagation during MI is a promising area of current research. The role of antioxidant as a therapy for reperfusion

injury has thus been tried in clinical trials with mixed results. Polymeric materials immobilized with antioxidant enzymes for the management of ischemia reperfusion has been tried for management of ROS at the infarct site. However, reports on the application of hydrogels for scavenging of ROS after MI or ischemic heart disease are not adequately available. Therefore, the ROS and associated oxidative damage at the infarct site is one of the hurdles for the cardiac tissue engineering approaches. Cardiac tissue engineering hydrogels having inherent ROS scavenging activities are required for the regenerating/repairing myocardium to restore the functional heart.

Cell growth and response on most tissue engineering scaffolds are studied in static culture conditions, where the cell attachment mainly depends on the cell density. The cell attachment cannot be further increased beyond an optimum level even when 3 D cultures are employed. In actual *in vivo* cardiac conditions, the cells have to overcome hydrodynamic shear stress, which may arise due to flow of biological fluids or forces generated because of movements of tissues or organ parts. The role of these stress in eliciting appropriate functional responses and adaptations to the native cells are also crucial. Simulating such hydrodynamic conditions and the response of the cells in eliciting adherence to the scaffolds and establishment of better communications among the cells are essential before going for implantation.

The native cardiac tissue is composed of several types of cells, cardiac fibroblasts, cardiomyocytes, endothelial cells etc., functioning in a coordinated manner. Each type of cells has influence on the activity and proliferation of the other types. The cells grown together may secrete nutrients, trophic factors or cell adhesion molecules,

which will benefit all the cell types to perform their functions. As far as cardiac tissue engineering hydrogel are concerned, it should not evoke any hindrance to the growth and activities of cells grown together. However, such hydrogel based co-cultured cardiac constructs are very rare in the literature. More optimization of co-culture based evaluations is still needed in terms of hydrogel scaffolds for construction of engineered heart tissue.

The stem cell therapies for the regeneration of infarcted heart have been gaining pace due to the absence of potent side effects and easy availability. The differentiation of stem cells from different sources to cardiac lineage has achieved. On dealing with cardiac tissue engineering hydrogel scaffolds, the chemistry and properties of these biomaterials have implications on directing the differentiation of stem cells to desired lineage. Evaluations of potential of the scaffolds to promote the effective differentiation profile are also necessary. Therefore, the selective tuning of favorable properties from these classes of biomaterials is necessary for generating successful tissue constructs with sustainable characteristics mimicking the native myocardium.

The development of tissue engineered myocardial patch lies with judicial selection of biodegradable hydrogel with adequate strength, compatibility of degradation products to the host tissue, interconnected pore architecture for supply of nutrients to cells, maintenance of cellular viability and differentiation, favoring cell integration, controlled degradation as well as survival with contractile function under ischemic conditions of the in the injured heart. With biodegradable polymers, biodegradation and formation of inflammatory byproducts alters the host response significantly. The inflammatory response to implanted hydrogel material is a great concern as slight inflammation may lead to fibrotic capsule around the implant, which may inhibit tissue remodeling and function as barrier to the transport of nutrient and angiogensis. To the best of our knowledge none of the hydrogel materials developed so far has met all these stringent and diagonally opposite requirements.

Based on this background, the present studies were designed with the major objective of synthesis of biomechanically favourable and biodegradable biosynthetic hydrogel scaffolds involving 1,2-propanediol , maleic anhydride, mannitol, sebacic acid and sodium alginate, which can elicit favourable cellular responses for the engineering of heart tissue. The specific objectives of the study are as follows.

1).Synthesis and characterization of novel biomechanically favourable and biodegradable hydrogel scaffolds using biosynthetic comacromers of polyester (1,2-propanediol, maleic anhydride, mannitol, sebacic acid) and sodium alginate.

2). Studies on cell-material interaction and genotoxicity of biosynthetic hydrogels.

3).Studies on biological responses of biosynthetic hydrogels for cardiac tissue engineering.

i). Studies on fibroblast infiltration and long-term viability

ii). Studies on protective effects of hydrogels from ROS induced oxidative stress

iii). Studies on cardiomyoblast growth and adhesion under hydrodynamic conditions

iv).Studies on co-culture of cardiomyoblast and fibroblast

v).Studies on the influence of hydrogels for differentiation of bone marrow MSC to cardiomyocyte.

Chapter 3
MATERIALS AND METHODS

9 Materials and Methods

9.1 Materials

Sodium alginate (guluronic acid (39%) and mannuronic acid (61%) from brown algae, medium viscosity, Product No.A2033), sodium chloride, maleic anhydride, acrylic acid, calcium chloride, 2-hydroxy ethyl methacrylate (HEMA), L-ascorbic acid, ammonium per sulfate, etc. were obtained from Sigma Aldrich, Spruce Street, St. Louis, USA. Calcium chloride, sodium acetate, N N' methylene bisacrylamide (NMBA), methyl methacrylate (MMA), poly(ethylene glycol diacrylate) (PEGDA), disodium hydrogen phosphate and sodium hydroxide were supplied by Merck specialties Pvt. Ltd,

Mumbai, India. n-butyl methacrylate (BMA) was purchased from Polyscience Inc, Warrington. 1,2 propylene glycol, morpholine etc were provided by SD fine chemicals India Ltd. Mannitol, sebacic acid etc. were purchased from HiMedia laboratories Pvt. Ltd, India. All other chemicals used were of analytical grade.

9.2 Preparation of biosynthetic hybrid hydrogel scaffolds

9.2.1 Synthesis of hydroxyl terminated-poly (propylene fumarate) (HT-PPF)

Hydroxyl terminated-poly (propylene fumarate) (HT-PPF) macromer was synthesized by refluxing maleic anhydride with 1-2,propylene glycol at 140 ^{o}C for 2 h in the presence of sodium acetate and morpholine. The mixture was then subjected to vacuum condensation at 190 ^{o}C for 20 min. The native resin obtained was purified by dissolving in acetone, washed in aqueous methanol and re-precipitated in petroleum ether (Gnanaprakasam Thankam and Muthu, 2013a).

9.2.2 Synthesis of poly(mannitol fumarate-co-sebacate) (PMFS)

Poly(mannitol fumarate-co-sebacate) (PMFS) was synthesized.0.72 M Mannitol, 0.67 M maleic anhydride and 0.42 M sebacic acid were taken in a 500 ml RB flask along with 1g each of catalysts (sodium acetate and morpholine) and refluxed to 140 ^{o}C for 25 min under N_2 atmosphere in an oil bath attached to the hot plate stirrer (IKA RH basic KT/C). The molar ratio of [OH] to [COOH] in the reaction mixture was set to 2 for getting hydroxyl terminated ends. Then the temperature was raised to 195 ^{o}C and vacuum condensation was carried out for 5 min. The viscous resin PMFS so formed

became solidified at room temperature. The resin was dissolved in DMSO and stored at room temperature for further studies.

9.2.3 Preparation and characterization of poly (propylene fumarate)-alginate and poly(mannitol fumarate-co-sebacate)-alginate graft comacromers

Poly (propylene fumarate)-alginate (HPAS) and poly(mannitol fumarate-co-sebacate)-alginate (PMFSA) graft comacromers were synthesized by copolymerizing poly (propylene fumarate) and poly(mannitol fumarate-co-sebacate) macromers with alginate under acidic conditions (Thankam and Muthu, 2013b). The macromers were warmed at 70 – 80 ^{o}C under acidic condition and Na-Alginate powder was immediately added under stirring condition, mixed well and allowed to set for more than 30 min. The ratio of Na-Alginate to macromer was 2:1. The entire mixture was then slowly dissolved in minimum distilled water under constant stirring to form corresponding HPAS and PMFSA comacromers. The comacromers were stored at room temperature for further studies.

The comacromers were analysed for molecular weight and functional group formation. The molecular weight was determined by gel permeation chromatography. 50 µl of 0.1% solution of comacromer in tetrahydrufuran (THF) was injected to the HPLC system (Waters) connected with 600 series pump and 2414 refractive index detector. The styragel columns (HR-5E/4E/2/0.5) were connected in series and THF was pumped at a flow rate of 1 ml/min and the relative calibration was done with polystyrene standards (Mp- 100000, 9130, and 162). The functional groups in the poly(mannitol fumarate-co-sebacate) macromer were analysed by FTIR analysis using FT-IR impact

410- spectrophotometer as per the standard ASTM E 1252-94. The spectrum was recorded using a resin smear on the KBr window. The functional groups in the poly (propylene fumarate)-alginate and poly(mannitol fumarate-co-sebacate)-alginate were analysed by AT-IR analysis using FT-IR impact 410- spectrophotometer as per the standard ASTM E 1252-98 (E 573-01). The spectrum was recorded using a freeze-dried thin film.

9.2.4 Preparation of HPAS and PMFSA based biosynthetic hydrogel scaffolds

The biosynthetic hydrogel scaffolds were prepared from the comacromers by crosslinking the alginate fractions with calcium ions and the unsaturation of the esters with different vinyl monomers by free radical induced crosslinking. A panel of 12 different monomodal and bimodal hydrogel scaffolds was synthesized from PPF-Alginate (HPAS) comacromer. Of these 5 bimodal hydrogels were synthesized by employing single vinyl crosslinkers. The vinyl crosslinkers used were methyl methacrylate (MMA), N N' methylene bis acrylamide (NMBA), 2-hydroxy ethyl methacrylate (HEMA), n-butyl methacrylate (BMA) and acrylic acid (AA) respectively for the hydrogel scaffolds HPAS-MMA, HPAS-NMBA, HPAS-HEMA, HPAS-BMA and HPAS-AA. No vinyl crosslinking agent was used for HPAS-No monomodal hydrogel scaffold (Thankam and Muthu, 2014a).

The remaining 6 bimodal hydrogel scaffolds were synthesized by crosslinking with two vinyl crosslinkers. HPAS was copolymerized with polyethylene glycol diacrylate (PEGDA) to form HPAS-P (HPAS-Co-PEGDA). Then the double bonds of PEGDA segments of HPAS-P was crosslinked with the above vinyl crosslinkers (MMA,

AA, BMA, HEMA, NMBA) to form HPAS-PM, HPAS-PA, HPAS-PB, HPAS-PH and HPAS-PN respectively (Thankam and Muthu, 2014b).

Similarly, PMFA-Alginate (PMFSA) comacromer was crosslinked with divinyl crosslinkers like PEGDA, NMBA and diethylene glycol dimethacrylate (DEGDMA) to form corresponding PMFSA-PEGDA, PMFSA-NMBA and PMFSA-DEGDMA bimodal hydrogel scaffolds respectively.

All the samples were casted at 60 ^{o}C for overnight. The sheets so formed were allowed for ionic crosslinking with calcium. The hydrogel scaffolds so formed were washed in tap water and distilled water at room temperature for 24 h for the leeching out of unreacted molecules. The samples were then freeze-dried overnight, sterilized by EtO (ethylene oxide) and stored aseptically for further studies.

9.2.5 Morphologically modified HPAS-P based hydrogels for improved biological performance

9.2.5.1 Modification of morphology by inducing unidirectional porosity

Dynamic mechanical cyclic stretching of hydrogels was carried out on water swollen HPAS-P based hydrogels system to introduce unidirectional porosity to form morphologically modified hydrogels (MM-hydrogels). The stretching cycles were limited to 1/4th cycles of the complete fatigue life of each hydrogel scaffolds as per the procedure described in section ***3.3.2.2***. These stretched hydrogel samples were freeze-dried and used for evaluations.

9.2.5.2 Effects of physiochemical parameters of MM- hydrogels on biological response

The MM-hydrogels were assessed with contact angle measurements, percentage swelling and equilibrium water content (EWC), DSC, ESEM and cell infiltration as described in the above sections. The amount of collagen adsorbed on the hydrogel scaffolds pre and post modification was compared by Sirius red method as per published procedures (Thankam and Muthu, 2014). The attachment and spreading of H9c2 cardiomyoblast cells was investigated for five days using fluorescence diacetate (FDA).

9.3 Characterization of biosynthetic hybrid hydrogel scaffolds

3.3.1.Physiochemical characterizations

9.3.1.1 ATR spectral analysis for surface functional groups

The surface functional group analysis of freeze-dried HPAS and PMFSA based hydrogels were carried out using AT-IR spectrum recorded with Nicolet 5700 FTIR Spectrometer based on ASTME 1252-98 standards.

9.3.1.2 Water content and holding capacity

Dry weight of six samples (2 cm x 1 cm) of freeze-dried hydrogels was accurately measured. Then these samples were immersed in distilled water for 24 h at room temperature and allowed to attain maximum swelling. The swollen samples were wiped softly to clear away the surface water and instantly measured the weight in an electronic weighing balance. The equilibrium water content and water holding capacity (%S) of the hydrogels were determined using the equations (Gnanaprakasam Thankam et al., 2013).

$$EWC = \frac{Wet\ weight - Dry\ weight}{Wet\ weight}\ X\ 100$$

$$\%S = \frac{Wet\ weight}{Dry\ weight}\ X\ 100$$

9.3.1.3 Surface hydrophilicity/hydrophobicity evaluation by contact angle

The hydrogel samples (n=6) for contact angle measurements were swelled in distilled water and cut to the dimensions 4 cm x 1.5 cm. The thickness was measured using a screw gauge. The samples were cleaned in a sonicate bath prior to the measurements. The contact angle was determined in water using Wilhelmy method using KSV sigma 701 tensiometer. The immersion depth was set to 10 mm with the speed of immersion of 5 mm/min. The initial 2 mm length from each samples were ignored during the measurements. Six measurements from each samples were recorded and the average of consecutive three values from each samples were taken (Gnanaprakasam Thankam et al., 2013).

9.3.1.4 Surface morphology and average pore diameter evaluation by ESEM

The surface morphology of all the hydrogels were investigated by environmental scanning electron microscopy (ESEM) at low vacuum mode. Freeze-dried samples were used. The average pore diameter of scaffolds was calculated using the imaging software ImageJ 1.46r using the multi-measure plugin (Gnanaprakasam Thankam and Muthu, 2013a).

9.3.2 Mechanical characterizations

9.3.2.1 Determination of tensile strength

Tensile strength of the water-swollen hydrogels were determined using universal automated mechanical test analyzer (Instron, model 3345) connected with long travel extensometer. Dumb bell shaped specimens were punched out (ISO 527-2 type 5A) using a shear cutting die. Tensile strength was tested with a load cell of 100 N at 25 ^{o}C with a crosshead speed of 10 mm/min. The stress-strain data were recorded using Bluehill software (Thankam and Muthu, 2014b).

9.3.2.2 Determination of accelerated fatigue life in water

The ability of water-swollen HPAS-AA, HPAS-P, HPAS-PA, HPAS-PB, HPAS-PM, HPAS-PN, PMFSA-PEGDA and PMFSA-DEGDMA hydrogels (n=6, 4 cm x 1.5 cm) to withstand cyclic stretching were determined using the biomaterial testing instrument connected to a biobath chamber and associated temperature controller (Test Resources, Model-BioBath, USA). The test was carried out in distilled water at physiological temperature at a frequency of 6 cycles/sec and amplitude 2.5 mm using the load 0.91 N. The fatigue lives of the hydrogels were recorded by the desktop computer using the MTL-Windows-v7.1 software. The instrument was stopped manually immediately after the rupture of the sample (Gnanaprakasam Thankam and Muthu, 2013a).

9.3.3 Thermal evaluation for determining the status of water in hydrogels

The status of water in the hydrogels was determined by differential scanning calorimetry (DSC) equipped with a low-temperature cooling apparatus based on the ASTM 537-07 method (DSC-2920, TA Instruments.Inc). The hydrogel was placed in an aluminum pan and hermetically sealed. The weight of the sample used was 10 mg. The sample was first cooled to (-)50 °C and then heated to 100 °C at the rate of 5 °C/min in nitrogen atmosphere. The cooling and heating processes were monitored. From the DSC thermogram freezing free water, freezing bound water and non-freezing bound water was calculated (Gnanaprakasam Thankam et al., 2013).

9.3.4 Biostability of hydrogels

The stability of hydrogels were evaluated in the cell culture medium DMEM containing 10% FBS by aging at temperature 37 ^{0}C for 7 days. Then the long-term biostability and degradation of the hydrogels were determined at pH 7.4 in the simulated biological fluid, PBS. Dried hydrogels of known weight were incubated in 20 ml PBS at physiological pH and temperature. Then the relative loss of dry weight, changes in pH and conductivity and total dissolved solids were monitored at regular intervals of 7 days using a pH meter (cyber scan pc510). The aged hydrogels were freeze-dried and the dry weight was noted for the evaluation of biodegradation (Gnanaprakasam Thankam et al., 2013).

9.4 Studies on cell-material interaction

9.4.1 Assessment of hemocompatibility

9.4.1.1 Evaluation of hemolytic potential of hydrogels

The hydrogel scaffolds of 1 cm diameter were incubated in PBS (pH 7.4) at 37 ^{0}C and for 48 h. RBC suspension was prepared from the blood collected from healthy human donors with informed consent. The blood was washed with sterile normal saline and diluted with the same. Then 100 µl of the hydrogel extract was mixed with 100 µl dilute RBC suspension and incubated at 37 ^{0}C for 3 h. After incubation 2.6 ml saline was added, centrifuged at 2000 rpm for 5 min and the OD of the supernatant was read at 541 nm. Distilled water was used as positive control and saline as negative control. From the OD values, the % hemolysis was calculated (Gnanaprakasam Thankam et al., 2013).

9.4.1.2 RBC aggregation assay to evaluate hemocompatibility

100 µl of the PBS extract of the hydrogels were mixed with 100 µl dilute RBC suspension (prepared as in hemolysis assay) and incubated at 37 ^{0}C for 30 min. The cells were microscopically examined for RBC aggregation with respect to negative (saline) and positive (poly ethylene imine) controls (Gnanaprakasam Thankam and Muthu, 2013a).

9.4.1.3 Evaluation of thrombogenic potential of hydrogels by platelet adhesion

Platelet rich plasma (PRP) was prepared from anticoagulated human blood by centrifuging at 2500 rpm, for 5 min. Again, the blood was centrifuged at 4000 rpm for 15 min to collect platelet poor plasma (PPP). PRP count was adjusted to 2.0 - 2.5 x 10^8 /ml with PPP. All the hydrogels (except HPAS-No, HPAS-MMA, HPAS-HEMA, HPAS-BMA and HPAS-PH) were swelled in PBS initially. PRP was added and agitated for 30 min at 37 ^oC in an incubator shaker. After incubation, the PRP was washed with PBS and the adhered platelets were fixed with 3% glutaraldehyde overnight at 2-8 ^oC and dehydrated with ethanol at different concentrations (30%, 50%, 70% and 100%). The samples were then observed using the ESEM under low vacuum mode (Gnanaprakasam Thankam et al., 2013).

9.4.1.4 Determination of plasma protein adsorption on hydrogels surface

1 ml of diluted plasma (1:10) was added to the PBS swelled HPAS based hydrogel scaffolds and incubated for 2 h at 37 ^oC on a shaker incubator. Then the scaffolds were removed and the protein fraction left out was determined by Lowry's method using BSA standard**.** Then percentage of proteins adsorbed on to the hydrogels was quantified with respect to total plasma protein content as control (Gnanaprakasam Thankam and Muthu, 2013a).

In order to distinguish the types of plasma proteins adsorbed to the hydrogels, SDS-PAGE analysis was done. Then the adsorbed protein fractions on the hydrogels were removed by vortexing, denatured and electrophoresis was done in 10% acrylamide gel. A 65V was supplied for stacking gel and 130V for resolving gel. After the

completion of electrophoresis, the gel was stained with coomasie brilliant blue dye for overnight, then destained and the image of the resolved gel was acquired by a scanning system. A well was loaded with bovine serum albumin as control (Gnanaprakasam Thankam and Muthu, 2013a).

9.4.2 Assessment of cytocompatibility

9.4.2.1 Cell culture

For biological studies, mouse fibroblast L929 cells and rat H9c2 cardiomyoblasts were used. Both the cell lines were purchased from National Centre for Cell Science, Pune, India. The cells were grown in DMEM supplemented with 10% FBS and antibiotics penicillin, streptomycin and amphotericin B in a humidified incubator at 5% CO_2 at 37 ± 0.2 ^{o}C. The cells were regularly monitored by phase contrast inverted light microscope. The medium was changed once in three days. The confluent monolayer was trypsinized for sub-culture and maintained for further studies.

9.4.2.2 MTT cell viability assay

The cytotoxicity of hydrogels was checked by MTT assay as per ISO 10993-5 on L-929 mouse fibroblast cell culture after extracting in DMEM. Cell suspension containing around $1x10^5$ cells/ml were seeded on to a 24 well tissue culture plate and incubated at 37 ˚C and 5% CO_2 for 72 h using the medium extracted with hydrogels. The percentage of the surviving fibroblast cells were quantified by the standard MTT assay. For the assay, the medium was removed, added 50 µl MTT solution (5 mg/ml in PBS) and incubated at 37 ˚C for 3 h. Then 200 µl DMSO was added to dissolve the

formazan crystals formed. The absorbance was read at 540 nm. From the absorbance values % of viable cells were determined with respect to scaffold free control (Gnanaprakasam Thankam and Muthu, 2013a).

9.4.2.3 Direct contact assay

The toxicity of the hydrogels under the direct influence of cell contact was determined by direct contact assay. L929 fibroblast cells were (1 x 10^4 cells/ml) seeded on to a 12 well plate (BD Falcon) and allowed to proliferate for 24 h to form a sub-confluent layer. Then the hydrogel samples of 1 cm diameter was placed over the monolayer and allowed to proliferate for 24 h in a CO_2 incubator. After the incubation, the cells were evaluated with respect to a control (cells grown without hydrogels) under inverted phase contrast microscope attached with an imaging camera. The images were captured and stored in the desktop computer with the help of imaging software (Gnanaprakasam Thankam and Muthu, 2013a).

9.4.2.4 Live/dead assay for the assessment of apoptosis

L929 cells were grown onto DMEM-swollen hydrogel for 5 days. After rinsing with PBS, the cell loaded hydrogels were incubated with a mixture of acridine orange (100 µg/ml) and ethidium bromide (100 µg/ml) at room temperature for 3 min and viewed under an epifluorescence microscope (Optika SRL). A blue filter for acridine orange and green filter for ethidium bromide was used. Two images were taken from the same field using both filters and the images were merged by the imaging software Photoshop8 CS (Gnanaprakasam Thankam and Muthu, 2013a).

9.4.3 *In vitro* evaluation of genocompatibility by comet assay

In order confirm the absence of genotoxic effects of the hydrogel upon contact with the cells, the DMEM-swelled HPAS-No, HPAS-MMA, HPAS-HEMA, HPAS-BMA and HPAS-PH hydrogels were placed over a sub-confluent layer of L929 fibroblasts and incubated at 37 ^{o}C for 48 h. These cells were then subjected to comet assay as per the following procedure. The microscope slides were pre-coated with 1 ml of 0.75% normal melting point agarose (NMA) and stored at 4 ^{0}C. This layer was removed before use and 120 µl of 0.75% NMA was pipetted on to the slides, which were then covered with cover slips. Cells were trypsinized, mixed with 50 µl of low melting point agarose and pipetted over the first layer of agarose. NMA (80 µl) was used as a final protective layer. Slides were placed in cold lysing solution (2.5 M NaCl, 100 mM Na_2EDTA, 10 mM Tris pH 10 & 1% SDS to which 10% DMSO and 1% Triton X 100 were added immediately before use) for overnight at 4 ^{o}C. After lysis slides were placed in electrophoresis buffer (300 mm NaOH and 1 mM Na_2EDTA $P^{H}13$) for 20 min to allow unwinding of DNA. Then electrophoresis was conducted in the same buffer by applying an electric current of 0.8 V/cm (300 mA) for 15 min. Finally, slides were washed in neutralization buffer (0.4 µL Tris, pH 7.5) three times for 5 min and stained with 50 µl ethidium bromide (20 µg/ml). The excess stain was washed with PBS and viewed under fluorescent microscope using green filter. The extent of DNA damage was quantified by the comet reading software TriTek cometScore Freeware 1.6.1.13 with respect to a control and H_2O_2 treated cells (200mM H_2O_2 was added to the culture and incubated for 24 h) (Thankam and Muthu, 2013a).

9.5 Stuidies on biological responses of hydrogels for cardiac tissue engineering

9.5.1 Quantification of fibroblast cell infiltration and long-term viability

All the hydrogels (except HPAS-No, HPAS-MMA, HPAS-HEMA, HPAS-BMA and HPAS-PH) were incubated in the medium containing FBS for 24 h in a CO_2 incubator. Then the medium was removed and 100 µl L929 cell suspensions, containing around $3x10^5$ cells/ml, was added on the scaffolds and kept undisturbed in CO_2 incubator at 37 ^oC for 45 min for cell attachment to the scaffolds. After the attachment 1 ml cell culture medium was added carefully through the wall of the wells. The cells were grown for a period of 1 month. Media was changed once in 3 days and the cell infiltration was quantified by modified MTT assay on every week. The cell-grown scaffolds were taken out from the wells, washed twice with PBS and incubated for 3 h with 1 ml MTT solution (1 mg/ml in PBS) under standard cell culture conditions. After incubation the scaffolds were extracted with isopropanol containing 0.01 N HCl, vortexed for 10 min, kept for 30 min, centrifuged at 10000 g for 5 min to settle the scaffold and cell debris. The OD of the supernatant was read at 570 nm. A control well without scaffolds and blank containing scaffolds without cells were also maintained in the same manner. From the OD values the percentage viability was calculated (Gnanaprakasam Thankam and Muthu, 2013a).

9.5.2 Evaluation of protective effects of hydrogels from cellular oxidative stress

9.5.2.1 Induction of oxidative stress

The free radical scavenging activity of biosynthetic hydrogels against reactive oxygen species (ROS) was determined on H9c2 cardiomyoblast cells using H_2O_2 model.

200 µM H_2O_2 was added to the culture to induce an oxidative stress as reported elsewhere (Thankam and Muthu, 2013a). Immediately the hydrogel (1 cm diameter swelled in DMEM) was placed on the stress-induced cell layer and incubated at 37^{o}C for 24 h. HPAS-AA, HPAS-PA, HPAS-NMBA, PMFSA-PEGDA and PMFSA-NMBA hydrogels were evaluated with oxidative stress induced H9c2 cardiomyoblasts.

9.5.2.2 Responses of stress induced H9c2 cells

9.5.2.2.1 Determination of ROS production of H9c2 cells

The production of reactive oxygen species (ROS) in cardiomyoblast cells induced by the hydrogel scaffolds (HPAS-AA, HPAS-PA, HPAS-NMBA, PMFSA-PEGDA and PMFSA-NMBA) were determined using luminol (5-amino-2-3-dihydro-1,4 phthalazinedione; Sigma) by generating a chemiluminescence signal. The hydrogel-exposed cells were detached from the culture by adding 40 µl trypsin and were suspended in serum free DMEM. The luminol solution for the assay was prepared by 0.014 g luminol in 10 ml solution containing 0.556 g NaOH and 0.618 g boric acid. 1:1000 dilution of luminol solution was used for the assay. Immediately before the assay equal volume of the working luminol solution and cell suspension were mixed and the luminescence was determined using luminescence counter for a time period of 15 min at an interval of 1 min (Smith et al., 2009). The results were reported as luminescence counts per second (LCPS). A negative control without scaffolds, a positive control containing 200 µM H_2O_2 and without scaffolds and a reagent blank were treated in a similar way.

9.5.2.2.2 Determination of ROS content

The ROS stressed cells were grown in presence of our hydrogels and were stained with 20 µM dichlorodihydro fluorescein diacetate (DCDHFDA). The stained cells were imaged under fluorescent microscope using blue filter after washing with PBS (Masaki et al., 2009). The settings of the microscope were kept unchanged for all the samples. The images were then analyzed using ImageJ software.

9.5.2.2.3 Determination of apoptosis by live/dead assay

Live/dead assay of the hydrogel treated cells under oxidative stress were determined as per the above-described protocol.

9.5.2.2.4 Metabolic activity of ROS stressed cells upon contact with hydrogels

ROS stress was induced to the H9c2 cell culture by the above procedure and the cells were allowed to proliferate for 24 h at standard culture conditions. Then the metabolic activity of the cells was determined by MTT assay with respect to the above-mentioned controls.

9.5.2.2.5 Estimation of lipid peroxidation products

Polyunsaturated fatty acid peroxides from the cell membrane, malondialdehyde (MDA), generated upon decomposition by interacting with ROS. For MDA estimation, 500 µl of 70% alcohol and 1 ml of 1% TBA was added to 50 µl of cell lysate and heated in a boiling water bath for 20 min. Then 50 µl of acetone was added at room temperature and absorbance was read at 535 nm. From the absorbance value, the concentration of MDA was calculated (Ogunro et al., 2012).

9.5.2.2.6 Estimation of reduced glutathione

To 1.0 ml of cell lysate 0.5 ml of phosphate buffer (0.2 M pH 8), 1.3 ml of distilled water and 0.2 ml of DTNB (0.6 mM) were added, mixed and OD was read at 420 nm. The GSH concentration in the lysate was calculated from the standard GSH plot (Shrikant Ashok Shete, 2012).

9.5.2.2.7 Estimation of cellular Nitrite Levels

To 0.5 mL of cell lysate, 0.1 mL of sulphosalicylic acid was added and vortexed for 30 min and centrifuged at 5,000 rpm for 15 min. This protein-free supernatant was used for the estimation of nitrite levels. To 200 µL of the supernatant, 30 µL of 10% NaOH and 300 µL of Tris-HCl buffer was added and mixed. Then 530 µL of Griess reagent was added and incubated in the dark for 15 min and the absorbance was read at 540 nm using Griess reagent as blank. The amount of nitrite present in the samples was estimated from the standard plot prepared by the above procedure using known concentrations of freshly prepared Sodium Nitrite solution (Lee et al., 2012).

9.5.3 Evaluations of growth of cardiomyoblasts (H9c2) cells under hydrodynamic conditions

In order to study the growth and activity of cells under hydrodynamic conditions, a Rotary Cell Culture System (RCCS) was used (Teo et al., 2012). The chamber of the RCCS was filled with cell culture medium (40 ml) without air bubbles. The DMEM swelled PMFSA based scaffolds (1cm diameter) were then put into the medium and subjected to rotation. After 24 h, 5 ml cell suspension containing approximately $5x10^5$ H9c2 cardiomyoblast cells/ml was added and the rotation was continued for 10 days.

The rotation speed was adjusted to maintain a steady state of the floating scaffolds and to avoid the collision between them. Cell seeded scaffolds grown under static condition were treated as controls. On 5^{th} and 10^{th} days scaffolds were removed from RCCS and cell infiltration assay was conducted. The cells on the scaffolds were imaged by staining with acrydine orange.

9.5.4 Coculture of fibroblasts and cardiomyoblasts

L929 fibroblast cells were allowed to attain confluence in a T75 flask and the cell cycle was arrested by incubating them with mitomycin, (10 µg/ml in serum free media) for 5 h. For removing the mitomycin the culture was washed with PBS and incubated with DMEM containing 10% serum for 1h. Then the cells were washed with PBS, trypsinized and around $3.2x10^6$ mitomycin treated cells were then seeded to PMFSA based hydrogel scaffolds which were prior swelled in DMEM and grown for 2 days. To these L929 grown scaffolds around $3.2x10^6$ H9c2 cardiomyoblast cells were also seeded and grown for another five days. Media change was done on every alternate day. MTT assay was conducted on 3^{rd} and 7^{th} days of the experiment. For comparison four controls were maintained (normal L929 cells, Mitomycin treated L929 cells, normal H9c2 cells and Mitomycin treated L929 cells + normal H9c2 cells). By analyzing the OD values the growth of H9c2 cells in presence of L929 cells were correlated.

9.5.5 Cell cycle analysis of H9c2 cardiomyoblasts grown on contact with PMFSA based hydrogels

The proliferation capacity and health of the H9c2 cardiomyoblast cells upon contact with MFSA hydrogel scaffolds were assessed by the determination of DNA content using flowcytometry analysis (Muse™ Cell Analyzer). The cell culture was carried out as per the above procedure. Then the cell cycle analysis was done by using MUSE cell cycle kit as per the manufacturer's instructions. The kit utilizes a premixed reagent which includes the nuclear DNA intercalating stains propidium iodide (PI) which discriminates cells at different stages of the cell cycle (G0/G1, S and G2/M) based on the differential DNA content in each phase. After 48 h the scaffolds were removed and the cells were trypzinized and washed thrice with PBS by spinning at 4500 rpm. The washed cells were then fixed overnight using absolute ethanol at (-)20 ^{o}C. The fixed cells were then washed twice with PBS as above and incubated with cell cycle reagent at room temperature in dark for 30 min and analyzed on Muse flow-cytometer (Millipore, USA).

9.5.6 Studies on differentiation of stem cells to cardiac lineage on PMFSA-PEGDA and PMFSA-DEGDMA hydrogels

Mesenchymal stem cells (MSCs) were isolated from the bone marrow of wistar albino rats. The bone marrow cells were grown in low glucose containing DMEM. After 2 passages the cells were confirmed by immunostaining using confocal microscopy for MSC markers like vimentin. The cells were then grown in differentiation medium containing 5-azacytidine. After 24 h the medium was replaced by normal DMEM and growth was continued for 2 weeks. The differentiation potential was confirmed by the gene expression analysis of cardiac specific biomarkers like GATA-4, NKX-2.5, MEF-

2, Troponin C and Troponin-C using conventional PCR amplification. The amplified genes were then subjected to electrophoresis and the band intensities were calculated by using ImageJ software.

9.6 Statistical analysis

All experiments were carried out with of 5 or 6 samples from each group. The values are presented as means ± standard deviations. Statistical analysis was done with one way ANOVA using online calculator, Statistics Calculator version-3 beta and the level of significance was set at $p < 0.05$ for all calculations.

Chapter 4
RESULTS

10 Results

10.1 Preparation of biosynthetic hydrogel scaffolds

Hydroxyl terminated-poly (propylene fumarate) (HT-PPF) macromer was synthesized by the condensation of maleic anhydride with 1-2,propylene glycol and subsequent isomerization of maleate to fumarate. Alginate was then graft copolymerized with HT-PPF under acidic conditions to form PPF-Alginate (HPAS) graft comcaromer. The GPC anaylses of HPAS reveal molecular weight 784 (Mn) and 2010 (Mw) and polydispersity 2.56.

AT-IR spectrum of HPAS comcaromer (Figure 3) reveals a broad band at ~3381 cm^{-1} for hydroxyl group of HT-PPF and alginate segments. The peak at 2983 cm^{-1} is due to C-H stretching vibration of the double bond = CH and to the symmetric stretching vibration of the aliphatic CH_2 groups of HT-PPF and alginate segments. The peak at 1715 and 1153 (C-O stretching) and, 1291 cm^{-1} (-OH bending) suggest PPF segments. The peaks appearing at 1642 and 1394 cm^{-1} are the asymmetric and symmetric stretching vibrations of the carboxyl group of alginate. The peaks appearing at 1642 is also due to C=C stretching vibration of HT-PPF segment (unsaturated fumarate groups). The peak appearing at 1024 cm^{-1} indicates C-O-C stretching of alginate. The strong peak appeared at 979 cm^{-1} reveals fumarate linkages of HT-PPF though a minor peak also

appeared at 773 cm^{-1} (C-H bending) for cis –CH=CH- end groups. The IR spectral anaysis thus provide evidence for the presence of PPF and alginate in the copolymer.

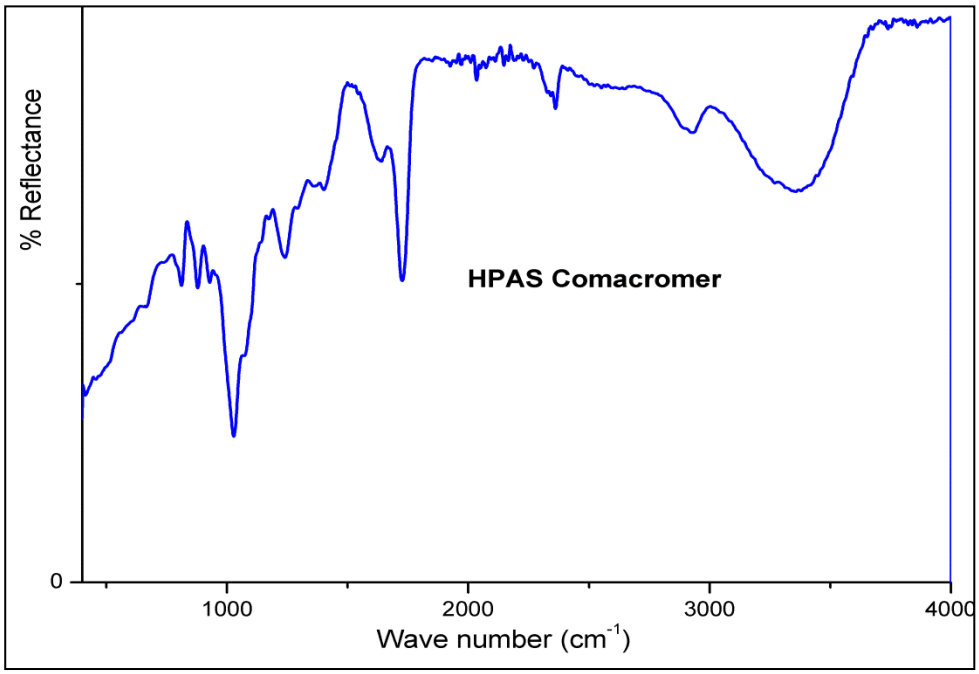

Figure 3. AT-IR spectrum of PPF-Alginate comcaromer (HPAS) showing peaks corresponding to the condensation of alginate and PPF.

Mannitol, maleic anhydride and sebacic acid were condensed for the synthesis of poly(mannitol fumarate-co-sebacate) (PMFS) macromer. Of the six –OH groups of mannitol four were left unreacted and two were allowed to esterify with one of the –COOH groups of the dicarboxylic acids sebacic acid and fumaric acid. The molar ratio of [OH] to [COOH] in the reaction mixture was set to 2 for getting hydroxyl terminated ends. Alginate was then graft copolymerized with PMFS under acidic conditions to form PMFS-Alginate (PMFSA) graft comcaromer. GPC analysis of PMFSA revealed number average molecular weight 849, weight average molecular weight 1022 and polydispersity 1.2.

The IR spectral analysis showed the presence of characteristic peaks revealing the surface functional groups of the scaffolds and the effective formation of the polymer and co-polymer. FT-IR spectrum of PMFS macromer (Figure 4) reveals a broad band at ~3400 cm^{-1} for hydroxyl group imparted by the mannitol residue. The peak at 2800 cm^{-1} and 2900 $cm^{-1}$is due to C-H stretching vibration of the double bond = CH of fumarate groups and also to the symmetric stretching vibration of the aliphatic CH_2 groups sebacic acid and mannitol residue. The slight peak around 1640 is due to C=C stretching vibration of fumarate groups. Peaks around 770 cm^{-1} indicates the C-H bending of cis –CH=CH- end groups. The peaks around 1700 cm^{-1} revealed the carbonyl stretch indicating the ester bond formation.

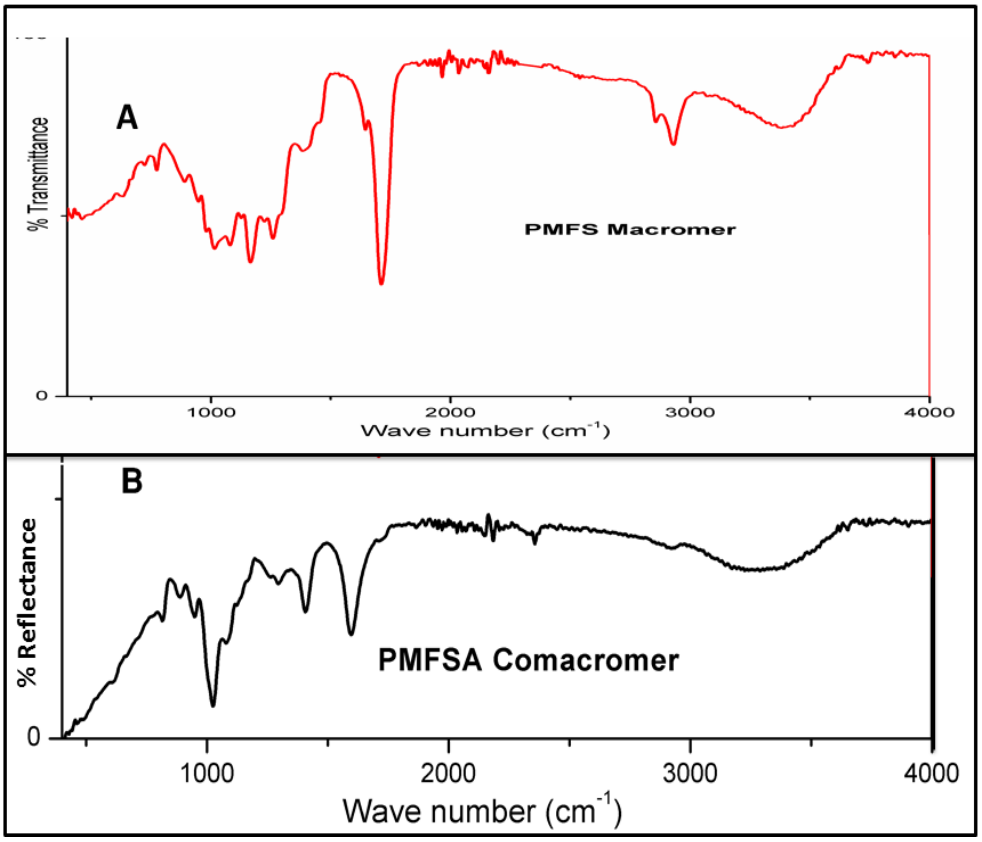

Figure. 4. FT-IR spectrum of poly(mannitol fumarate-co-sebacate)(PMFS) (A) and AT-IR spectrum of PMFSA graft comcaromer (B)

AT-IR spectrum of PMFSA graft comcaromer showed the broad spectrum of –OH groups of alginate and mannitol around 3300 cm^{-1}. The peaks appearing at ~1600 and ~1400 cm^{-1} are due to the asymmetric and symmetric stretching vibrations of the carboxyl groups. The peak around 2900 cm^{-1} indicates -OH bending suggesting mannitol fraction on the surface. The sharp peak appearing at 1020 cm^{-1} is due to the C-O-C stretching of alginate. The IR spectral analysis showed the presence of characteristic peaks revealing the effective formation of the macromer and comacromer.

The comcaromers were dissolved in minimum distilled water for the preparation of hydrogel scaffolds. The hydrogel scaffolds were prepared by crosslinking the alginate segments with calcium ions and the unsaturation of the polyesters with different vinyl

monomers. Of the twelve different hydrogel scaffolds from HPAS comcaromer, five were prepared using single vinyl crosslinkers. The vinyl crosslinkers used were methyl methacrylate (MMA), N N' methylene bis acrylamide (NMBA), 2-hydroxy ethyl methacrylate (HEMA), n-butyl methacrylate (BMA) and acrylic acid (AA) respectively for the bimodal hydrogel scaffolds HPAS-MMA, HPAS-NMBA, HPAS-HEMA, HPAS-BMA and HPAS-AA. Monomodal HPAS-No hydrogel scaffold was synthesized by crosslinking alginate fraction of the comcaromer with calcium ions by leaving the double bonds of PPF fraction in free form (Thankam and Muthu, 2013a), (Thankam and Muthu, 2013b). The details and scheme of the synthesis are given in the Figure-5.

The remaining six bimodal hydrogel scaffolds were prepared by crosslinking with two vinyl crosslinkers. HPAS was copolymerized with polyethylene glycol diacrylate (PEGDA) to form HPAS-P. Then the double bonds of PEGDA segments of HPAS-P was crosslinked with the above vinyl crosslinkers (MMA, AA, BMA, HEMA, NMBA) to form HPAS-PM, HPAS-PA, HPAS-PB, HPAS-PH and HPAS-PN respectively (Gnanaprakasam Thankam and Muthu, 2013a), (Thankam and Muthu, 2014b). The details and scheme of the synthesis are given in the Figure-6.

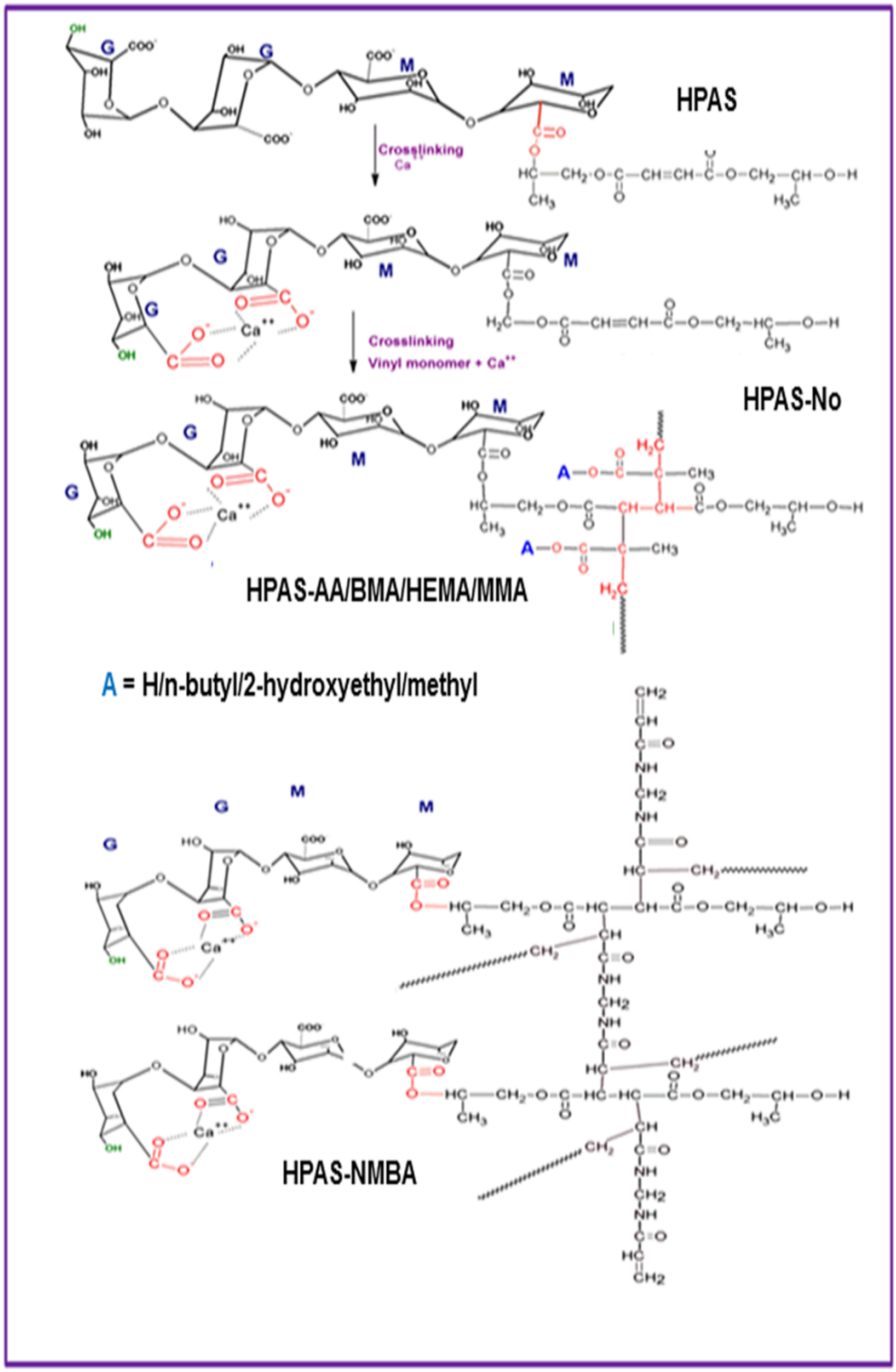

Figure-5. Synthesis of HPAS based monomodal (HPAS-No) and bimodal (HPAS-AA/BMA/HEMA/MMA/NMBA) hydrogel scaffolds using single vinyl crosslinkers.

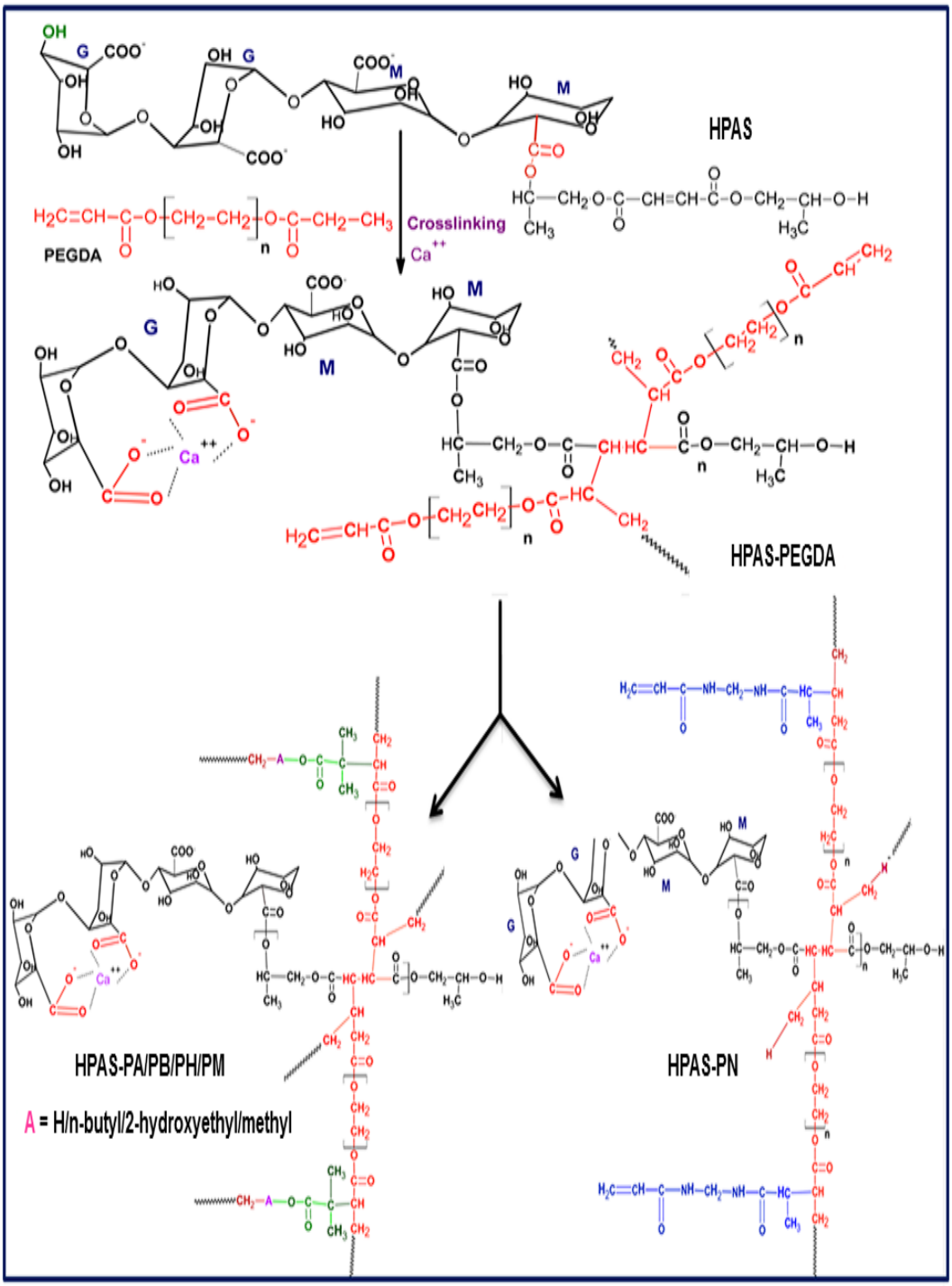

Figure-6. Synthesis of HPAS based bimodal hydrogel scaffolds using two vinyl crosslinkers, (HPAS-P/PA/PB/PH/PM/PN).

PMFSA comcaromer was crosslinked with divinyl crosslinkers like PEGDA, NMBA and diethylene glycol dimethacrylate (DEGDMA) to form corresponding PMFSA-PEGDA, PMFSA-NMBA and PMFSA-DEGDMA hydrogel scaffolds respectively. The details and scheme of the synthesis are given in the Figure-7.

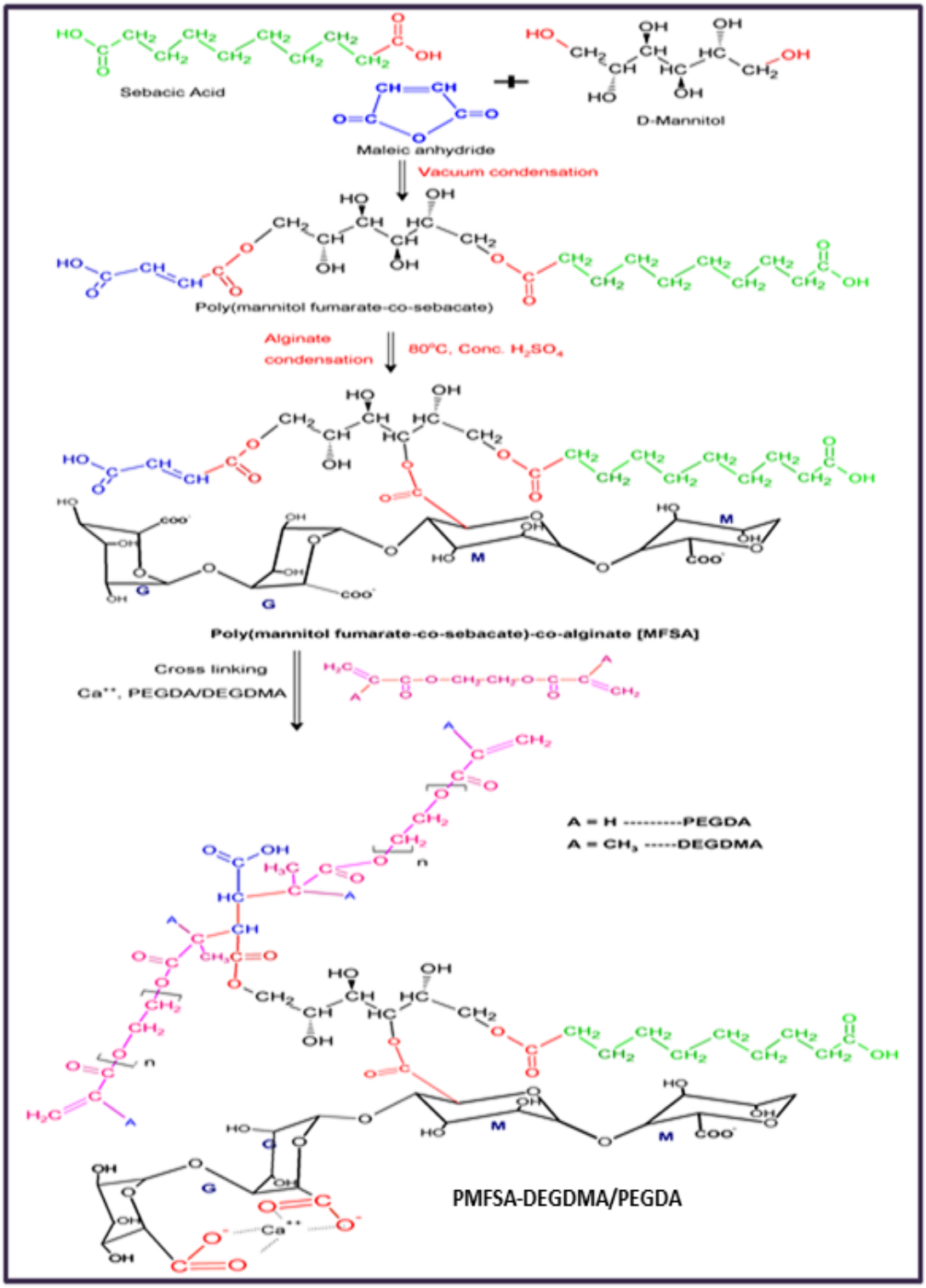

Figure-7. Synthesis PMFSA based bimodal (PMFSA-PEGDA / DEGDMA / NMBA) hydrogel scaffolds.

All the samples were freeze-dried overnight, and sterilized by EtO and stored aseptically for further studies.

10.2 Physiochemical characterizations of biosynthetic hydrogels

10.2.1 AT-IR spectral analysis

AT-IR spectral analyses of freeze-dried HPAS based hydrogels showed peaks around 1720 cm^{-1} (C-O stretching) of HT-PPF segments. The strong peaks appearing around 1600 and 1400 cm^{-1} are the asymmetric and symmetric stretching vibrations of the carboxylate group of alginate and also due to C=C stretching vibration of unsaturated fumarate groups of HT-PPF segment. The results are displayed in figures-8 and 9.

The strong peak appearing around 1030 cm^{-1} (C-O-C stretching) also indicates the presence of alginate. However the disappearance of peaks at 1291cm^{-1} (-OH bending), 1153 (C-O stretching), 979cm^{-1} (fumarate groups) for HT-PPF segments and the peak appearing around 1200cm^{-1} and 1030 cm^{-1} (C-O-C stretching) for alginate provide evidence for the presence of PPF and alginate on the surface of both hydrogels. The broad peak around 3200cm^{-1} indicated the presence of ample –OH groups of the alginate clustered on the surface of the hydrogel and due to the stretching of –NH groups in the case of NMBA crosslinked hydrogels.

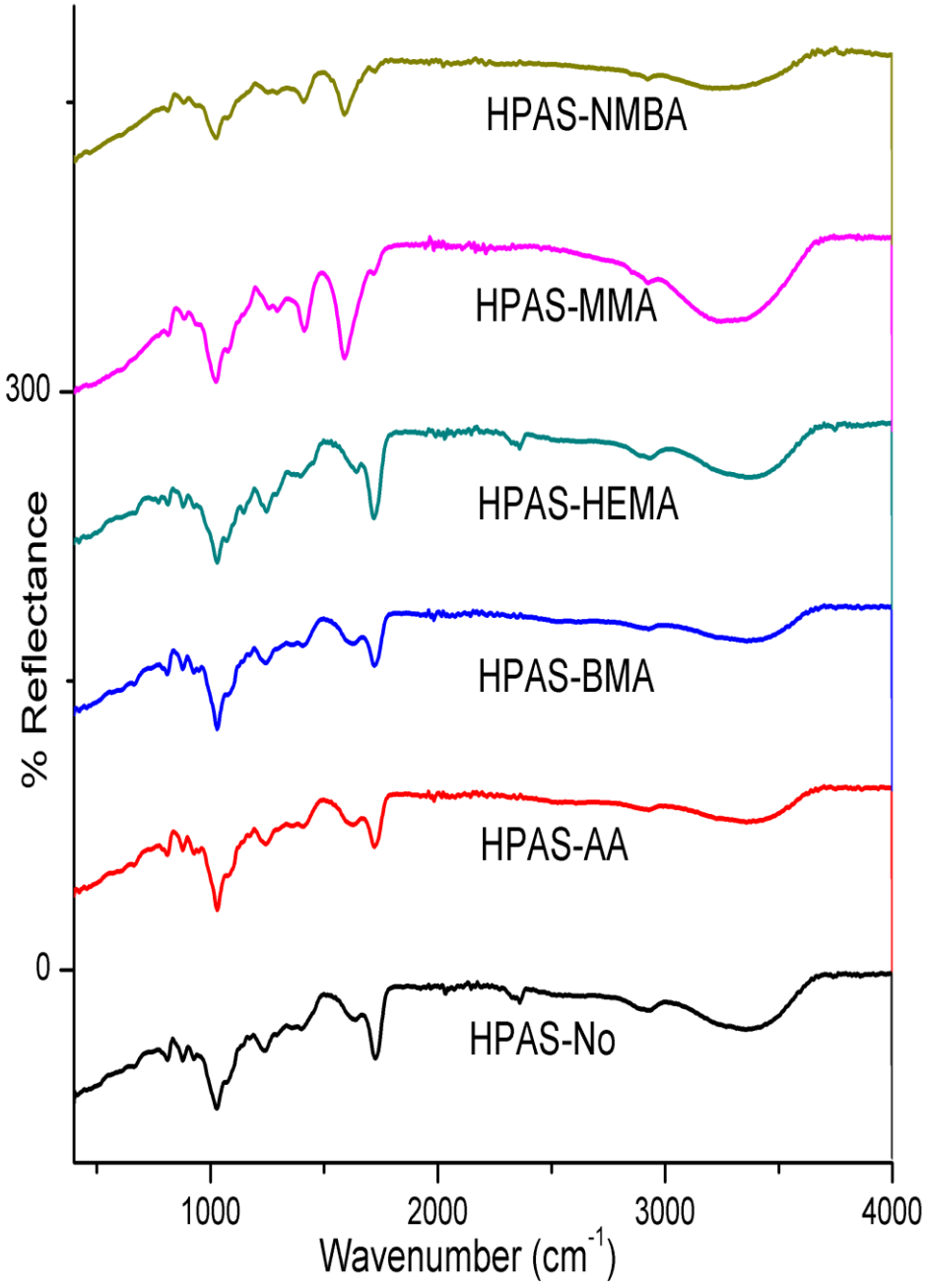

Figure 8.AT-IR spectra of freeze-dried monomodal (HPAS-No) and bimodal (HPAS-AA/BMA/HEMA/MMA/NMBA) hydrogel showing the characteristic peaks indicating effective condensation, ionic cross linking with Calcium and vinyl cross linking.

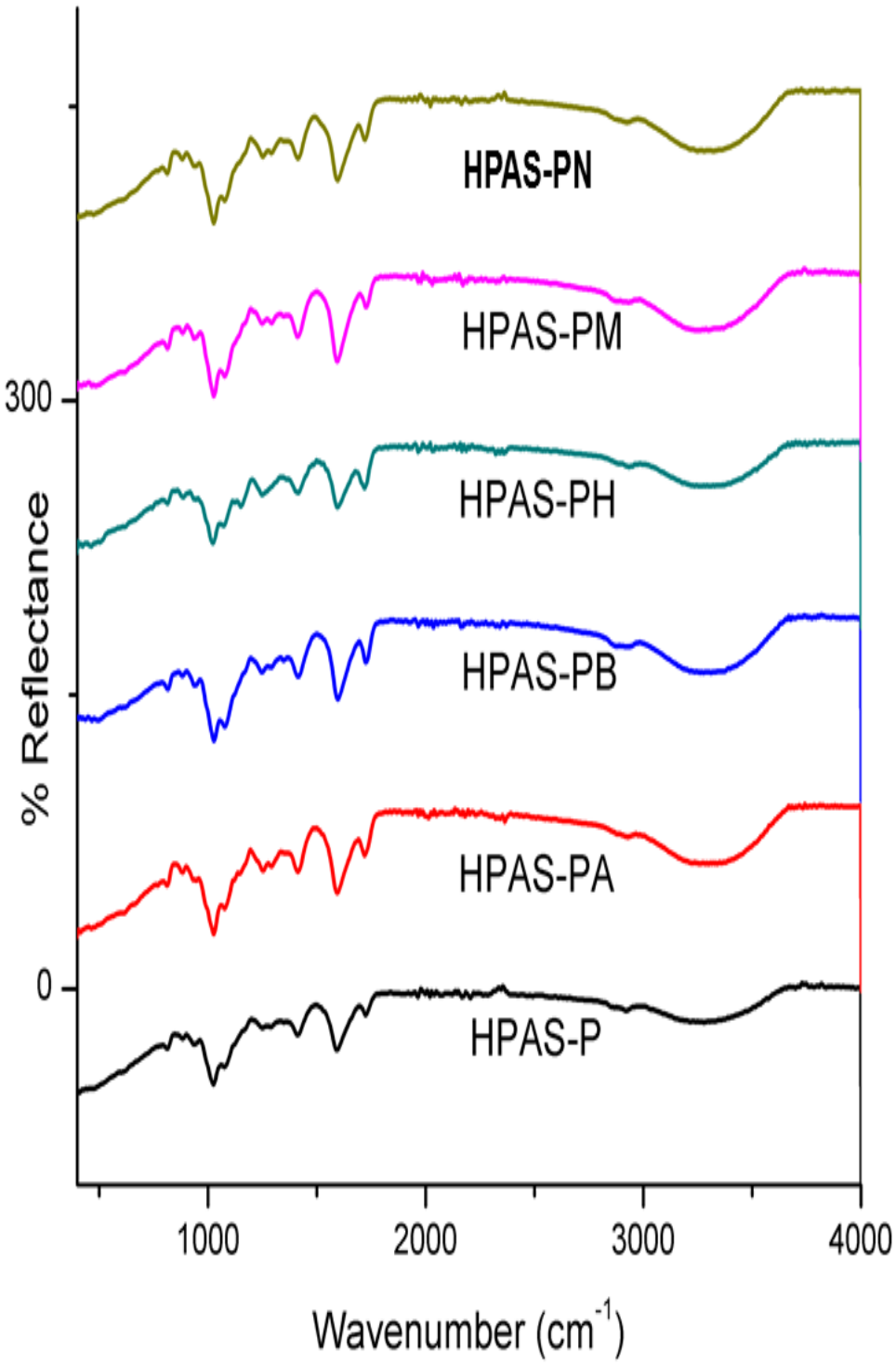

Figure 9. AT-IR spectra of freeze-dried HPAS based bimodal hydrogel scaffolds using two vinyl crosslinkers, (HPAS-P/PA/PB/PH/PM/PN) indicating effective cross linking.

The AT-IR spectral analysis of PMFSA based hydrogels also displayed similar peaks (Figure-10). The broad peaks around 3300 cm-1 imply the presence of –OH groups of alginate and mannitol. The peaks for asymmetric and symmetric stretching vibrations of the carboxyl groups, C-O-C stretching of alginate, C-O stretching and C=C stretching vibration of unsaturated fumarate groups of PMFS were also evident as in HPAS system.

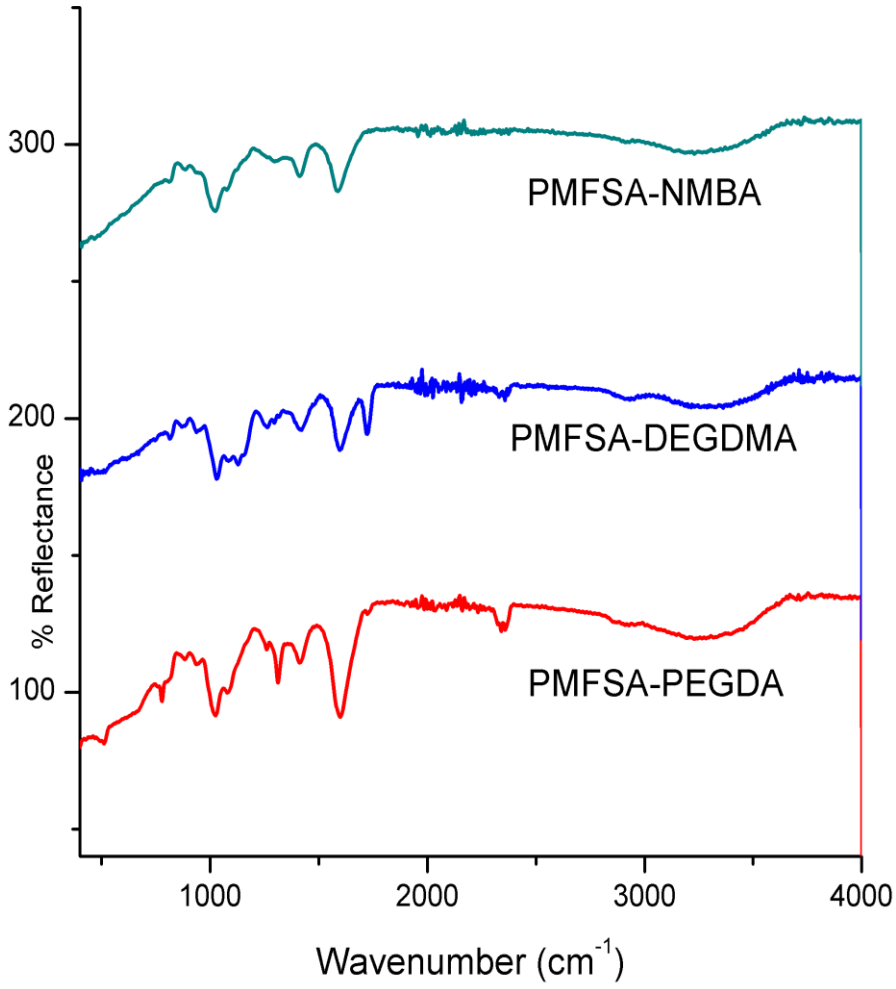

Figure 10.AT-IR spectra of freeze-dried PMFSA based bimodal (PMFSA-PEGDA/DEGDMA/NMBA) hydrogel scaffolds

10.2.2 Equilibrium water content (EWC) and % swelling

The EWC and % swelling for the HPAS and PMFSA based hydrogel are given in the table-2. From the results, it was clear that the single crosslinker based HPAS scaffolds showed relatively lower swelling and EWC. HPAS-PEGDA based hydrogels and PMFSA based hydrogels were superior in this aspect with a EWC greater than 60%. However, HPAS-PM and PMFSA-PEGDA hydrogels were found to have swelling values greater than 400% and EWC more than 80%.

Table-2. Equilibrium water content, % swelling and contact angle measurements of hydrogels

Hydrogels	**% Swelling**	**EWC**	**Advancing angle**	**Receding angle**
HPAS-No	164.06 ± 3.54	62.13 ± 0.5	51.66 ± 14.59	51.75 ± 14.57
HPAS-AA	188.49± 16.8	65.23± 2.02	37.17 ± 9.2	36.45 ± 10.73
HPAS-BMA	74.42 ± 4.61	42.63 ± 1.53	47.44 ± 9.11	47.2 ± 9.61
HPAS-HEMA	61.44 ± 18.35	37.46 ± 6.21	50.38 ± 2.88	50.67 ± 2.84
HPAS-MMA	59.06 ± 1.17	37.13 ± 0.46	63.34 ± 5.3	62.21 ± 4.87
HPAS-NMBA	135.47 ± 9.15	57.48 ± 1.58	55.32 ± 1.07	55.55 ± 1.19
HPAS-P	157.48 ± 11.94	61.12 ± 1.79	38.94 ± 3.99	43.42 ± 2.42
HPAS-PA	273.35 ± 22.29	73.36 ± 1.77	40.89 ± 4.69	43.7 ± 2.39
HPAS-PB	371.69 ± 2.55	78.76 ± 0.99	35.03 ± 2.8	35.8 ± 2.6
HPAS-PH	260.62 ± 17.24	72.22 ± 1.33	38.87 ± 2.86	39.63± 2.81
HPAS-PM	444.72 ± 54.11	81.49 ± 1.88	32.67 ± 2.9	34.28 ± 2.94
HPAS-PN	267.16 ± 67.58	71.95 ± 5.13	33.06 ± 3.68	34.01 ± 3.36
PMFSA-DEGDMA	241.49 ± 41.35	70.34 ± 3.52	57.21 ± 4.29	58.15 ± 3.83
PMFSA-PEGDA	400.5 ± 28.5	79.95 ± 1.14	55.33 ± 5.95	56.16 ± 5
PMFSA-NMBA	228.71 ± 9.14	69.36 ± 0.51	50.67 ± 6.05	51.58 ± 6.53

10.2.3 Surface hydrophilicity/hydrophobicity evaluation by contact angle

The surface properties of hydrogels play a crucial role in cell growth and function in tissue engineering. The surface hydrophilicity and wettability of the hydrogel

scaffolds were determined by water contact angle measurements. Both the advancing and receding angles of the present two batch of hydrogels showed values around 30-60^{o} revealing their amphiphilic nature (Table-2). The similarity in advancing and receding angles is an indication of the absence of phase transition of surface functional groups of the hydrogels.

10.2.4 Evaluation of surface morphology and average pore diameter by ESEM

The ESEM images of the hydrogel scaffolds displayed their characteristic morphology. A significant increase in pore length was observed for HPAS-AA and HPAS-NMBA hydrogels (Figure-11, Table-3).

However, the PEGDA crosslinked HPAS based hydrogels and PMFSA based hydrogels displayed relatively lower pore length in the range 5-15 μm. This is favourable for the invading cells for penetration by availing the metabolites from the medium circulating through the pores.

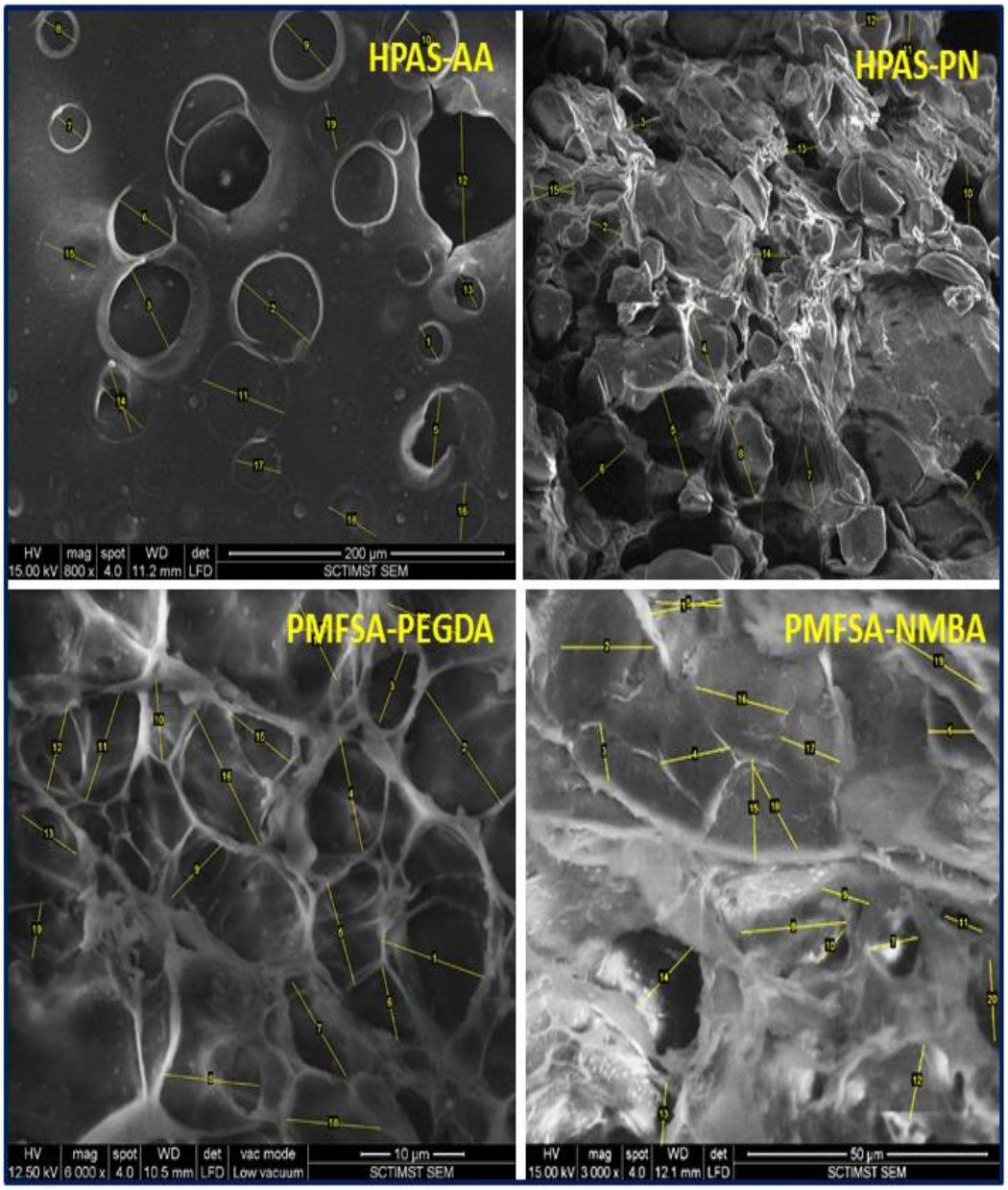

Figure-11. The average pore length of hydrogel scaffolds as determined by ESEM after ImageJ analysis showing the average pore length in the range 5-15 µm.

Table-3. The average pore length of hydrogel scaffolds determined by ESEM

Hydrogels	**Pore length (μm)**
HPAS-AA	36.91 ± 8.8
HPAS-NMBA	45.00 ± 7.98
HPAS-P	6.01 ± 1.32
HPAS-PA	10.18 ± 3.02
HPAS-PB	8.00 ± 2.86
HPAS-PM	16.86 ± 4.72
HPAS-PN	9.66 ± 2.91
PMFSA-DEGDMA	5.06 ± 0.73
PMFSA-PEGDA	7.50 ± 1.95
PMFSA-NMBA	14.11 ± 3.91

10.2.5 Mechanical characterizations

The tensile properties of HPAS and PMFSA based hydrogels are given in Table 4. HPAS-AA possessed lower strength among the HPAS system. PMFSA-DEGDMA had lower tensile value and elongation. The Youngs modulus was greater for HPAS-PN, while others except HPAS-AA possessed values greater than 1MPa. These hydrogels were able to withstand appreciable fatigue life (Table 5). PMFSA based hydrogels predominated in this aspect. Mechanical studies revealed that the hydrogel samples could tolerate appreciable force.

Table-4. Tensile properties of HPAS and PMFSA based hydrogels

Hydrogels	**Tensile Strength (Kpa)**	**% Elongation**	**Modulus (kPa)**
HPAS-No	2399 ± 151	133.2 ± 17.31	3783 ± 345
HPAS-AA	187 ± 19	24.43 ± 3.07	816 ± 48
HPAS-BMA	316 ± 51	39.85 ± 15.27	1508 ± 424
HPAS-HEMA	709 ± 55	84.77 ± 12.91	1499 ± 250
HPAS-MMA	2446 ± 146	136.2 ± 8.66	2538 ± 338
HPAS-NMBA	1689 ± 349	86.97 ± 15.24	3350 ± 122
HPAS-P	581 ± 165	56.33 ± 9.54	1533 ± 219
HPAS-PA	886 ± 126	116.83 ± 2.47	1155 ± 201
HPAS-PB	867 ± 126	97.86 ± 15.52	1235 ± 70
HPAS-PH	1051 ± 140	105.32 ± 8.65	2002 ± 311
HPAS-PM	615 ± 108	79.66 ± 10.38	1212 ± 200
HPAS-PN	1640 ± 173	61.54 ± 9.87	6032 ± 1441
PMFSA-DEGDMA	266 ± 23	24.16 ± 4.14	2455 ± 599
PMFSA-PEGDA	525 ± 60	53.29 ± 6.46	2213 ± 464
PMFSA-NMBA	392 ± 44	34.3 ± 3.5	2766 ± 539

Table-5. Fatigue life of HPAS and PMFSA based hydrogels

Hydrogels	**No. of cycles of cyclic strectching before breaking**
HPAS-AA	>52000
HPAS-P	> 30,000
HPAS-PA	>70,000
HPAS-PB	> 3,000
HPAS-PM	> 26,000
HPAS-PN	>8,000
PMFSA-DEGDMA	> 6,00,000
PMFSA-PEGDA	>7,30,000

10.2.6 Biodegradation of hydrogels

The bio-stability of the HPAS and PMFSA based hydrogel scaffolds were tested in both DMEM containing 10% FBS and in PBS at physiological conditions. In DMEM the solubility of the three hydrogel scaffolds were monitored qualitatively for a period of 1 week. Five scaffolds from HPAS system, HPAS-No, HPAS-BMA, HPAS-MMA, HPAS-HEMA and HPAS-PH were stable up to 1-week time. All the other hydrogel scaffolds were stable for more than 1 week and were analyzed for the long-term degradation studies in PBS (Figure-12).

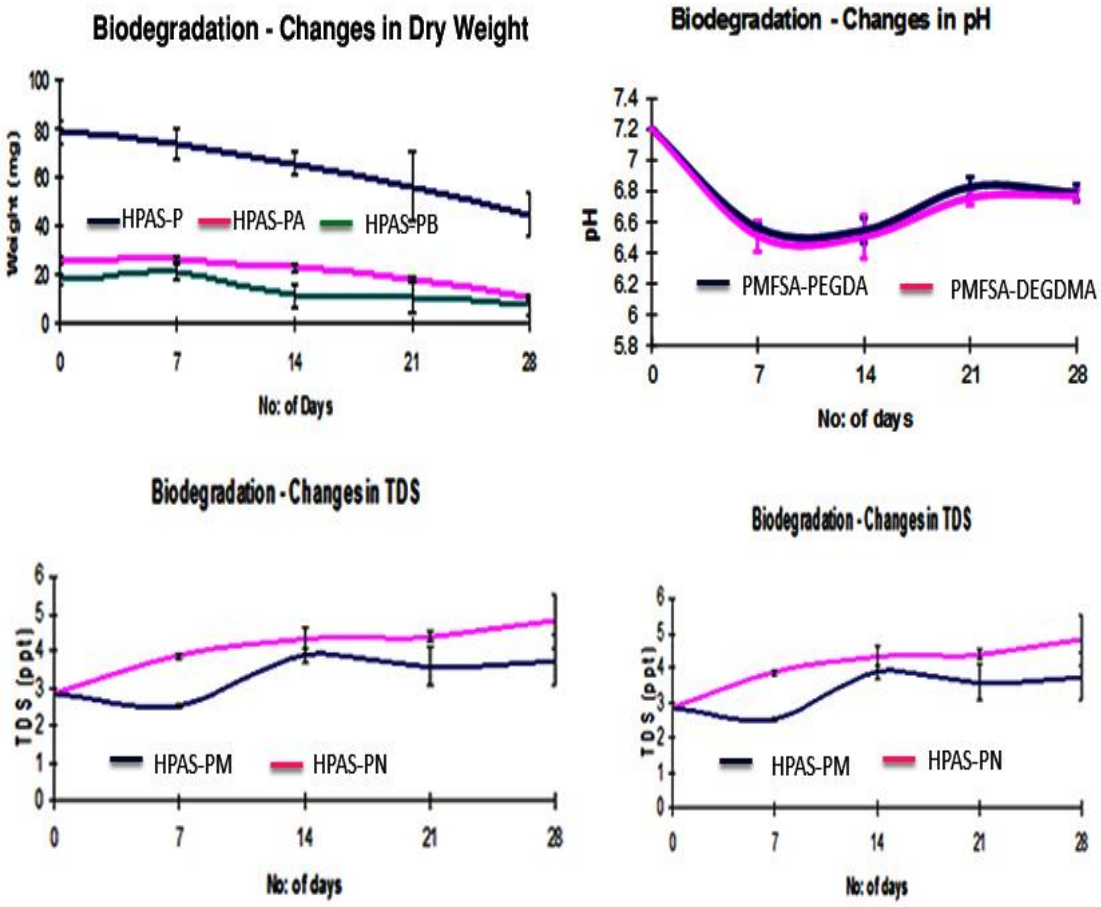

Figure-12. Biodegradation profile of hydrogels showing progressive decrease in dry weight, pH and changes in conductivity and TDS

The dry weight of the scaffolds was found to be decreased progressively during the course of time. The pH of the PBS was dropped to slightly acidic range for all the scaffolds. This trend is in agreement with total dissolved solids (TDS) and conductivity during the one-week duration. The total dissolved solids (TDS) and conductivity were increased appreciably on progression towards one month.

10.2.7 Thermal evaluation for determining the water status of hydrogels

Water swollen HPAS and PMFSA based hydrogel scaffolds were analyzed for thermal properties to assess the nature of water present in the hydrogels. The DSC

cooling curves of hydrogel samples displayed exothermic peak due to crystallization of freezing water and heating curves showed endothermic peak due to the melting of frozen water (Figure-13).

The freezing water content (W_f) was calculated from the enthalpy of melting endotherm and enthalpy of melting of pure water ($334Jg^{-1}$) using the equation $W_f = (\Delta H_{Endo}/\Delta H_w)$ X 100 where ΔH_{Endo} is the enthalpy of melting of frozen water in the hydrogel calculated from the area under the endothermic peak, ΔH_w enthalpy of melting of frozen pure water ($334Jg^{-1}$). The non-freezing bound water content (W_{nb}) was calculated from the difference between the equilibrium water content (EWC) and freezing water content (W_f). The non-freezing bound water content of all the hydrogels fall in the range of 30-65% except to that of HPAS-PA. However, the freezing water content varied significantly among the hydrogels. The results are displayed in table-7.

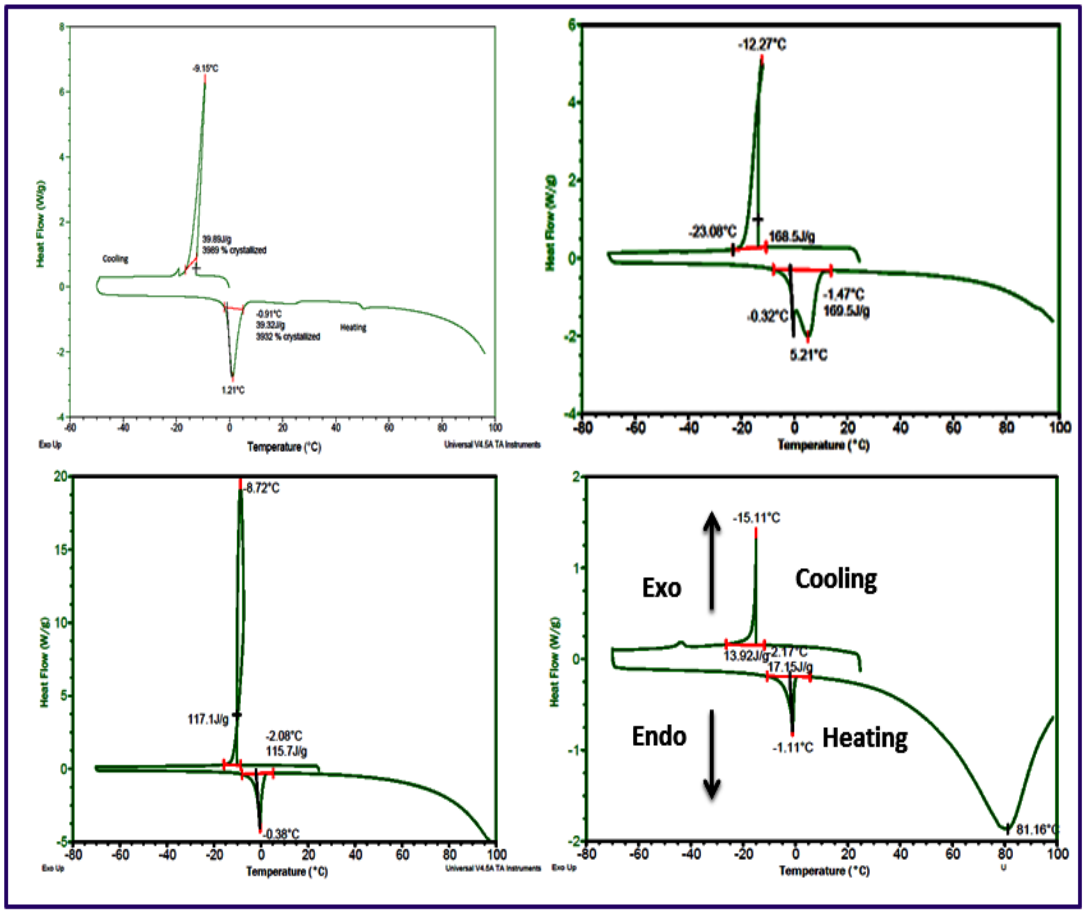

Figure-13. DSC thermogram of HPAS and PMFSA based hydrogels showing crystallization of freezing water and melting of frozen water

Table-7. Determination of the freezing and non-freezing water content in hydrogels.

Hydrogels	**ΔH(endo)(J/g)**	**Freezing water (%)**	**Non-freezing water (%)**
HPAS-NMBA	121.7	21.01	36.47
HPAS-AA	39.32	11.77	53.46
HPAS-P	57.01	17.07	44.05
HPAS-PA	169.5	50.75	22.61
HPAS-PB	47.4	14.19	64.57
HPAS-PM	76.69	58.74	29.26
HPAS-PN	97.74	29.26	42.69
PMFSA-DEGDMA	90.23	26.95	43.39
PMFSA-PEGDA	117.1	34.64	45.31

PMFSA-NMBA	17.15	5.13	64.23

4.3. Studies on cell-material interaction

4.3.1. Assessment of hemocompatibility

The hydrogels were tested for their hemocompatibility by RBC aggregation assay and hemolytic assay. The hemolysis assay is based on RBC lysis and the release of hemoglobin to the surrounding medium. The hemolytic potential of both the hydrogel systems were found to be negligible and fell within the acceptable limit of 5% (Table-8).

Table-8. Determination of hemolytic potential of hydrogels

Hydrogels	**% Hemolysis**	**Hydrogels**	**% Hemolysis**
HPAS-No	0.35 ± 0	HPAS-PB	0.35 ± 0.01
HPAS-AA	0.59 ± 0.4	HPAS-PH	0.71 ± 0.02
HPAS-BMA	0.94 ± 0.2	HPAS-PM	0.71 ± 0.02
HPAS-HEMA	0.35 ± 0	HPAS-PN	0.71 ± 0.02
HPAS-MMA	1.19 ± 0.55	PMFSA-DEGDMA	3.71 ± 0.04
HPAS-NMBA	0.47 ± 0.2	PMFSA-PEGDA	3.57 ± 1.2
HPAS-P	0.35 ± 0.01	PMFSA-NMBA	2.3 ± 0.61
HPAS-PA	0.71 ± 0.02	--	--

The microscopic analysis of the RBCs treated with hydrogel extracts were failed to aggregate revealing their hemocompatibility (Figure-14).

The thrombogenic potential of the hydrogels was evaluated by ESEM analysis after incubating with PRP (Figure-15). The images showed no platelet adhesion to the hydrogel surface revealing the non-thrombogenic effects of the hydrogels.

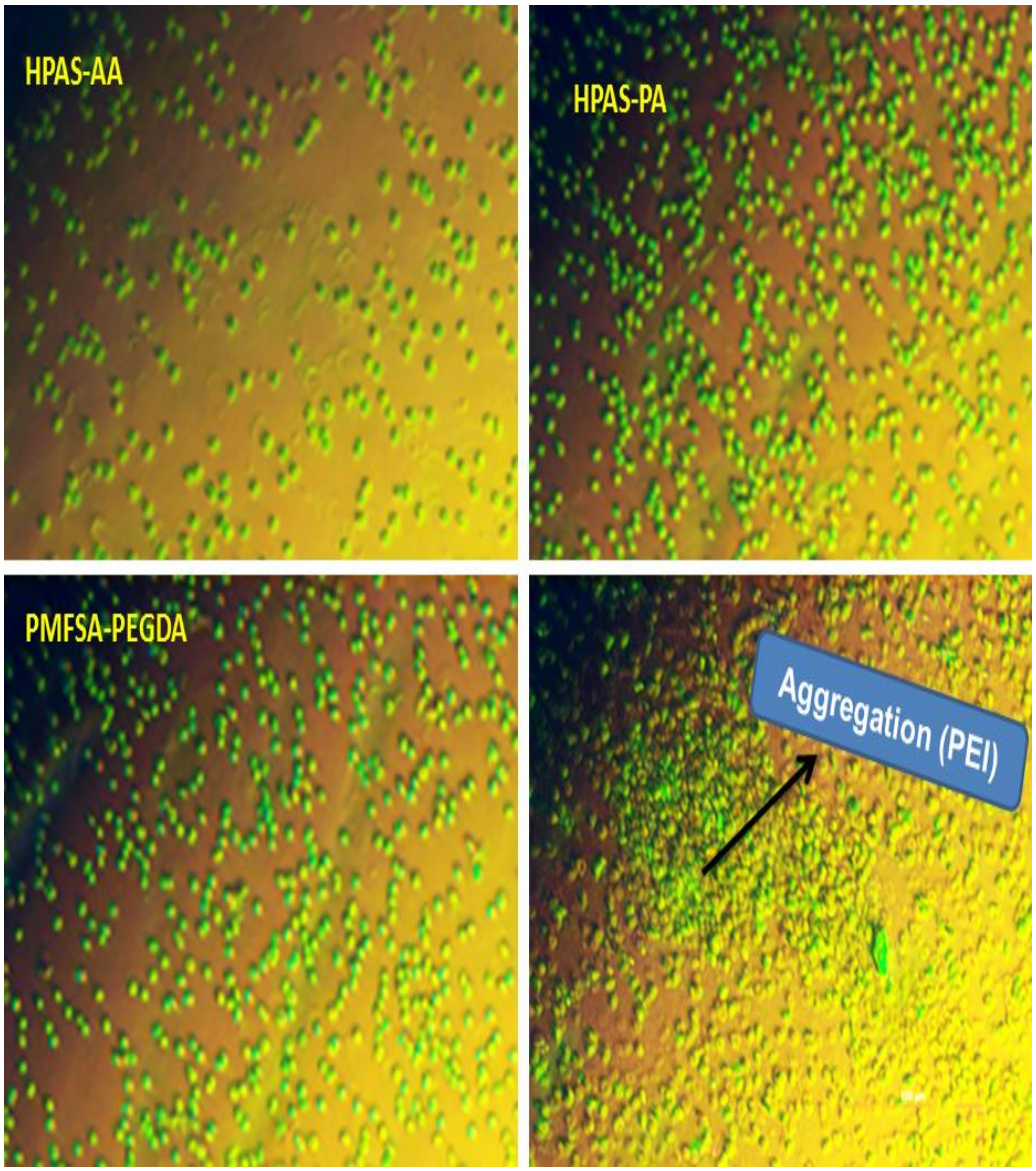

Figure-14. Phase contrast microscopic images showing the absence of aggregation of RBC in HPAS-AA, HPAS-PA and PMFSA-DEGDMA on comparison with positive control (PEI).

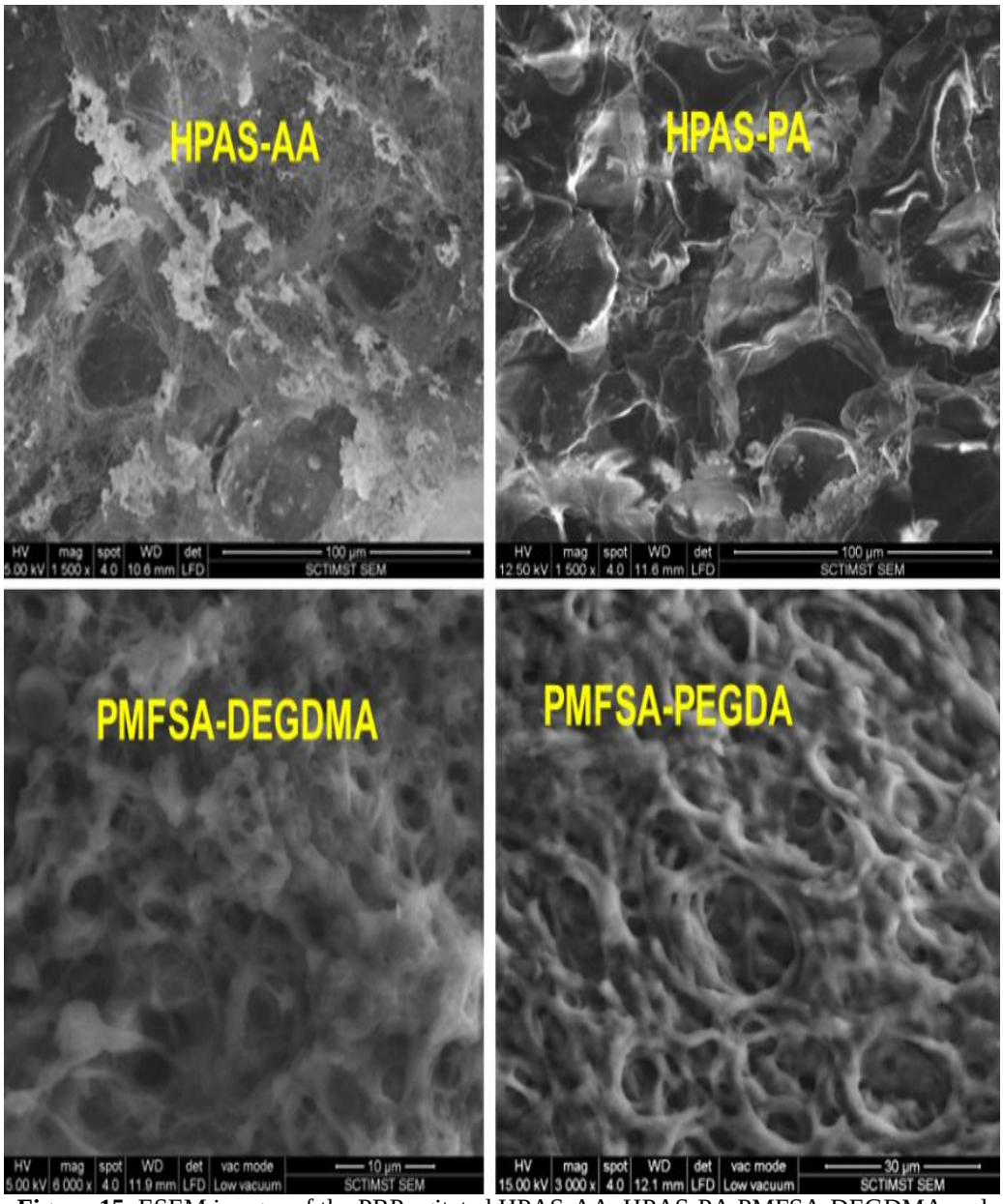

Figure-15. ESEM images of the PRP agitated HPAS-AA, HPAS-PA PMFSA-DEGDMA and PMFSA-PEGDA hydrogels showing absence of platelet adhesion

4.3.1.1.Plasma protein adsorption

The present hydrogel scaffold systems were subjected for plasma protein exposure at physiological conditions. All the hydrogels based on HPAS, except HPAS-

PB, HPAS-PH and HPAS-PM, exhibited appreciable plasma protein adsorption (Table-9).

Table-9. Protein adsorption on HPAS based hydrogels

Hydrogels	**% Protein Adsorption**
HPAS-No	35.36
HPAS-AA	50.09
HPAS-BMA	37.57
HPAS-HEMA	40.88
HPAS-MMA	26.7
HPAS-NMBA	43.09
HPAS-P	33.15
HPAS-PA	46.85
HPAS-PB	2.09
HPAS-PH	4.45
HPAS-PM	3.92
HPAS-PN	26.7

Figure-16. SDS-PAGE analysis of the plasma proteins after adsorption on the HPAS and PMFSA based hydrogels with respect to albumin standard and plasma control.

SDS-PAGE analysis showed that the majority of the protein adsorbed on the hydrogels constitutes the bands corresponding to the molecular weight of albumin (Figure-16**)**. From this, it can be confirmed that albumin adsorption is prominent in these hydrogels.

4.3.2. Assessment of cytocompatibility

The cytotoxicity of the hydrogels was determined by MTT assay and direct contact assay using L929 fibroblast cells. All the hydrogels were incubated with culture medium for 48 h and L929 cells were grown on this medium for another 48 h. As per the assay both PMFSA and HPAS based hydrogel systems displayed viability more than 80% (Figure-17) indicating the absence of the release of any toxic particles from the hydrogels.

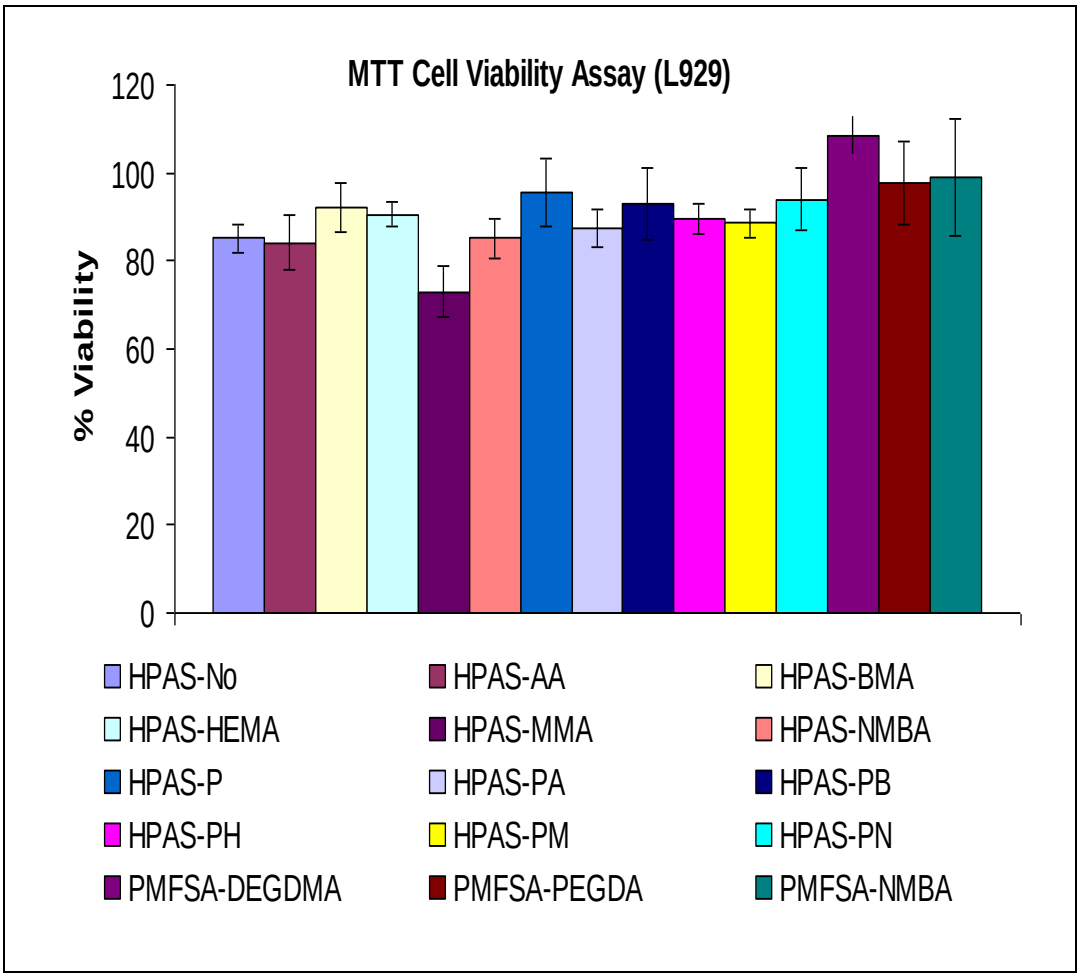

Figure-17. MTT cell viability assay of L929 cells grown on hydrogel extracts showing viability greater than 85% indicating the absence of toxic leaching products.

In order to observe the real time morphologies of the cells upon contact with the hydrogels, the direct contact assay was carried out. The phase contrast images of the L929 cells grown with the hydrogels displayed no changes in their normal morphology when compared with the control, confirming the non-toxic nature (Figure-18).

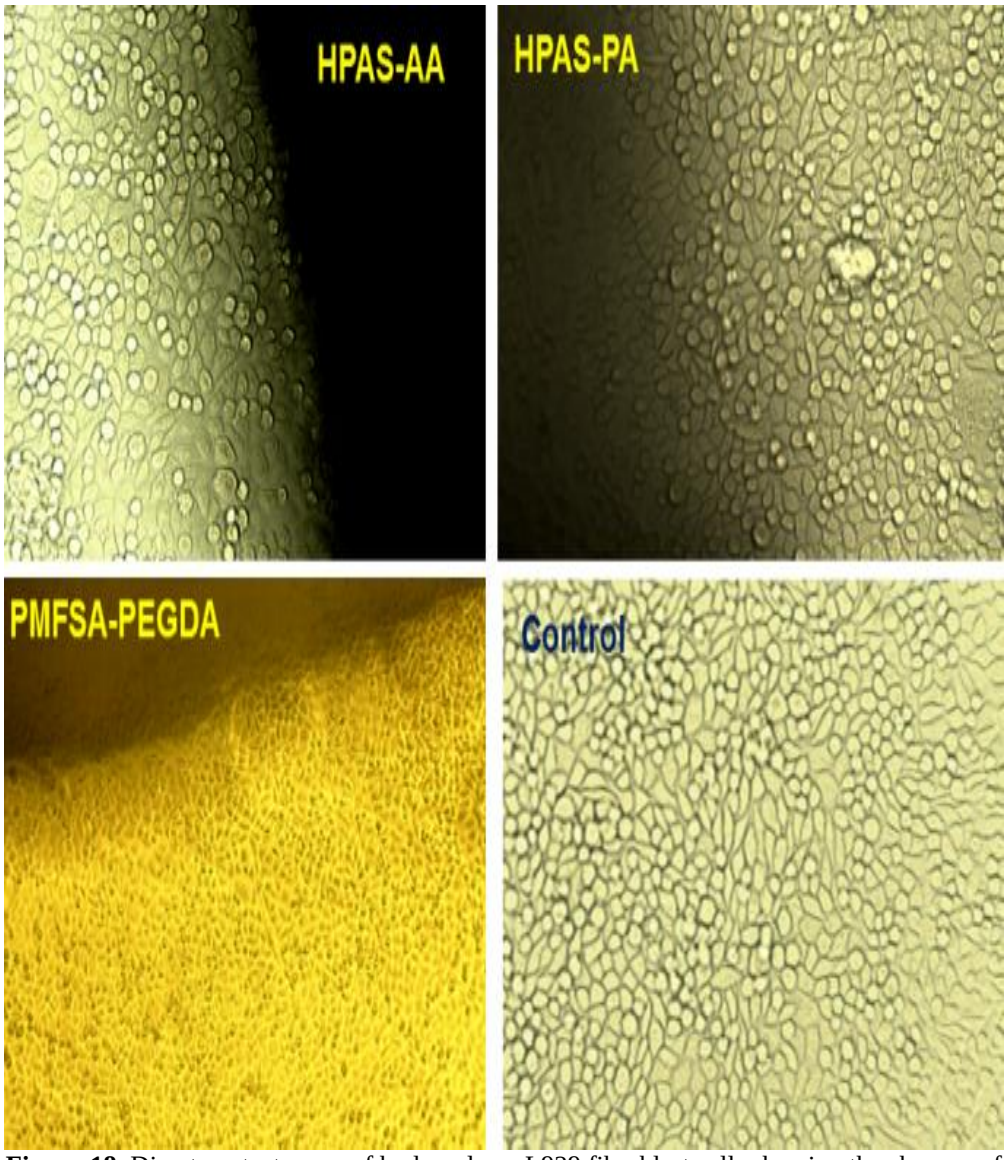

Figure-18. Direct contact assay of hydrogels on L929 fibroblast cells showing the absence of characteristic changes in cell morphology revealing the non toxic nature of the hydrogels.

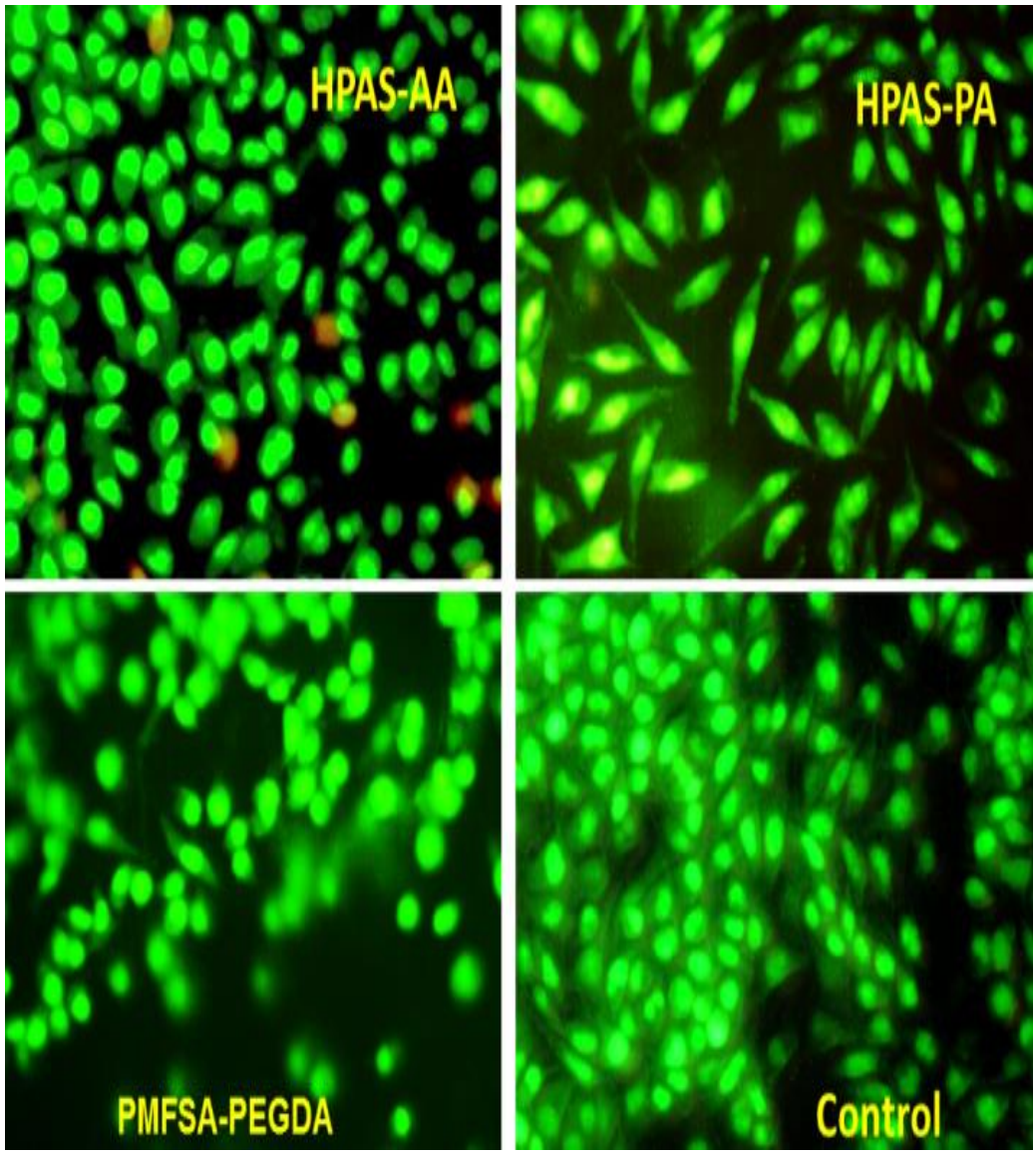

Figure-19. Live/dead assay of L929 cells grown on hydrogel scaffolds on comparison with control showing non-apoptotic nature.

Live/dead assay also brought out that most of the cells were non-apoptotic showing the healthy well-being of the cells grown on all the hydrogels after five days, which was evident from the presence of mostly green nucleus (Figure-19).

4.3.3. Evaluation of genocompatibility by comet assay

The determination of DNA damage of cells grown on medium extracted with hydrogel materials give a clear idea about the genotoxic potential of the hydrogel scaffolds. The comets resulting from exposure to the extracts of the test hydrogels, HPAS-No, HPAS-MMA, HPAS -HEMA, and HPAS-BMA did not differ from that of the control. With control and test hydrogels the relatively undamaged cells give comets consisting of a compact head without any prominent tail, indicating double-stranded intact DNA (Figure-20). The mean comet lengths for the L929 exposed to test hydrogels as compared with control are presented in Table-10. For test hydrogels, DNA in the head region is more than 99% and in the tail region, it is less than 1%. The diameter of the head region is also maximum.

Table-10. Determination of genotoxic effects of HPAS based hydrogels by comet assay

Samples (n=30)	**Head diameter (px)**	**% DNA in Head**	**% DNA in Tail**
Control	22.78 ± 3.5	99.72 ± 0.38	0.62 ± 0.33
HPAS-BMA	23.25 ± 4.88	99.38 ± 0.7	0.62 ± 0.7
HPAS-HEMA	24.1 ± 4.53	99.5 ± 0.55	0.69 ± 0.53
HPAS-MMA	24.5 ± 5.92	99.37 ± 0.64	0.91 ± 0.61
HPAS-No	26.4 ± 3.62	99.49 ± 0.63	0.89 ± 0.62

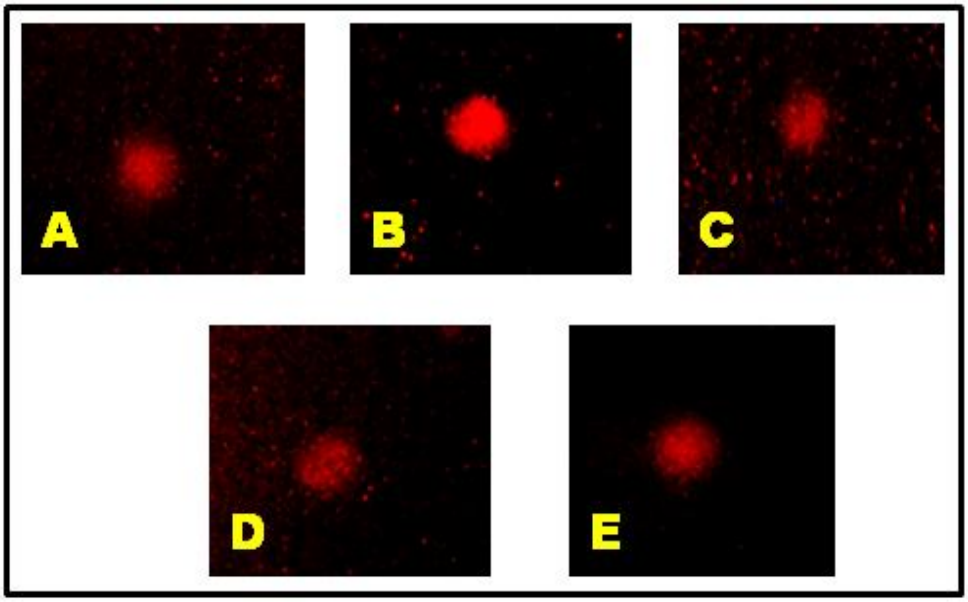

Figure-20. Representative images of L929 cells after comet assay. Control (A), HPAS-BMA (B),HPAS-HEMA (C), HPAS-MMA (D) and HPAS-No (E).
The assay reveals absence of genotoxicity.

4.4. Biological responses of hydrogels for cardiac tissue engineering

4.4.1. Cell infiltration and long-term viability

The fibroblast cells were found to be effectively penetrated inside the present hydrogel networks that resulted in a sustained viability as determined up to one month. Both the hydrogel systems were able to maintain the better viability of fibroblasts. The fibroblast cell infiltration on the PMFSA based hydrogels was quantified for 1 month and for HPAS based hydrogels for 18 days (Figure-21).

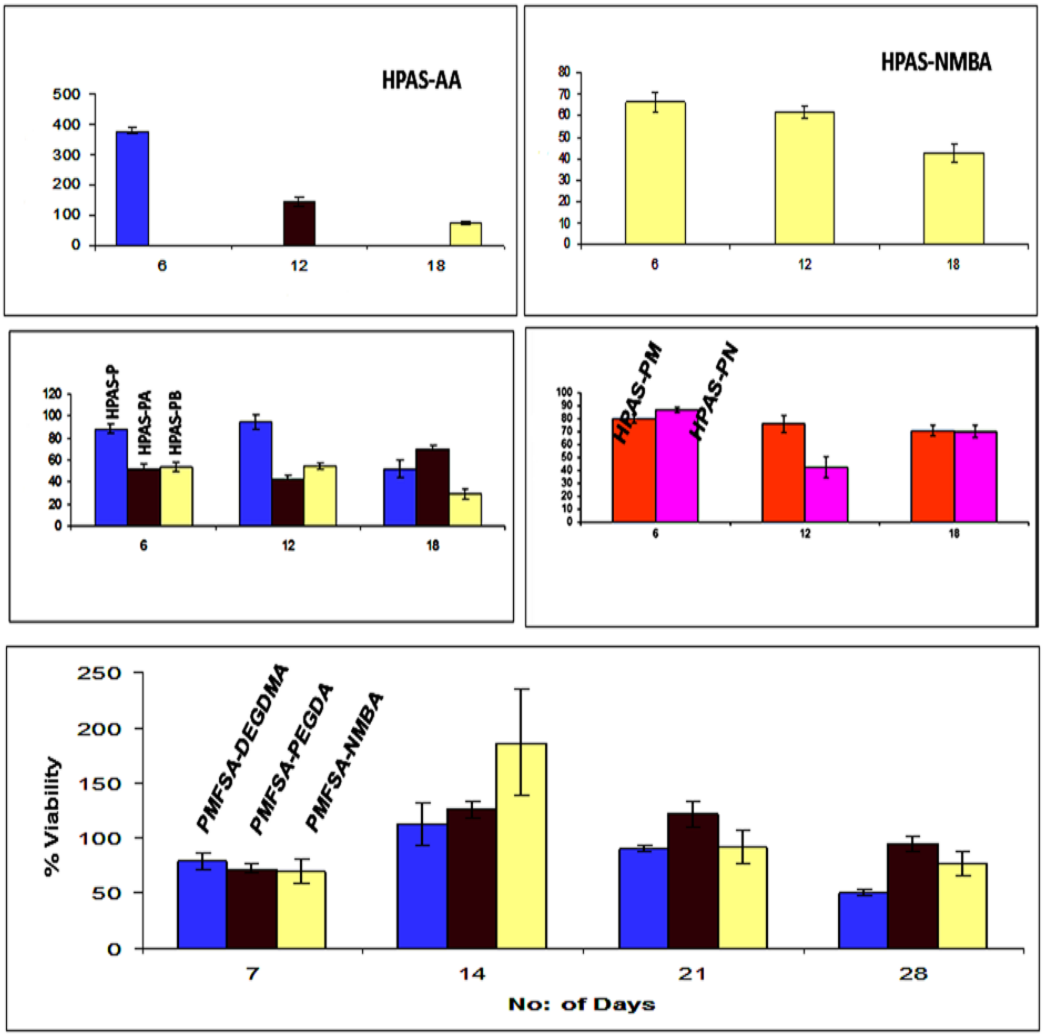

Figure-21. Fibroblast cell infiltration and long-term viability on hydrogels

Even though both the hydrogel systems displayed appreciable cell penetration, the extend of penetration was higher in PMFSA based hydrogel system than that of HPAS ones. PMFSA-PEGDA hydrogels maintained more than 90% viability after 1 month. Of the HPAS based hydrogels, HPAS-AA and HPAS-PA predominated in this aspect while HPAS-P, HPAS-PM, HPAS-PN and HPAS-NMBA were also displayed appreciable long-term viability response.

4.4.2. Morphologically modified HPAS-P based hydrogels for improved biological performance

Modification of morphology by uniaxial cyclic stretching of HPAS-PEGDA based hydrogels could introduce unidirectional porosity (MM-Hydrogels). The cyclic stretching introduced complex macro and micro interconnected pores on MM-Hydrogels, which was evident from ESEM analysis. The pore length was found to be increased after stretching as quantified by ImageJ software (Table-11).

Table-11. Physiochemical properties of MM-Hydrogels

Parameters (n=6)	**ALGP-P**	**ALGP-PA**	**ALGP-PB**	**ALGP-PM**	**ALGP-PN**
Onset of melting temp. of freezing water (^{o}C)	-0.60	-0.55	-1.31	-0.37	-1.38
Enthalpy of melting of freezing water (Jg^{-1})	162	166.2	64.2	125.5	93.47
Advancing contact angle (deg)	44.06 ± 6.89	43.42 ± 2.42	50.23 ± 5.2	38.21 ± 11.34	42.77 ± 5.49
Receding contact angle (deg)	40.89 ± 4.69	43.7 ± 2.39	50.32 ± 6.21	39.18 ± 11.11	43.55 ± 5.64
Swelling (%) (P<0.01)	264.4 ± 37.33	252.68 ± 114.96	77.49 ± 3	202.16 ± 8.89	137.7 ± 9.58
EWC (P<0.001)	72.33 ± 3.05	69.53 ± 8.8	43.65 ± 0.95	66.88 ± 0.98	57.77 ± 1.52
Freezable water content (W_f) (%)	48.5	49.76	19.16	37.43	27.99
Non freezing water content (W_{nf}) (%)	23.83	19.77	24.49	29.45	29.78
Pore length (µm) (n=20) (P<0.001)	6.01 ± 1.32	10.18 ± 3.02	8.00 ± 2.86	16.86 ± 4.72	9.66 ± 2.91
Pore length (µm) (n=20) (MM-Hydrogels) (P<0.001)	13.11 ± 4.16	14.89 ± 6.18	7.76 ± 2.03	20.64 ± 3.14	11.26 ± 5.03

There was no considerable difference in other physiochemical parameters were observed among the MM-Hydrogels on comparing with unmodified hydrogels. Biological performance was found to be enhanced in MM-Hydrogels, which was evident from the increased collagen deposition and cell viability and infiltration (Figure-22).

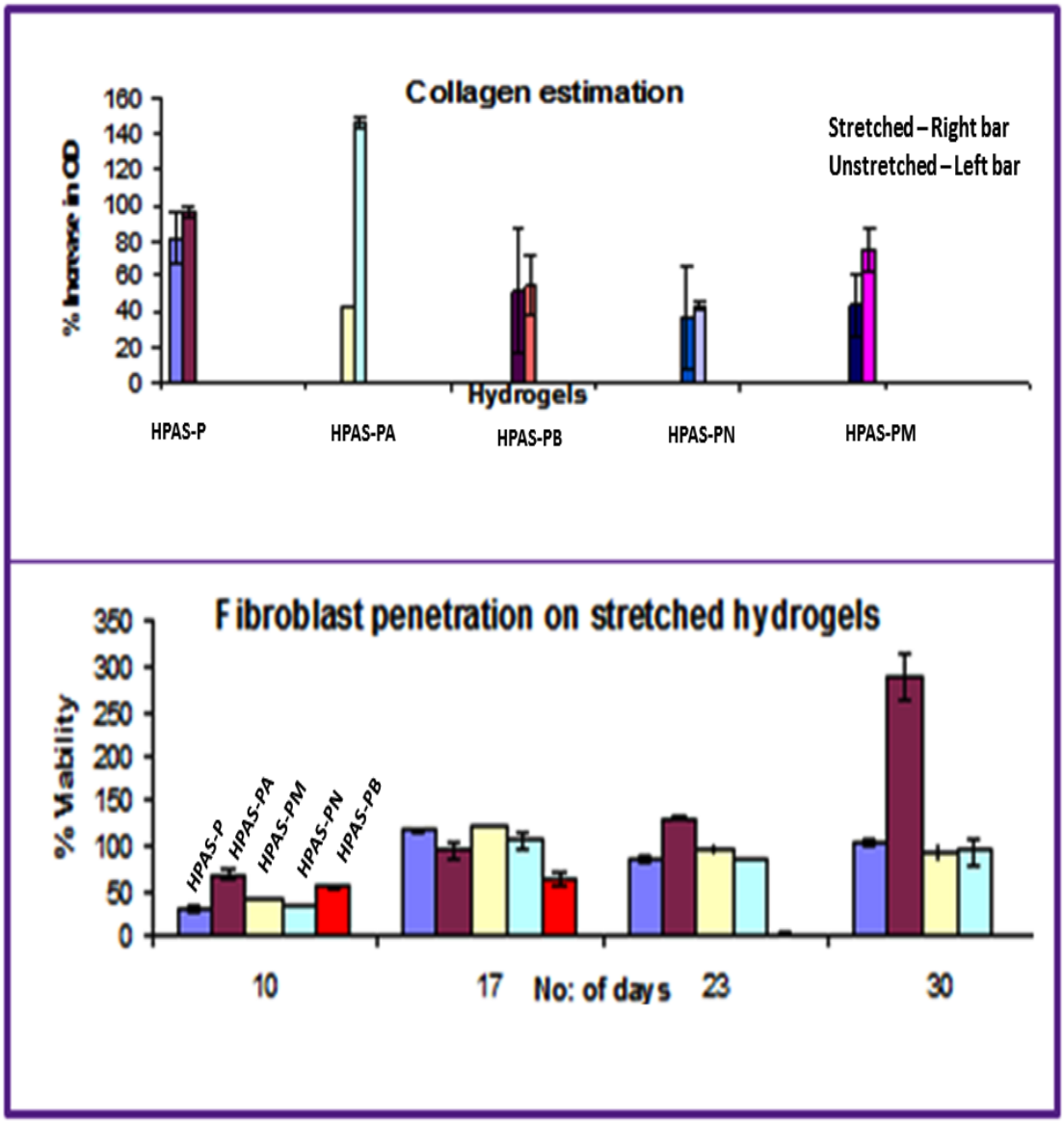

Figure-22. Collagen estimation and fibroblast infiltration on MM- hydrogels. MM hydrogels displayed an increase in collagen content and penetration.

Fibroblast infiltration was greater for HPAS-PA even after one month (288%) while the cell viability on HPAS-PB hydrogels declined drastically. All these MM-Hydrogels promoted cardiomyoblast growth on to their interstices (Figure-23) signifying their potent applications in cardiac tissue engineering.

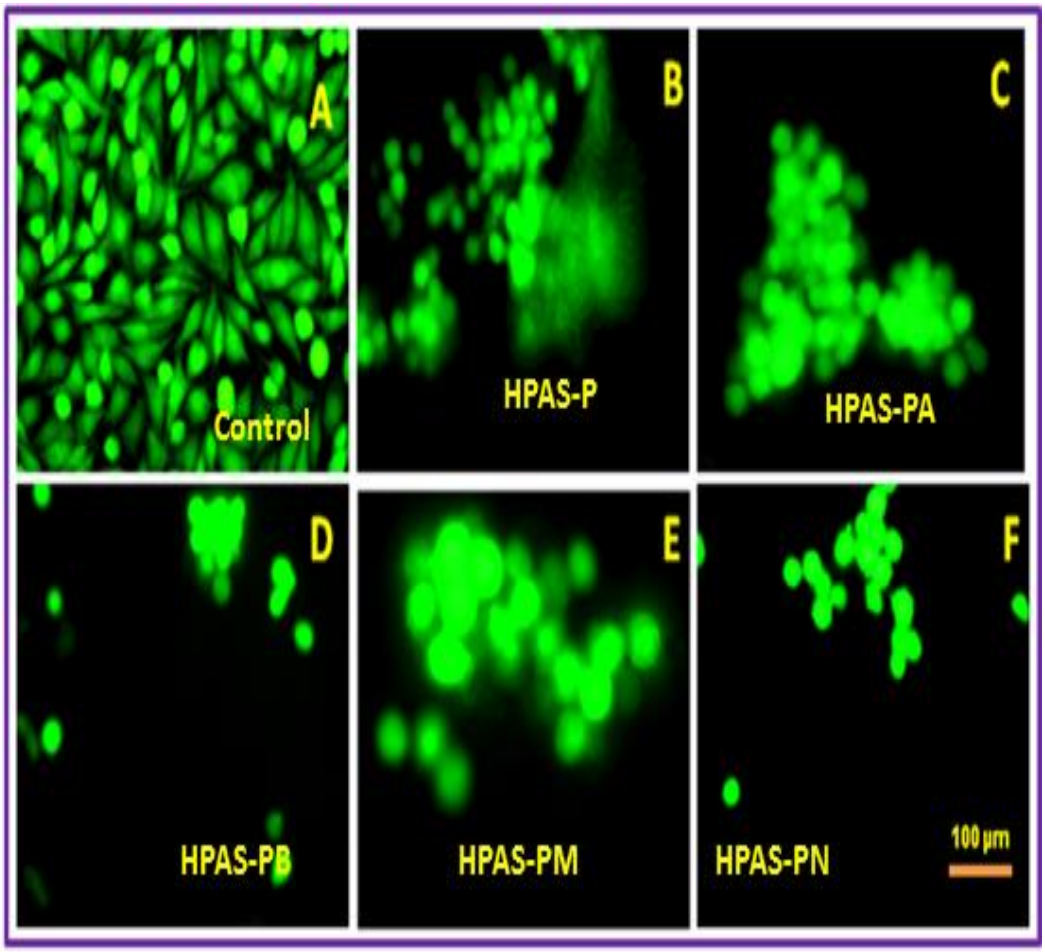

Figure-23. FDA stained images of H9c2 cells grown on MM- hydrogels showing the cell infiltration on the hydrogel interstices. The performance of HPAS-P, HPAS-PA and HPAS-PM were found to be better than the other two.

4.4.3. Protective effects of hydrogels from cellular oxidative stress

The possibility of production of reactive oxygen species (ROS) from the cells upon contact with these hydrogels was evaluated. The assay was based on luminescence determination produced because of ROS inside the cells. All the five hydrogels displayed luminescence counts very closer to that of control cells grown without scaffolds (Figure-24).

The chemiluminescence signal of all the samples were found to be decreased in a time dependent manner and reached a value very near to the control after 15min. A blank and H_2O_2 were also evaluated as control for comparison; those readings were not included in the figure due to their extreme values. H_2O_2 control displayed values ranging from 12385.23 (1^{st} min) to 5716.85 (15^{th} min). The blank showed a reading from 31.67 to 22.9 respectively for 1^{st} and 15^{th} min. From this, it was obvious that the presence of our hydrogel scaffolds will not evoke any ROS generation on H9c2 cardiomyoblast cells.

DCDHFDA staining of the hydrogels-exposed cells under oxidative stress showed a lower intra cellular ROS. This was evident from the relative lower fluorescence intensity of cells on comparing with H_2O_2 control. Live/dead assay results showed lower number of apoptotic cell death in hydrogels-exposed cells under oxidative stress (Figure-25**)**.

Most of the cells were apoptotic in H_2O_2 control, which were evident by the reduced cell number and red nuclei. Vitamin C, the natural antioxidant, was able to scavenge appreciable amount of ROS, which was evidenced by the retention of cell morphology (Figure-26**)**. Still most of the cells were in early apoptotic stage as evident from light orange nucleus. The hydrogel-exposed cells were able to retain their normal morphology and health even under high oxidative stress. This effect was minimal in HPAS-NMBA hydrogels where most cells were apoptotic. The protective effect was greater in HPAS-AA and PMFSA-NMBA, which was evident from the green fluorescence corresponding to acridine orange, which stains the live cells. However, in

HPAS-PA the cells were healthy; but the cell number was found to be reduced. In the case of PMFSA-PEGDA the cells were green but the cell morphology was slightly altered.

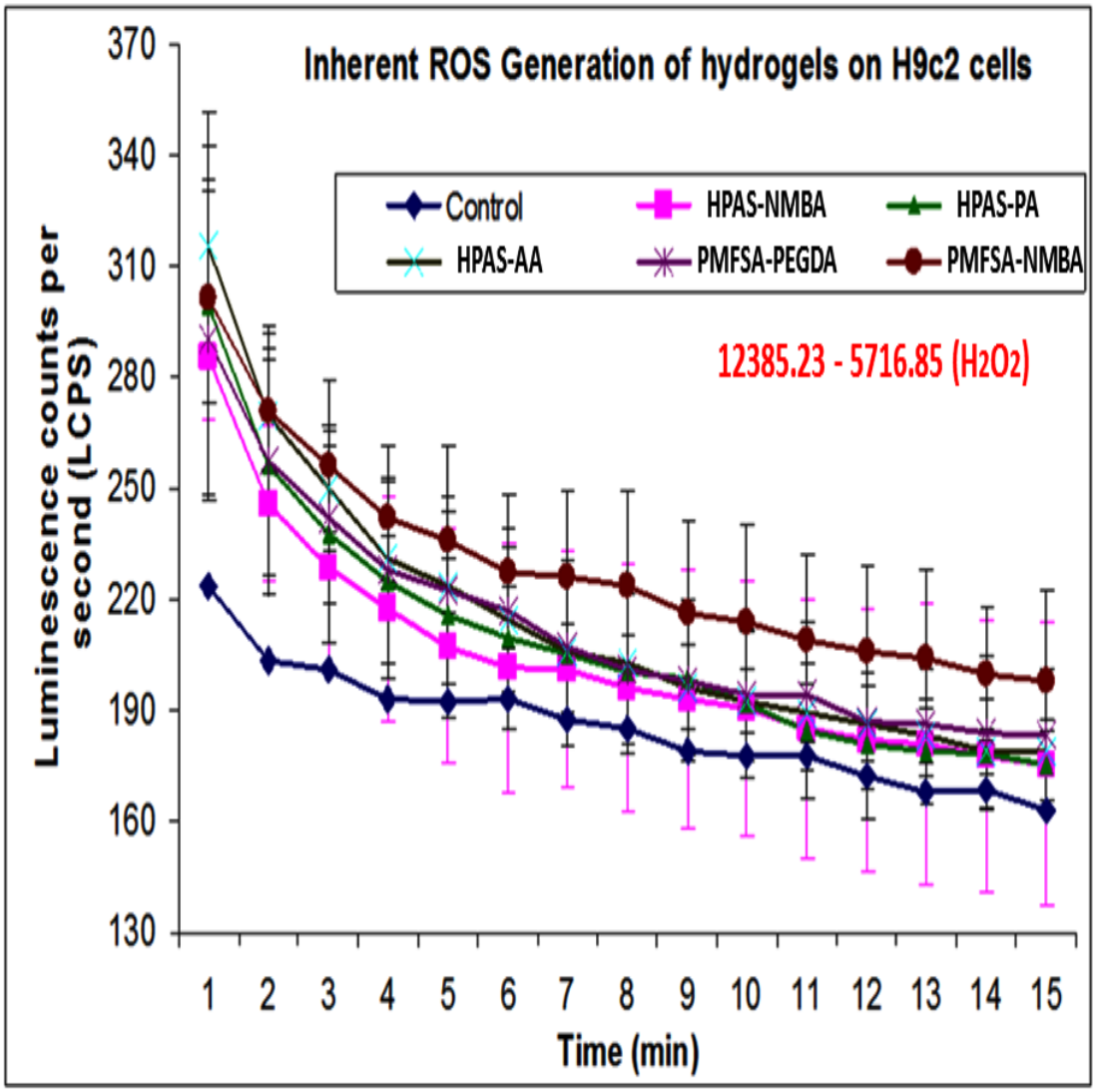

Figure-24. Luminol based chemiluminescence assay showing the minimal inherent ROS generation of hydrogels upon contact with H9c2 cells.

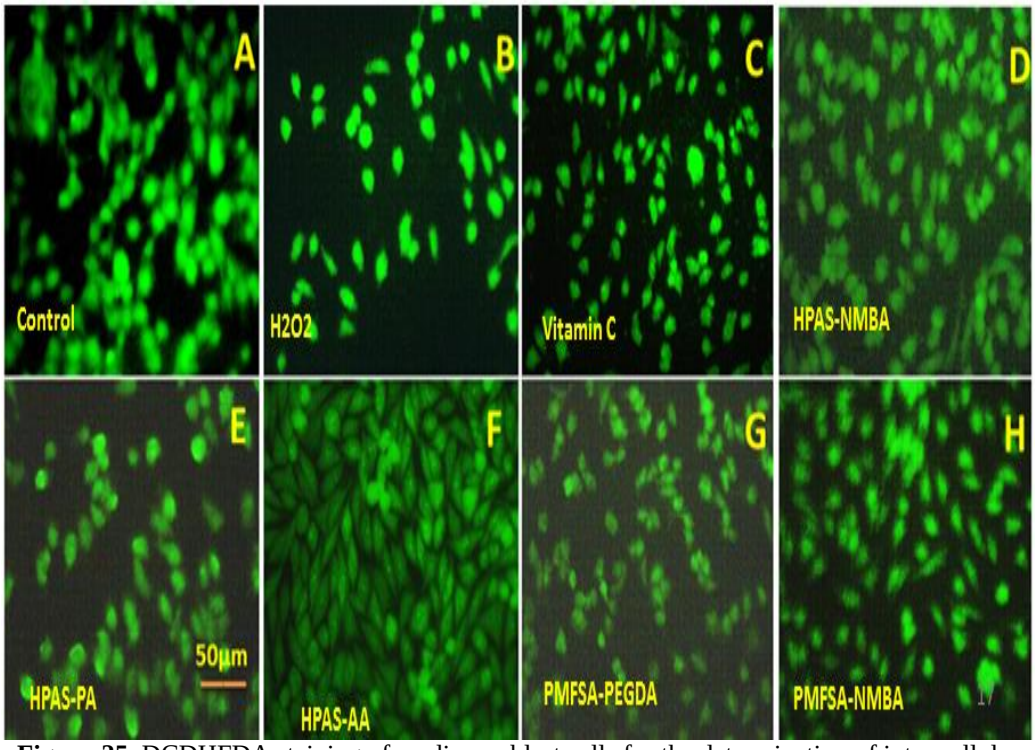

Figure-25. DCDHFDA staining of cardiomyoblast cells for the determination of intra cellular ROS content after scavenging with hydrogels. From the fluorescence intensity it was evident that HAPA-AA possesses better scavenging potential than the others.

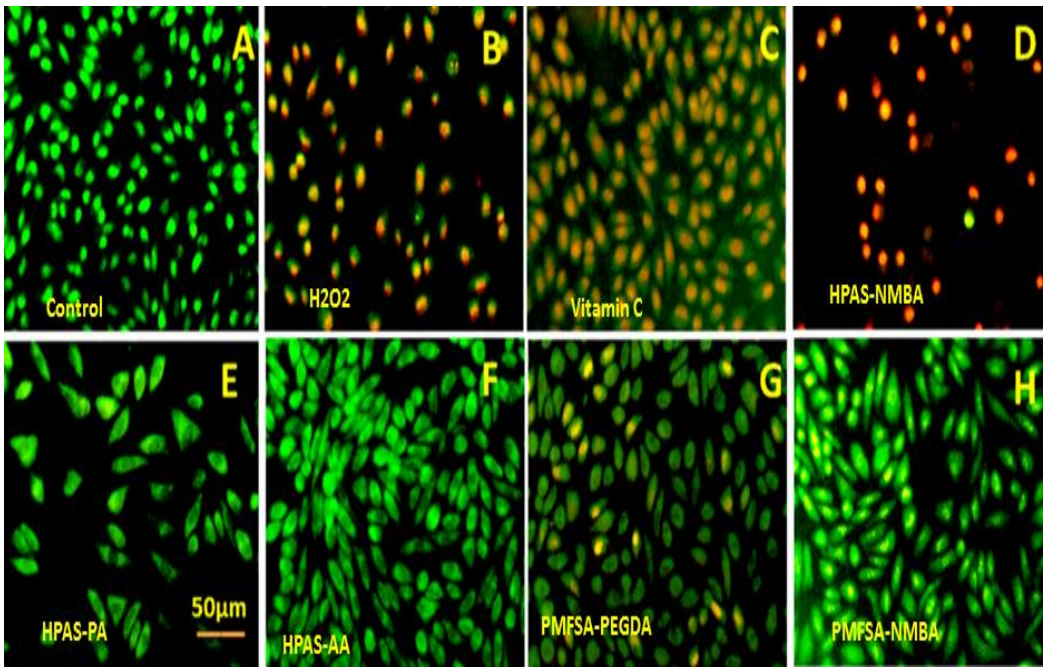

Figure-26. Live/dead assay of H9c2 cells under ROS stress and the efficiency of hydrogels in scavenging ROS.

The hybrid hydrogels were able to prevent the oxidation of the membrane lipids, which was evident from the lesser amount of MDA products (Figure-27). All the hydrogels except PMFSA-PEGDA exhibited an appreciable prevention of peroxidation of membrane lipids of cardiomyoblast cells under oxidative stress.

The protective capacity of the other four hydrogels was similar to that of Vitamin C. Similar results were obtained for metabolic activity determination and RNS scavenging potential. The increase in intra cellular GSH level in the hydrogel-exposed cells again confirmed the scavenging capability. In short, the hydrogels except HPAS-NMBA was found to be capable of protecting the cells from undergoing apoptosis due to the harsh effects of ROS.

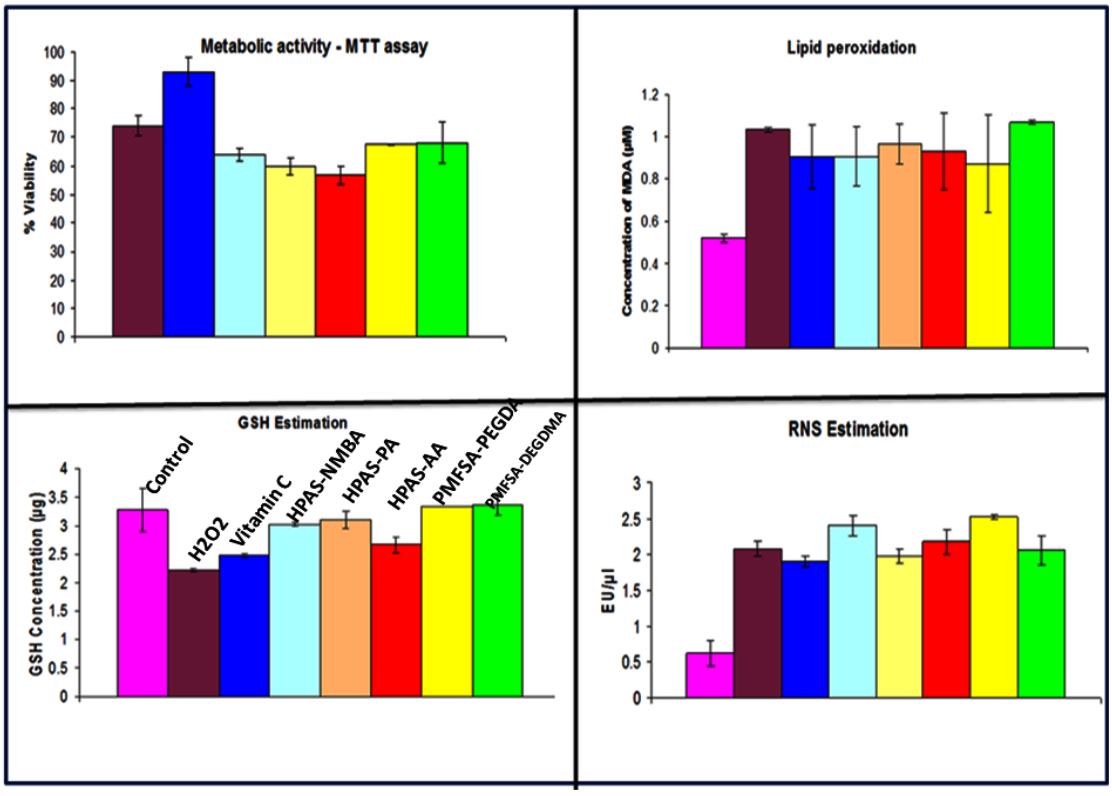

Figure-27. ROS effects of hydrogels – effect on metabolic activity, lipid peroxidation, GSH content and RNS scavenging.

4.4.4. Growth of cardiomyoblasts cells (H9c2) under hydrodynamic conditions

The growth, attachment and infiltration of H9c2 cells on PMFSA based hydrogels under hydrodynamic conditions were monitored using the dynamic rotary cell culture system (RCCS) for 10 days. The viability assays showed all the three PMFSA based hydrogels were able to maintain the viability greater than 50% after 10 days (Figure-28).

The AO stained images showed the crowded population of cells homed on the pores of both the hydrogels (Figure-29). The sizes of the cell crowd were found to be increased on the 10^{th} day when compared with that of 5^{th} day. Effects that are more prominent were obtained for PMFSA-NMBA hydrogels when compared to the others.

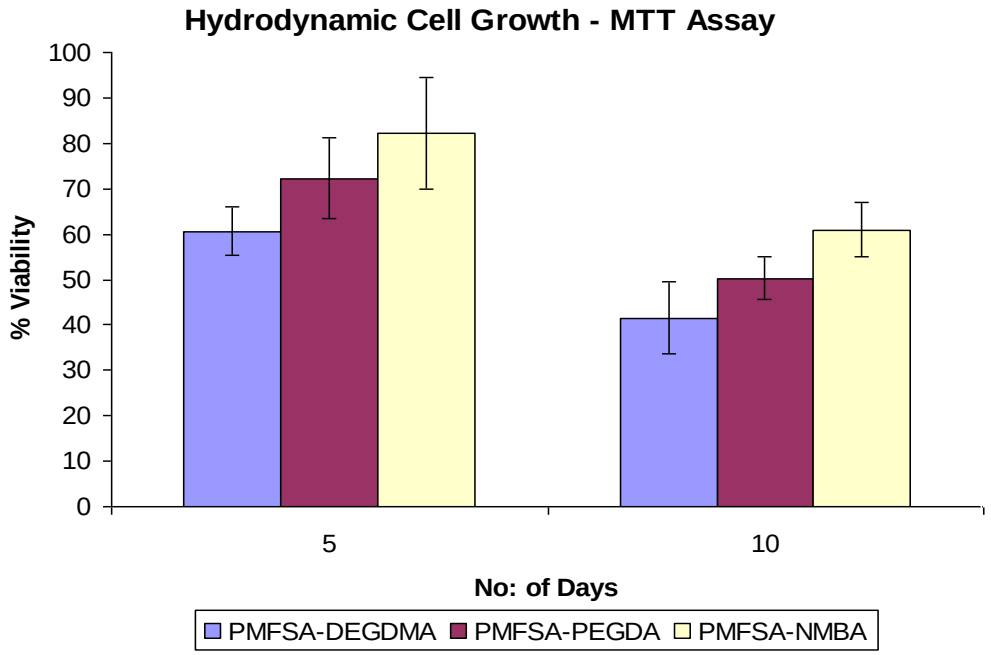

Figure-28. H9c2 cell growth under hydrodynamic conditions showing viability greater than 50% even after a period of 10 days.

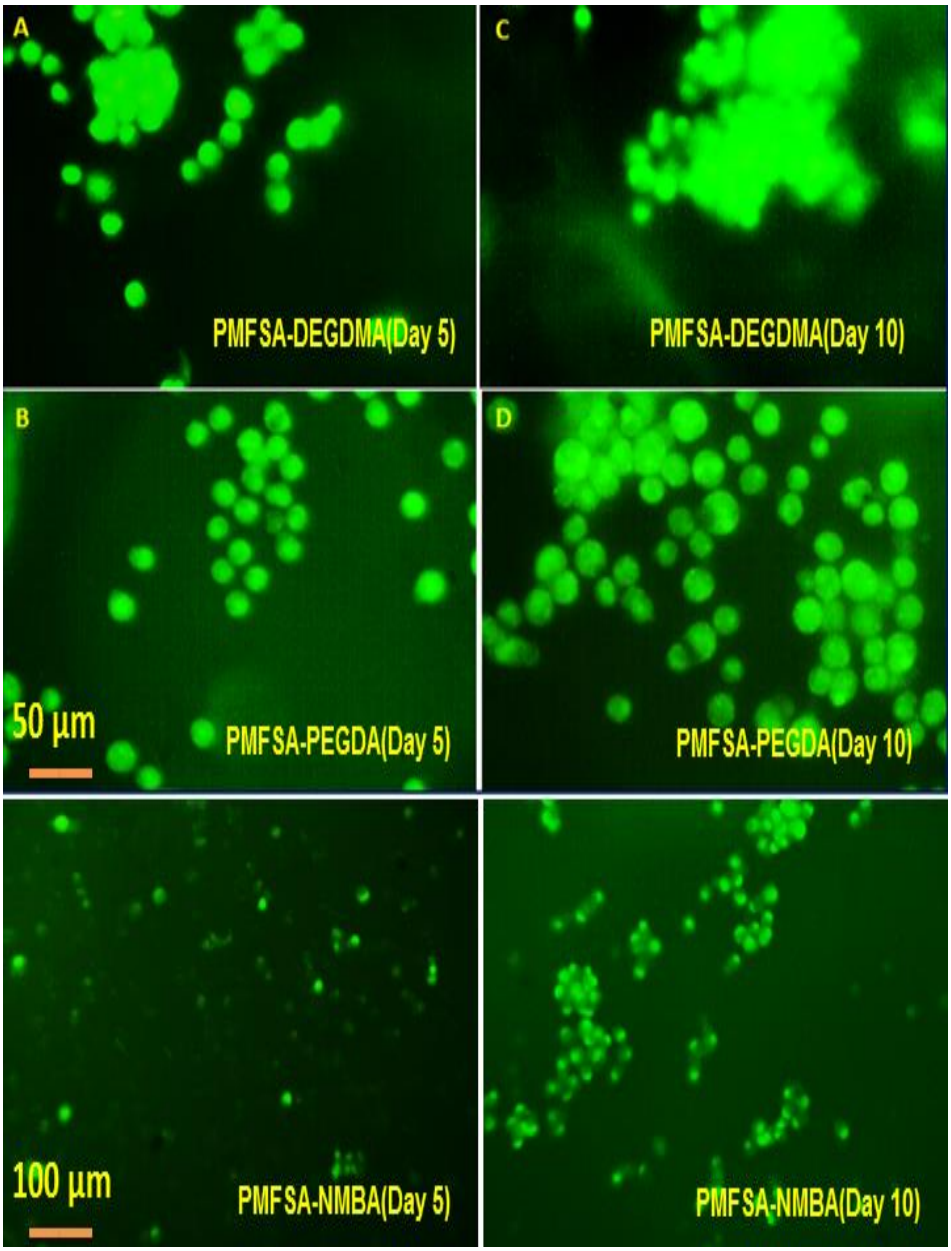

Figure-29. Adhesion and spreading of H9c2 cardiomyoblast cells grown under hydrodynamic conditions on PMFSA based hydrogel on 5^{th} and 10^{th} day.

4.4.5. Co-culture of fibroblasts and cardiomyoblasts

The co-culture studies of L929 fibroblast cells and H9c2 cardiomyoblast cells revealed that both the hydrogels support the adhesion and growth of the cells cultured together. That is the coexistence of one type of cells will not hamper the growth and functioning of the other (Figure-30).

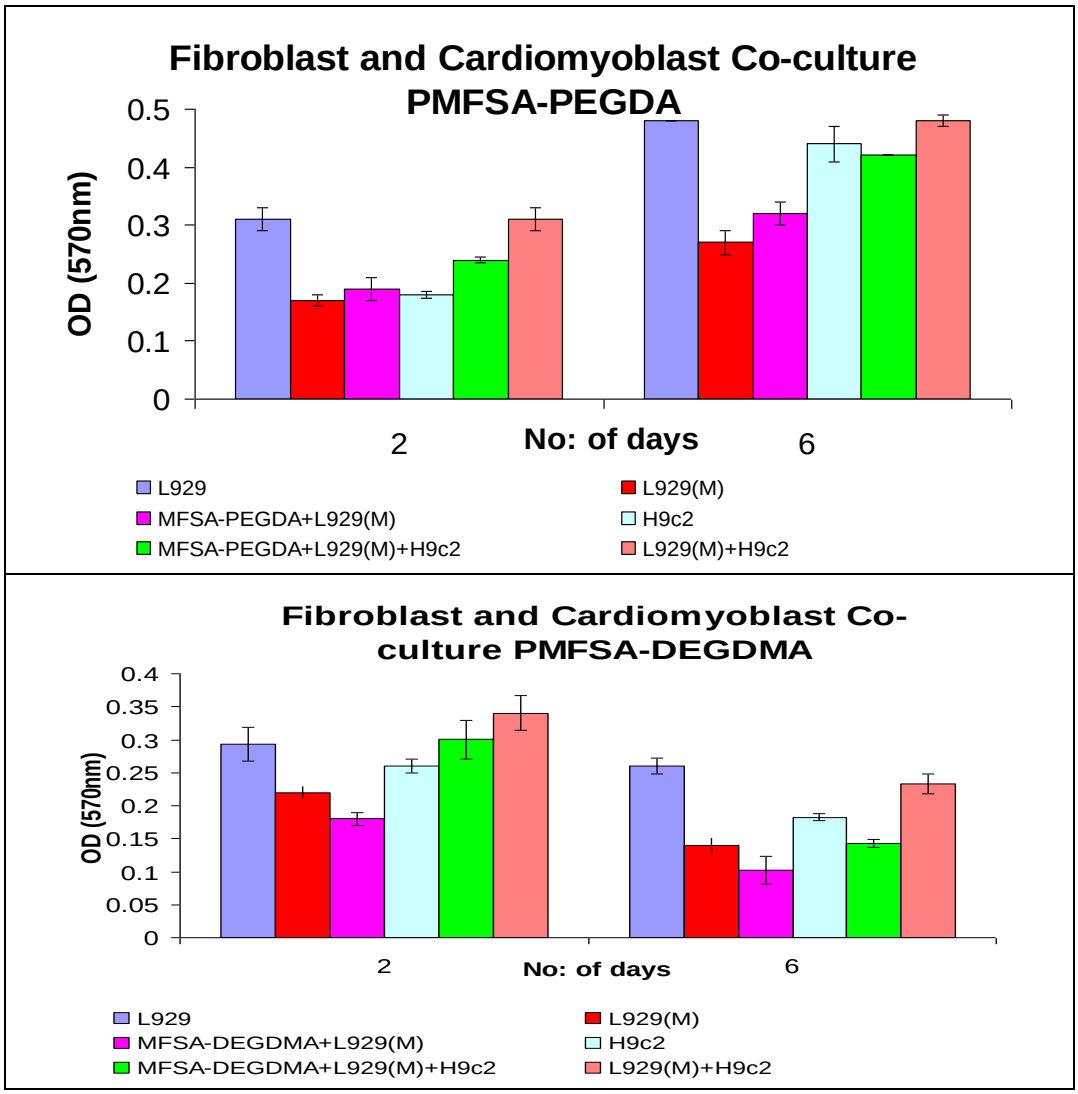

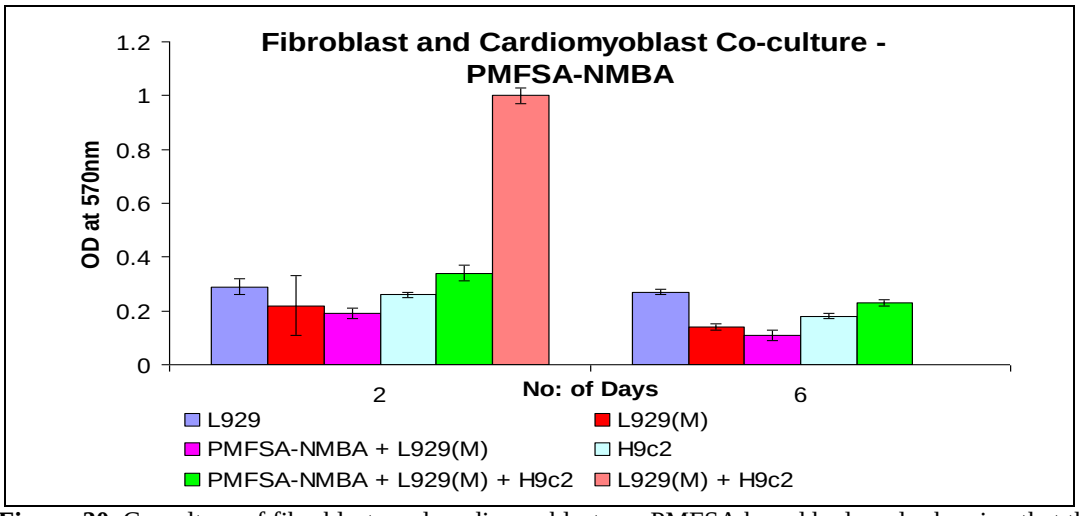

Figure-30. Co-culture of fibroblasts and cardiomyoblasts on PMFSA based hydrogels showing that the presence of fibroblasts in the hydrogels did not altered the viability of cardiomyoblasts.

From the bar diagram it is clear that the growth of co-cultured cells were greater than that of individually grown cells. All the three PMFSA based hydrogels were found to promote the simultaneous growth of both the cells together in the interstices.

4.4.6. Cell cycle analysis of H9c2 cardiomyoblasts grown on PMFSA based hydrogels

The cell cycle analysis of H9c2 cells grown on PMFSA based hydrogels showed around 60% of the cells in the G0/G1 phase of the cell cycle (Figure-31). These cells were actively proliferating and functionally healthy similar to the control. There was no considerable difference between the DNA content of the cells in corresponding phases when the control and hydrogel treated cells were compared. In short there was no arrest in cell cycle during any of the phases of cell cycle.

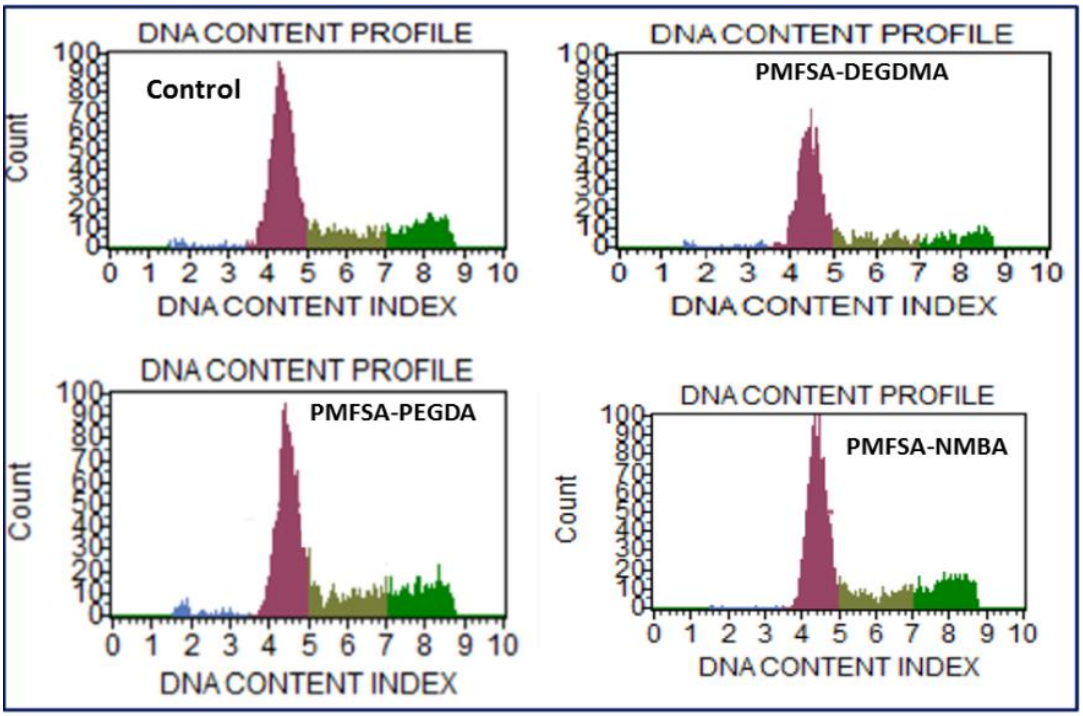

Figure-31. Cell cycle analysis of H9c2 cells grown on contact PMFSA hydrogel scaffolds in comparison with control.

4.4.7. Studies on differentiation of stem cells to cardiac lineage on hydrogels

The ability to support the differentiation of MSC to cardiac lineage was investigated with PMFSA-PEGDA and PMFSA-DEGDMA hydrogels. Confocal microscopy analysis of MSC marker vimentin confirmed that the isolated cells were of mesenchymal lineage (Figure-32). Gene expression analysis of cardiac specific biomarkers like GATA-4, NKX2-5, MEF-2, Troponin T and Troponin C showed the differentiation of MSC grown on two scaffolds to cardiac lineage. This result shows the potential of these scaffolds to differentiate MSC.

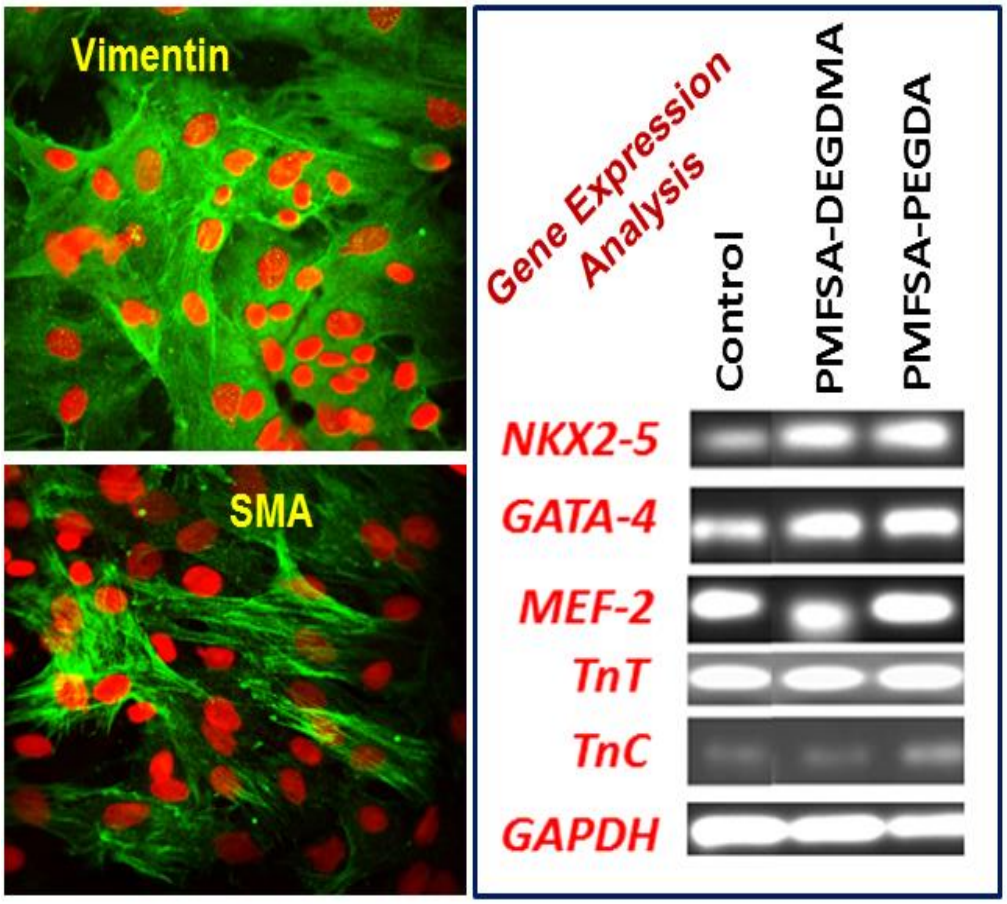

Figure-32. Confocal microscopy images of vimentin and smooth muscle alpha actinin (SMA) positive MSC and gene expression of cardiac specific biomarkers after differentiation.

Chapter 5
DISCUSSIONS

11 Discussions

11.1 Preparation of poly (propylene fumarate)-alginate (HPAS) and poly (mannitol fumarate-co-sebacate)-alginate (PMFSA) based biosynthetic hydrogel scaffolds

The performance of biodegradable hydrogel as myocardial patch largely depends upon the integrity of the hydrogel with adequate mechanical strength, controlled degradation and non toxic degradation products, interconnected pores for supply of nutrients to cells, maintenance of cellular viability and differentiation, favoring cell integration and contractile function under ischemic conditions of the in the injured heart. We addressed these challenges by hybridizing mechanically stable synthetic polyester with biocompatible natural polysaccharide, alginate, to form biosynthetic hybrid hydrogels. These hydrogels were prepared from the graft comcaromers poly (propylene fumarate)-alginate **(**HPAS) and poly(mannitol fumarate-co-sebacate)-alginate (PMFSA).

The GPC analysis of molecular weight of poly (propylene fumarate)-alginate reveals polydispersity, 2.56 which implies that the molecular mass is not uniformly distributed and effective grafting has occurred. GPC analysis of poly(mannitol fumarate-co-sebacate)-alginate also confirmed the macromeric nature. The polydispersity, 1.2 revealed the effective condensation and uniformity in molecular size. The relatively higher polydispersity value of HPAS was due to the result of copolymerization of monodisperse alginate with PPF is an indication of interpenetration of these polymers to form a graft comcaromer that results in the uneven distribution of the functional groups on the HPAS interface.

The vinyl crosslinkers, N N' methylene bisacrylamide (NMBA), 2-hydroxy ethyl methacrylate (HEMA), methyl methacrylate (MMA), n-butyl methacrylate (BMA), poly(ethylene glycol diacrylate) (PEGDA), used for the scaffold prepararion were biocompatible with biomimmetic characteristics (Lee and Chen, 2001)(Gnanaprakasam

Thankam et al., 2013). The hydrophilicity and the strength of the poly (propylene fumarate)-alginate (HPAS) were enhanced by reacting with PEGDA. This has further increased the unsaturation of the system, which was crosslinked with the vinyl and alginate crosslinking to form bimodal hydrogels. Similarly the poly(mannitol fumarate-co-sebacate)-alginate (PMFSA) based hydrogel scaffolds were prepared by crosslinking with divinyl crosslinkers like DEGDMA, PEGDA and NMBA. The ionic crosslinking of alginate fractions of the comcaromers by Ca^{2+} ions offer additional advantage to the biosynthetic hybrid scaffolds in terms of biocompatibility, amphiphilicity, and cell growth.

11.2 Physiochemical characterizations of biosynthetic hydrogel scaffolds

11.2.1 ATR spectral analysis

The ATR analyses confirmed the effective crosslinking of graft comcaromers, HPAS and PMFSA, with vinyl crosslinkers in the formation of hydrogel scaffolds. The presence of characteristic peaks revealed the presence of PPF/PMFS and alginate segments on the surface of hydrogels. The peaks for double bonds reflect the presence of free fumarate fractions on the surface of the hydrogels. These double bonds are effective in arresting the ROS progression at the hostile environment of the infarct zone. The peaks for –OH functional groups on the surface of hydrogels were prominent. This will impart water holding, hydrophilicity and swelling behavior. The density of –OH groups will be greater on the surface of PMFSA based hydrogels which can be attributed to the presence of both alginate and mannitol fractions. In short, the functional groups present in the hydrogel surfaces are responsible for their biological performance. The

carbonyl peaks indicates the presence of alginate fraction on the surface of all the hydrogels.

11.2.2 Eqilibrium water content (EWC) and % swelling

The swelling and EWC of a hydrogel is proportional to the amount of water entered and imbibed on to the hydrogel networks. This water plays a significant role in the diffusion of solutes from the surrounding medium. The microarchitecture resulting from crosslinking also influences the water holding efficiency of the hydrogel. The adsorption of water by the hydrogels and their subsequent swelling is a function of the availability of the hydrophilic functional groups present on the polymer backbone. Swelling is favored by the osmotic force, which drives the water inside the polymer network. At the same time, the dispersing forces generated by the polymer chains resist the osmotic water drive. The dispersive forces are the reverberation of the extent of crosslinking of the polymer networks (Gnanaprakasam Thankam et al., 2013).

The HPAS based hydrogels, HPAS-MMA, HPAS-NMBA, HPAS-HEMA, HPAS-BMA and HPAS-AA, with single crosslinker produced lower swelling and EWC than the HPAS-PM, HPAS-PA, HPAS-PB, HPAS-PH and HPAS-PN hydrogels. From these outcomes, it is clear that the introduction of PEGDA fraction to HPAS have enhanced the hydrophilicity of the system. The crosslinking with other monomers have significantly altered the crosslinks and pore morphology that enhanced the uptake of more water molecules. In the case of PMFSA based hydrogels, the presence of both mannitol and alginate –OH groups have increased the hydrophilicity of the system, which resulted in relative higher water content and holding capacity. This difference is

attributed to the nature of crosslinkers used. Being more hydrophilic PEGDA attracted more water molecules than DEGDMA and NMBA.

11.2.3 Evaluation of surface hydrophilicity/hydrophobicity by contact angle

Contact angle measurements quantify the hydrophilicity of the hydrogels. The values between 30 and 90 degrees can be regarded as amphiphilic and that above 90 are the indications of hydrophobicity. Our hydrogels are amphiphilic and this amphiphilicity can be attributed to the greater amount of free –OH groups contributed by alginate fraction. The introduction of PEGDA segments to the HPAS based hydrogels caused a decrease in contact angle more towards the hydrophilicity. But among the HPAS based hydrogels without PEGDA, HPAS-AA possessed a contact angle values similar to that of which containing PEGDA. This is due to the hydrophilicity imparted by the –COOH group of acrylate. The presence of the polyol mannitol in the PMFSA comcaromer also contributed to the hydrophilicity to the corresponding hydrogel scaffolds. However, the values are greater than that of HPAS-PEGDA based hydrogels. This is due to the hydrophobicity imparted by the hydrocarbon tail of sebacic acid.

The hydrogels having the contact angles ranging from hydrophilic to amphiphilic range are hailed for their better blood compatibility and cell attachment for tissue engineering applications (van Wachem et al., 1987). It was reported that the hydrogels with lower contact angles (high wettability) have appreciable hemocompatibility and *vice versa*. The materials with lower contact angle values exhibit better cell adhesion, spreading and proliferation. The surface hydrophilicity enhances plasma protein adsorption especially that of albumin, which in turn activates cell adhesion and

improves the compatibility of the material (Pal et al., 2009). Wei *et al.* reported that cell attachment was greater in hydrogels having contact angle values around 55 deg which is similar to our results (Wei et al., 2009). But Shu *et al.* reported that extreme hydrophilicity of poly anionic hydrogels based on the hyaluronic acid hinders the cell attachment and spreading (Shu et al., 2004). Our hydrogels showed optimal surface hydrophilicity to be applicable for cell attachment and growth.

11.2.4 Surface morphology and evaluation of average pore diameter by ESEM

Freeze-dried HPAS-AA and HPAS-NMBA hydrogels possessed considerably higher pore length than others. These differences in pore morphology reflect their crosslinking interactions. The structural rearrangements and associated crosslinking imparted by the PEGDA segments in the HPAS-P based hydrogels may contribute to the decrease in their pore lengths. This shows the increase in crosslinking densities in HPAS-P based hydrogels. Similarly, the presence of divinyl crosslinkers in PMFSA based hydrogels contributed to the lower pore length. Moreover the pore morphology and porosity will also depend on the fabrication process (Karageorgiou and Kaplan, 2005). We employed the simple freeze-drying technique for the fabrication of the hydrogels. The evaluations were made on freeze-dried hydrogels. Swelling in the medium will increase the pore volume and facilitate effective transport of metabolites and cell infiltration.

The porosity and pore size of the hydrogels play a direct and significant role in the functionality of the hydrogels for their biomedical applications. Because, this is vital for the cell nutrification, proliferation and infiltration of the seeded cells and formation of

neo tissue. In addition the pores facilitate mechanical interlocking with the host tissue at the implant site and partially enhance the mechanical stability of the implant (Loh and Li, 2007). Madden *et al.* reported that the scaffolds with average pore length of 11µm supported cell infiltration and 3D growth and that with average pore length of 8µm allowed the cell growth on the surface only; the cell penetration in the latter was limited (Madden et al., 2010). Interestingly, our scaffolds have appreciable pore length, which can promote cell infiltration to a greater extent. In cardiac tissue engineering point of view, the interconnected pores with lower pore length is suitable for rapid vasculogenesis with negligible fibrosis and also aid in the synchronization and propagation of the electrical signals for contraction of cardiomyocytes with excellent mechanical compilation (Rnjak-Kovacina et al., 2011). The pore length and morphology of our scaffolds revealed its potential for cardiac tissue engineering.

11.2.5 Evaluation of mechanical properties

During the cardiac cycle, the heart muscle exhibit contrasting mechanical events. According to Starling relationship, in the systole it becomes ductile while in diastole it will be more elastomeric. So the mechanical properties of the cardiac tissue engineering hydrogel scaffolds are very crucial (Bhana et al., 2010). Our hydrogels possessed appreciable mechanical properties to be applicable for cardiac tissue engineering (Table-4 and 5).

Relatively higher tensile strength is observed with HPAS-NMBA and HPAS-PN, which may be due to its higher crosslinking of NMBA with respect to its two vinyl functional groups. The relatively lower tensile strength observed with HPAS based

hydrogels with single crosslinker than that with two crosslinker is due to lower degree of crosslinking in the former. Interestingly, HPAS-MMA has maximum tensile strength, which may be sue to higher hydrophobicity. In the case of PMFSA based hydrogel system the tensile strength of water-swollen PMFSA-PEGDA was found to be higher than that of the other two. This may be due to the presence of ample hydrogen bonding in PMFSA-PEGDA imparted by more hydrophilic PEGDA segments. The hydrogen bonding partners will interact with the functional groups, especially –OH, within the hydrogel and from the surrounding medium. However, these types of interactions are minimal in PMFSA-DEGDMA and PMFSA-NMBA due to the less hydrophilic nature of the crosslinkers. Relatively higher fatigue life has been overved with PMFSA-PEGDA hydrogel.

Cardiac tissue consists of a well-defined extra cellular matrix (ECM) with inherent mechanical properties, which is crucial for the proper functioning of cardiovascular system. Therefore, the hydrogels mimicking the cardiac ECM should be able to bear appreciable mechanical load until the repair and regeneration is completed. The removal of entire cells from the cardiac tissue will not significantly change the mechanical properties of the cardiac ECM (Berry et al., 1975). The elastic modulus of elastic arteries including aorta of the heart lies within a short range of 0.3-1MPa for most organism; this is achieved by regulating the expression of ECM proteins (Thankam and Muthu, 2014b). The myocardium of rat was reported to have the stiffness of 70kPa (Boublik et al., 2005). The stiffness of circumferential and longitudinal right ventricle were 54 ± 8 kPa and 20 ± 4 kPa (Engelmayr et al., 2008) respectively. The stiffness of

the adult rat left ventricle was found to be 18 ± 2 kPa (Thankam and Muthu, 2014b). The adult left ventricle was found to have an ultimate tensile strength of 108 kPa with 63.8% elongation (Kallukalam et al., 2009)**.** The mechanical properties of the water-swollen HPAS and PMFSA based hydrogels showed values greater than the ultimate tensile strength of 108 kPa showing their applicability for cardiac tissue engineering. Since these hydrogels possess higher values than the reported ones it can compromise the loss of mechanical properties due to the exchange of Ca^{2+} ions of alginate segments with monovalent ions from the physiological fluid.

A functional cardiac construct must possess a tensile strength greater than the mammalian left ventricular myocardium (0.15MPa for canine models) (Isaka et al., 2006). The elastic modulus of the one of the most successfully used material, Dacron, was reported to be around 600kPa. Our hydrogels have ultimate tensile strength greater than the reported values signifying their mechanical compatibility for cardiac applications. Since our materials are hydrogels it can efficiently promote cardiac tissue orchestration, since the cardiomyocytes and associated cells prefer a softer microenvironment for growth and function (Pok et al., 2013).

11.2.6 Evaluation of biostability of hydrogels

The biodegradation occurs due to the entrapment of water molecules inside the highly crosslinked networks of hydrogel scaffolds as the initial degradation phase allows more water particles to penetrate these scaffolds. This will initiate the hydrolysis of the labile bonds of the crosslinked networks. In the present study, the medium attained a slight acidic pH after the aging. These slight acidity is due to the hydrolysis products of

the ester bonds (free –COOH functional groups). This can be easily be buffered by the physiological buffers *in vivo* after implantation. The increase in the ionic composition of the medium because of hydrogel aging indicates the accumulation of degradation products. This ionic content contributes to the conductivity and TDS of the medium, which is an indication of biodegradation. The TDS and conductivity of all the hydrogel systems increase in a time dependent manner, which signifies the biodegradation of these scaffolds in the simulated biological fluid, PBS. It was reported that if the rate of degradation on the surface is constant, the bulk structure of the scaffold will be maintained; such degradation provides better opportunities for tissue regeneration and repair (Gnanaprakasam Thankam et al., 2013).

Both the PMFSA system and HPAS based hydrogel systems exhibited a similar biodegradation profile. The monomers and the crosslinkers used for the scaffold fabrication were reported to be compatible and have been employed for several biomedical applications. Sebacic acid is a natural intermediate of the medium and long chain α-carboxylic acid metabolism. So the sebacic acid monomer released from PMFSA based hydrogel degradation can be effectively utilized by the body. It can be converted to acetyl (CoA) and succinyl CoA. The former is one of the key factors in TCA cycle and is involved in cholesterol biosynthesis and several other biochemical reactions. Succinyl CoA is also a key component of TCA cycle and serves as component for porphyrin biosynthesis (Barrett and Yousaf, 2009). Similarly the other possible products, mannitol can enter the glycolytic pathways. PPF degrades by simple hydrolysis of the ester bonds and the degradation products; primarily fumaric acid and

propylene glycol are proven non-toxic and can enter the mitochondrial TCA cycle to be utilized by the cell. The unsaturation present in the PPF allows the crosslinking of the polymer into a covalent polymer network (Gnanaprakasam Thankam and Muthu, 2013b).

Alginate fraction of both the hydrogels systems will be released due to the replacement of Ca^{2+} with monovalent ions form the medium. Even though alginate will not undergo any enzymatic degradation, it will be cleared very slowly from the implant site. The degradation profile of both HPAS and PMFSA based hydrogels reveals its safe use in cardiac tissue engineering applications.

11.2.7 Evaluation of thermal property and status of water in hydrogels

The water in a hydrogel exists in three phases: nonfreezing-bound water, freezing-bound water and freezing-free water. The freezing-free water (water that does not form hydrogen bonds with the polymer and behaves similarly with pure water) is associated with melting of free water at about 0°C and provides an endothermic peak. The freezing-bound water (one which interacts weakly with the polymer chains) crystallizes below 0°C with an exothermic peak (cold-crystallization) (Tanaka et al., 2000). As nonfreezing water is bound to the polymer chains through hydrogen bonds; it never crystallizes even at less than (-) 100°C. Moreover, the freezing and non-freezing bound water content in different polymer-water systems depends on both chemical as well as higher order structure of a polymer.

Thus, the increased nonfreezing bound water content (W_{nb}) in the present hydrogels except in HPAS-PA and HPAS-PM is resulted from the changes in

hydrophilicity, presence of free –OH or –COOH groups, degree of crosslinking in the hydrogels and also due to the presence of alginate fraction in HPAS system and both alginate fraction and mannitol in PMFSA based hydrogels. The difference in freezing water content is attributed to the nature of different the vinyl crosslinkers employed.

The structured water (nonfreezing-bound water) along with free water favors the micro-niche of the surviving cells mainly by accomplishing the easy transportation of biomolecules. For a metabolically active tissue like myocardium, there will be a continuous transport of nutrients and metabolic waste to and from the ECM. Because of myocardial infarction (MI), there will be a leakage of more solute from the infarcted tissues to the ECM. This will further increase the extra cellular solute concentration, which is a vital issue to be addressed by hydrogels intended for cardiac applications. As per the regulatory volume decrease (RVD) mechanism (Gnanaprakasam Thankam et al., 2013), the hydrogels easily allow the transfer of solutes from the surrounding medium into the pores where the cells are stationed. The permeable solutes will take advantage of this situation to enter the membrane barriers of the adjacent cells along with the associated solvent layer. As a result, the cellular volume will increase; if this persists, it will ultimately end in the loss of normal cell morphology and function. In order to restore the normal volume, the cells will try to expel the inorganic solutes like K^+, Cl^- etc. and organic osmolytes that result in the osmolytic efflux of water.

Since all the hydrogels are amphiphilic, it can repel more freezing-free water from its voids than a highly hydrophilic one. This property may be advantageous especially while implantation; the hydrogel implant may prevent the entry of excess

water and solutes into the surviving cardiomyocytes at the site of infarction. Moreover, the hydrogel implant may transfer metabolic water and the water and solutes formed by RVD process at the injury site to the circulation for clearance. This process would sustain the otherwise apoptotic or necrotic cardiomyocytes. Still more *in vivo* studies are needed to validate these aspects.

11.3 Cell-material interaction

11.3.1 Assessment of hemocompatibility

Hemolysis analysis is one of the key tests recommended by ISO for implantable biomaterials as the particles leaching from the materials or the degradation products can interfere with host circulatory system (Peng and Shen, 2011). RBC aggregation, leading to rouleaux formation, is mainly depends on the composition and concentration of the medium where it suspends. This will interfere with the local shear forces encountered by native RBCs and contribute the non-Newtonian behavior of blood, a condition in which decreased blood viscosity and increased shear rate is attained. As a result, the rouleaux will arrest and hold more RBCs and disturbs the normal rheology of the blood (Baskurt and Meiselman, 2007). The lack of rouleaux formation and hemolysis in the present HPAS and PMFSA based hydrogel systems is a sign of absence of toxic degradation products revealing the compatibility to RBC integrity and blood flow.

All the hydrogel scaffolds were exposed to platelet rich plasma (PRP). ESEM analysis was carried out for assessing their thrombogenic potential. Generally, the platelets can adhere even on the surface of biocompatible biomaterials. But the

morphology of the adsorbed platelets determines their thrombogenic potential. If the adhered platelets retain their normal discoid morphology on the biomaterial surface, they are considered as normal without thromogenesis. On the other hand if the platelets exhibit some pseudopodia like extension, it will be an indication of their activation and subsequent thrombosis (Aldenhoff and Koole, 2003). The ESEM analysis of both the hydrogel systems revealed minimal platelet adhesion and morphological changes. From the platelet adhesion studies and hemocompatibility assays, it can be concluded that the present hydrogels will not evoke any adverse blood responses when implanted.

It has been reported that the platelet adsorption on a surface depends on the wettability. The hydrophobicity favors more platelet adsorption (Gnanaprakasam Thankam et al., 2013)**.** The retention of fibrinogen was reported to be higher in hydrophobic surfaces, which favors more platelet adsorption (Nygren, 1996). Thrombocyte aggregation is a pro-inflammatory process due to their secretion of cytokines like CD-40 ligand, IL-1β and the chemokines RANTES and platelet factor 4 by the activated platelets. The expression of these factors will enhance the monocyte recruitment via monocyte integrin activation. So the elimination of thrombosis is very crucial in ensuring the long-term viability of the tissue engineered construct *in vivo* (Gnanaprakasam Thankam and Muthu, 2013b). From the platelet adhesion studies, it is clear that the present hydrogel scaffolds are neutral in provoking the thrombosis. The surface amphiphilicity limits the extensive adhesion of platelets. This is very crucial for cardiac tissue engineering hydrogels since such materials have to be in continuous contact with blood.

11.3.1.1 Plasma protein adsorption

Protein adsorption was prominent in HPAS-AA, HPAS-NMBA and HPAS-PA, which may be mainly due to albumin that will defend the thrombocytosis. However, HPAS-PB, HPAS-PH and HPAS-PM hydrogel does not exhibit adsorption of protein significantly on the surface. This is due to the difference in surface properties imparted due to the different vinyl crosslinkers. The SDS-PAGE analysis of the plasma proteins adsorbed on the HPAS and PMFSA based hydrogels showed a thick band corresponding to that of albumin. From this, it is very clear that the major fraction of the protein adsorbed on the hydrogels was serum albumin. Immediately after implantation plasma protein adsorption onto the biomaterial surface occurs. Even in the case of *in vitro* cell culture on the hydrogels, the same events take place; the initial interaction of cells would be with the adsorbed proteins and not with the hydrogels. The response of the cells on the hydrogels will therefore mainly depend on the adsorbed protein layer. Of the three major plasma proteins, the predominant one, the plasma albumin is reported to have a passivation effect on the surface of the biomaterials.So it resist the acute inflammatory reactions thereby contribute to the biocompatibility of the material (Sultana and Khan, 2012).

The amount and the type of protein adsorption and their responses are mediated by the surface properties of the hydrogels like chemistry, charge, roughness and so on. The wettability and water content of the hydrogels is another key factor for the adsorption of desired proteins like albumin. There are reports that the albumin adsorption is favored by amphiphilic surfaces rather than hydrophobic or hydrophilic.

The hydrophobicity will results in the denaturation of native conformation and hydrophilicity will inhibit adsorption due to the formation of undesirable hydrogen bonds (Vasita and Katti, 2012). Contact angle measurements signify the amphiphilic character of our hydrogels. Reports on the computer simulation studies revealed that water molecules would compete with fibrinogen for binding the hydroxyl groups of the hydrogel surfaces. This binding will be very tight but the optimum concentration of –OH groups will favor albumin over fibrinogen. Still fibrinogen can interact hydrophobically to the methyl-functionalized surfaces. –COOH group also inhibit fibrinogen binding, as it prefer water molecules than the fibrinogen protein (Thevenot et al., 2008). Both our hydrogel systems bear ample –OH groups contributed by alginate and mannitol and sufficient –COOH groups by alginate, PPF and sebacic acid segments. Moreover, the freezing free and freezing bound water provide abundant water molecules for competition. The relative absence of fibrinogen adsorption and extensive albumin passivation on the hydrogels has provided better cell response and excellent biocompatibility.

11.3.2 Assessment of cytocompatibility

The resemblances of hydrogels with the native extracellular matrix made these class of biomaterials an ideal choice for the engineering of various tissues. The viability of cells on these hydrogels even in the absence of growth factors or signaling molecules without provoking apoptosis or necrosis is one of the limiting factors to determine the success of these hydrogels for a particular application (Geckil et al., 2010). Examination by MTT assay, direct contact assay and live/dead assay of the present hydrogels showed

excellent viability of the L929 cells without any morphological changes. No apoptosis was evident in the cells grown on these hydrogels as per live/dead assay displaying the cells were able to maintain their integrity even in the absence of specific growth factors or other biochemical. These cells are able to divide and proliferate on their hydrogel niche. This stimulates their specific functions. These qualities of hydrogels are ideal for tissue engineering applications.

MTT assay gives the percentage of viable cells by evaluating the metabolic activity of the cells by utilizing mitochondrial succinate dehydrogenese enzyme. The MTT assay confirmed the absence of toxicity of the hydrogel degradation products and leachates and its effect on the viability of fibroblast cells. Since the particles leaching out will be of very low concentration and will be diluted further in the culture medium. The absence of biologically harmful materials in the hydrogel extracts and greater viability is an indication of cytocompatibility of our hydrogels (Hago and Li, 2013). In order to observe the real time morphologies of the cells upon contact with the hydrogels, the direct contact assay was carried out. The phase contrast images of the L929 cells grown with the hydrogels displayed no changes in their normal morphology when compared with the control. Again, the direct contact assay results also signify that the contact of cells with materials will not alter the normal physiological or biochemical characteristics of the cells. This can be manipulated for the prediction of cellular responses like adhesion, spreading, proliferation, contact guidance and so on for cardiac tissue engineering (Fukuda et al., 2006). Klouda *et al.* reported that more than 75% viability is necessary for a material to be non-toxic by MTT assay employing their

acrylamide based hydrogels (Klouda et al., 2009). Both MTT assay and direct contact assay results signifies the cytocompatibility of the present hydrogels.

The fluorescent microscopic analysis after live/dead staining using AO/EtBr cocktail displayed green fluorescence of AO dye indicating the retention of nuclear integrity of the cells grown on both the hydrogels. This nuclear integrity is the sign of healthy and proliferating cells confirming the cytocompatibility of the hydrogels and their ability to support cell growth and function. Moreover, this is the indication of the absence of apoptosis, anoikis and necrosis. Since AO is a permeable dye, it can enter all the cells and makes the nuclei to fluoresce green. While EtBr can be taken up by the cells whose membrane integrity is lost, the ability of the membrane to exclude EtBr is very much limited, and stains the nucleus red. So the healthiness of the cells can be evaluated by analyzing the coloration of nuclei from green to red (Ribble et al., 2005).

In cardiac tissue engineering point of view, the attachments of cell types to hydrogel scaffolds are very crucial. Since hydrogels form an ECM substitute, the chances of anoikis is much higher than compared to actual *in vivo* situations. If the attachment of the cells in the substratum (native ECM or scaffold) is improper the apoptotic pathways is triggered leading to anoikis. In normal cellular physiology, anoikis is relevant for homeostasis and tissue development by preventing the detached cells from colonizing in wrong locations. But anoikis resistance will lead to tumor genesis and metastasis, especially while dealing stem cells for cardiac and other tissue engineering applications (Kim et al., 2012). Since both the hydrogel systems provided better cell attachment, viability and proliferation without apoptosis/anoikis the present

hydrogels are potent candidates for cardiac tissue engineering. Therefore, they can adhere and support stem cells and prevents teratoma formation.

11.3.3 Evaluation of genocompatibility by comet assay

The Comet assay or single cell electrophoresis is a sensitive and rapid technique for quantifying and analyzing DNA damage in individual cells for the evaluation of genotoxicity (Widziewicz et al., 2012). This assay can be used to detect DNA damage caused by double strand breaks, single strand breaks, alkali labile sites, oxidative base damage, and DNA cross-linking with DNA or protein. The Comet assay gain special significance in the field of biomaterials research due to the long latent period between exposure to genotoxic agent and genetic effect(s) becoming apparent. In the present investigation, the time (24 h) elapsed between exposures and measuring of the DNA damage is adequate for the repair of the possible lesions and enables to detect whether or not the chemical is able to produce the DNA damage. As per the assay the four HPAS based hydrogels, HPAS-No, HPAS-MMA, HPAS -HEMA, and HPAS-BMA, (degrades faster rate in DMEM) did not evoke a significant effect on DNA migration on the electric field at the applied concentrations and found to be non-genotoxic. From the assay it is very clear that the neither the hydrogels nor the degradation products or the particles leaching from them affect the genomic integrity of the genetic materials. These non-mutagenic effects suggest their long-term cardiac applications. Apart from the chemical nature, the physical properties like surface topography, hardness, porosity and surface energy also impart genotoxic effects to the biomaterials (Chauvel-Lebret et al., 2001). The relative absence of DNA in the tail region of comets of all the samples again

reveals that all the characteristics of these hydrogels are well suited for tissue engineering applications.

11.4 Biological responses of hydrogels for cardiac tissue engineering

11.4.1 Cell infiltration and long-term viability

The extent of cell infiltration and its metabolic activities inside the hydrogels were quantified by a modified version of MTT assay. The results showed that both the hydrogel systems were able to provide longer viability to the cells. Generally, the prolonged growth of the cells in culture plates after attaining confluence will reduce the viability; but the porous networks of the present hydrogel enables the cells to divide and function inside the pores. The relative higher viability in the present hydrogels is due to the cell friendly microenvironment orchestrated by the structured water along with more free water.

The porosity also has much relevance in directing the cells to the inner networks of the hydrogels for enhancing the tissue formation by assuring a homogeneous cell distribution. The increased porosity and optimum pore size will favor cell infiltration by promoting the easy diffusion of gases and metabolites towards the interior of the scaffolds, which will guide the cells to migrate. Upon implantation, the porosity favors angiogenesis to occur and this can be indirectly correlated with the extent of cell infiltration. More cell infiltration reflects the availability of inner pores for cell homing and this support neo-angiogenesis (Annabi et al., 2010). A recent report says that a minimum of 5 μm pores are necessary for vascular ingrowth and 5-15 μm for fibroblast

infiltration (Huang et al., 2012). The pore length of the present hydrogels lies within this limit revealing their potential to promote cell infiltration. Fan *et al.* reported that their double network hydrogels showed viability around 90% after 21 days of seeding (Fan et al., 2013). HPAS based hydrogels were able to maintain more than 60% viability after a period of 18 days. But, the PMFSA based hydrogels exhibited a better viability of 100% after 21 days. PMFSA-PEGDA hydrogel retained around 95% viability even after 30 days. The water content, amphiphilicity, albumin passivation, biocompatibility and long-term cell infiltration and survival make our hydrogels an excellent choice for long-term cardiac tissue engineering applications. Still PMFSA based hydrogels were superior in this aspect.

11.4.2 Morphologically modified HPAS-P based hydrogels for improved biological performance

The major demerits associated with most scaffoldshaving low pore volume are the limited cell penetration, non-homogeneous cell distribution, low cell viability, time consumption and so on (Chan and Leong, 2008). In such scaffolds, the surface area available for cell adhesion and protein adsorption is very limited, which will affect the cellular metabolism (Thankam and Muthu, 2014). Our controlled cyclic stretching (uniaxial direction) method adopted in the present study has triggered the pore opening and enhanced the pore inter connectivity on HPAS-P based hydrogels, prominently with HPAS-PA and HPAS-PM hydrogels. This approach succeeded in imparting an increased pore length without altering the physiochemical and thermal properties of parent hydrogels. The resultant increase in pore length is an indication of increase in

pore volume for accommodating more cell crowd. This increased pore length is favourable for enhancing the biological performance of the hydrogels. The seeded cells on these MM-Hydrogels can take up proliferation and penetration near elongated pores by responding to water content and amphiphilicity.

Biological performance was found to be enhanced in MM-Hydrogels, which was evident from the increased collagen deposition (Figure-22). The collagen synthesis on the MM-Hydrogels was displayed as percentage increase in OD with respect to the control. This indicates the availability of sufficient space on these hydrogels for accommodating more cells. The cells growing on the hydrogel scaffolds can overcome the mechanical and biological stresses by ECM secretion and deposition. These types of extra cellular responses are critical for the long-term viability and functioning of the seeded cells (Stock et al., 2001). Since collagen is the most abundant ECM component, its quantification will give a clear picture of the total ECM deposition (Cox and Erler, 2011). It has been reported that the porosity has a direct effect on the ECM secretion and deposition (Mandal and Kundu, 2009). The ECM produced by the seeded cells is deposited in the pores and fills the voids as the hydrogel degrades. This leads to the generation of a neo tissue equivalent (Bryant and Anseth, 2003). The MM-Hydrogels has increased the void volume and subsequent ECM deposition. This effect was found to be relatively greater in HPAS-PA and HPAS-PM hydrogels while the other hydrogels also exhibited an appreciable effect.

Biological performance was found to be enhanced in MM-Hydrogels, which was evident from the increased cell viability and infiltration. The stress induced by the

population of proliferating cells crowded on the pores force them to enter the unoccupied rooms of the interior network. The diffusion properties of the hydrogels were reported to be limited to 200 μm and the cells form a necrotic core beyond this distance if surplus nutrition is not available (Huang et al., 2012). The pore dimensions of all our hydrogels fall within the acceptable limit. Moreover, FDA stained H9c2 cells were found to be grown as crowded population in all the five HPAS-P, HPAS-PA, HPAS-PM, HPAS-PN, HPAS-PB hydrogels. The densities of the cells in the clusters were found to be greater in HPAS-PA followed by HPAS-PM. The two cells were able to maintain their viability and function on these bare hydrogels (without any growth factors or signaling molecules). Of the five, HPAS-PA and HPAS-PM possessed better porosity and water content, which made them to accommodate more cell population than the rest.

11.4.3 Protective effects of hydrogels from cellular oxidative stress

The prevention of progression reactive oxygen species (ROS) is very necessary for the repair and regeneration of heart muscle. To the best of our knowledge, limited research articles are available in the literature that focused on the ROS scavenging and management using tissue engineering hydrogels. In order to evaluate the ROS scavenging potential of our hydrogels we simulated an oxidative stress in the H9c2 cardiomyoblast cell culture by using 200μm H_2O_2, since H_2O_2 is a natural source of oxidative damage and its ability to produce other ROS by Fenton reaction (Thankam Finosh and Jayabalan, 2013). We first evaluated the inherent ROS production of the cardiomyoblast cells upon contact with the hydrogels. Because there are reports showing

that the presence of scaffolds provoke the ROS generation in the adjacent cells in a process mediated by cytokines (Shakya et al., 2013). This cytokine mediated ROS generation leads to the increased ROS level at the implant site. Subsequently immune responses are provoked resulting in implant rejection. Moreover, there are chances of ROS production by degradation products or leaching particles from the hydrogels.

From luminescence assay it is evident that the chances of ROS generation by H9c2 cell either directly or indirectly in contact with our hydrogels is minimal. ROS induced apoptosis forms one of the major reason for the progression of cardiovascular diseases especially myocardial infarction. The process of apoptosis occurs in mitotic and post mitotic cells during reperfusion and after ischemia. The exact trigger for apoptosis during these stages is still unknown. But, the role of ROS in this aspect was confirmed due to the hike in concentration at the infarct site during ischemia and reperfusion (von Harsdorf et al., 1999). The subnanomolar concentration of ROS were reported to be sufficient for inducing severe oxidation to macromolecules, membranes and organelles of the myocardium and lead to cardiac malfunction especially disturbances in calcium homeostasis. The slight disturbances in calcium homeostasis will affect the cardiomyocytes ionic balance and thereby excitation contraction coupling (Santos et al., 2011).

Reports on the application of hydrogels for scavenging of ROS after MI or ischemic heart disease are not adequately available. Yung-Hsin Cheng *et al* reported the application of injectable thermosensitive chitosan/gelatin/glycerol phosphate hydrogel for the delivery of an antioxidant compound ferulic acid to prevent free radical induced

vertebral disc degeneration (Cheng et al, 2012). Beukelman *et al* (Beukelman et al, 2008) has used liposome hydrogel with polyvinylpyrrolidone-iodine (PVP-I) as free radical scavenger for wound healing of burns and chronic wounds and reported that PVP-I inhibits production of reactive oxygen species by polymorphonuclear neutrophils. Cheung *et al* (Thankam Finosh and Jayabalan, 2013), (Thankam and Muthu, 2013a) have prepared hydrogels based on polymerisable superoxide dismutase mimetic meatalloporphyrin macromer, Mn (III) Tetarkis [1-(3-acryloxy-propyl)-4-pyridyl]porphyrin cross linked with polyethylene glycol diacrylate to scavenge superoxide anion associated with implantation of biomaterials. But we are lacking sufficient literatures on the application of hydrogels for scavenging of ROS in cardiac tissue engineering. Four of our hydrogels, HPAS-PA, HPAS-AA, PMFSA-PEGDA and PMFSA-NMBA were proven to be able to sustain the cell viability by preventing apoptosis in a highly ROS stressed environment. The relative lower responses of HPAS-NMBA are due to the excessive crosslinking owing to its two vinyl groups.

In the present hydrogels, the free radical scavenging activity is anticipated in two ways, (i) restricting the migration of free radicals and reduction of intracellular redox state in the cells and (ii) extra cellular scavenging by neutralization by freezing free water present in the hydrogel. The present cross linked hydrogel undergoes erosion in DMEM medium by exchanging Ca^{2+} with Na^{+} and other monovalent ions from the medium and leads to unwinding of alginate fraction as reported elsewhere (Thankam Finosh and Jayabalan, 2013), (Thankam and Muthu, 2013a). This will decrease the gelling behavior of Ca-alginate and increases the fragmentation with generation of free

calcium. The generated calcium has a vital role in controlling the intrusion of hydrogen peroxide in the cells. Calcium can induce conformational changes in membrane phospholipids as reported by Gutteridge (Thankam and Muthu, 2013a) (Luo et al., 2009) or by binding to the polar heads of phospholipids resulting in increased surface rigidity of membranes as reported by Benga and Holmes (Thankam and Muthu, 2013a). These calcium interactions might account for reduction of intracellular redox state in the cells. The neutralization of hydrogen peroxide free radical present in the extracellular milieu is carried out by dilution by freezing free water present in the hydrogel. It is known that hydrogen peroxide free radicals participate in the physiological processes in a concentration-dependent manner. At low concentrations, they play an important role as regulatory mediators in signaling processes. In the present hydrogels, the swelling (%) and freezing free and non-freezing bound water promote dilution of hydrogen peroxide free radical to very low concentration. Moreover, the double bonds generated during the unwinding of alginate gel will be crosslinked by utilizing the free radicals. This ROS induced crosslinking effectively scavenge the ROS and neutralize them. Still more evaluations at cellular and scaffold levels are needed to elucidate an apt mechanism for ROS scavenging effects.

11.4.4 Growth and adhesion of H9c2 cells under hydrodynamic conditions

Cell growth and response on most tissue engineering scaffolds were studied in static culture conditions where the cell attachment mainly depends on the cell density; the cell attachment cannot be further increased beyond an optimum level. In hydrodynamic conditions, the adherence of the cells to the scaffolds occurs because of the fluid flow

created by the rotary culture system. Here the cell establishes better communications while attaching to the scaffolds and improves the spatial distribution of cells in the scaffolds. The dynamic fluid flow enhances cell proliferation, differentiation, migration and function. Moreover, the dynamic system modulates the shear properties of a native tissue environment especially dealing with cardiac tissue engineering hydrogel scaffolds (Luo et al., 2009). McDevitt reported that around 10^9 functional cardiomyocytes were needed to replenish the damaged ventricles after infarction (McDevitt and Palecek, 2008).

The 3 D culture on hydrogels was found to be effective for the replication of physiochemical and structural components of the heart (Akins et al., 1997). Still the hydrodynamic conditions of the cells growing on a 3 D hydrogel scaffold also influence the success of the application. In order to address this issue we cultured H9c2 cardiomyoblast cells in rotary cell culture system [(RCCS, High-Aspect Rotating Vessel model (HARV)] as the rotation motion provide a homogenous distribution of cells and nutrients. The RCCS minimize the shear stress and provide an appreciable microniche for the cell culture (Teo et al., 2012).

The growth of H9c2 cardiomyoblast cells on PMFSA based hydrogel scaffolds under hydrodynamic conditions was observed with viability greater than 50% after 10 days. The results indicate the effective communication among the cardiomyoblast cells on the hydrogels to get crowded and to function as a single unit. During the course of time, these clusters cover the entire scaffold and provide better integration of the cells.

11.4.5 Co-culture of fibroblasts and cardiomyoblasts

In order to study the influence of L929 fibroblast cells on the growth and performance of H9c2 cardiomyoblast, we co-cultured these cells on PMFSA based hydrogel scaffolds. Though the excessive proliferation of fibroblast cells were controlled by arresting their cell cycle by mitomycin treatment, these fibroblasts are able to execute their ECM secretory function and act as a feeder layer for cardiomyoblast cells. The optical density (OD) of the cardiomyoblast cells co-cultured with cell cycle arrested fibroblast cells were found to be increased significantly on PMFSA based hydrogels when compared with the scaffold less controls.

The complexity of myocardial tissue architecture, the spatio-mechanical integration and the electrophysiological properties offers a huge challenge for the development of tissue engineered patch for cardiac applications. The chemistry of the scaffolds and their physiochemical and mechanical characteristics often determine the survival and functioning of different cell types grown together in the scaffolds. The maintenance of correct proportion of various cells in a particular tissue is another major concern when dealing with tissue engineering applications. In the case of native myocardium, the ratio of fibroblasts to myocytes must be in the 70:30 limits to replicate the physiological function. At this ratio, the fibroblasts are determined to conduct electrical signal to a distance of 100μm through the gap junctions there by synchronizing the heartbeat. Still all these factors were determined by the substratum where the cells were attached either native ECM or artificial scaffolds (Hussain et al., 2013).

It has been reported that the co-cultured cells may secrete nutrients, trophic factors or cell adhesion molecules which will benefit all the cell types to perform their tissue functions in the tissue engineering scaffolds (Kim et al., 2012). The presence L929 cells on our hydrogels did not affected much on the viability of H9c2 cells, even if the cells were from different source. This showed that both the cell types grow independently, but depending on the secreted molecules from the both.

Lu *et al.* reported the co-culture of mouse fibroblasts with human corneal cells and claimed that mouse fibroblast feeder layer is far better than explant culture. The report highlights the fact that in actual application the cells have to be replaced with the cells from the species of interest and has to be expanded *ex vivo* before implantation (Luo et al., 2009). Hussain *et al.* conducted a similar study like ours using chitosan scaffolds for cardiac tissue engineering by co-culturing rat cardiomyocytes and mouse fibroblasts (Hussain et al., 2013). The PMFSA based hydrogels also promoted the growth of different cells of cardiac tissue indicating the potency for cardiac tissue engineering applications. In the present study, we focused on the biomaterial aspect of the co-cultured fibroblasts and cardiomyoblast cells. In addition, the results showed that PMFSA based hydrogel scaffolds promoted the growth of these two cell types alone and together.

11.4.6 Cell cycle analysis of H9c2 cardiomyoblasts grown on contact with PMFSA based hydrogels

The health of cells and their function depend on its proliferation capacity, which in turn involves the different stages of cell cycle. The surrounding environment and the

substratum that they attach also influence the dividing capacity of the cells. The progression of cells through different phases of cell cycle gives a clear picture of the health status of the cell with respect to its microenvironment. The cell cycle analysis of H9c2 cardiomyoblast cells grown beneath PMFSA based hydrogel scaffolds suggest the the dividing capacity of cells in contact with the hydrogel. The cell cycle profiles of the hydrogels-expsed cells were very much similar to that of control cells (grown on tissue culture plates without scaffolds). Like the control cells, the cells grown on contact with the hydrogels exhibited a normal progression through G0/G1, S and G2/M phases of cell cycle. There was no considerable difference between the DNA content of the cells in corresponding phases. In short, there was no arrest in cell cycle with hydrogels-expsed cells during any of the phases of cell cycle.

The normal cell cycle involves G1 and G2 phases where the cells prepare itself for DNA replication and mitosis by synthesizing protein and RNA synthesis. The S phase involves the DNA replication and in M phase cytokinesis occurs. G0 is another phase where the cells become inactive and exist in a quiescent stage. The time taken for cell division and the relative lengths of the phases vary with cell type and growth conditions (Boccafoschi et al., 2007). The cell cycle analysis of PMFSA based hydrogels revealed that the cells are constantly progressing through all the phases of the cell cycle as in the case of control. This showed that the environment of cells grown beneath the present hydrogel scaffolds were very much supportive for the growth of cells and were able to propagate through all the phases of cell cycle in a normal manner. The dividing capacity and DNA replication of these cells were not affected by the

presence of the hydrogel scaffolds. The analysis revealed that these scaffolds are able to promote tissue formation without altering the viability and dividing capacity of the seeded cells. This signifies that the hydrogels can form a suitable micro niche for cardiac tissue engineering applications.

11.4.7 Differentiation of MSC to cardiac lineage on PMFSA-PEGDA and PMFSA-DEGDMA hydrogels

As cardiomyocytes are terminally differentiated, they do not regenerate after birth. Loss of cardiomyocytes leads to regional contractile dysfunction. The necrotized cardiomyocytes in infarcted ventricular tissues are progressively replaced by fibroblasts to form scar tissues (Keiichi Fukuda; 2000). Administration of stem cells that differentiate to cardiomyocytes at the infarct site can reverse the fibrotic scar tissue formation. Among the different stem cell sources, embryonic stem cells demonstrated a higher degree of success. But teratoma formation, immunologic rejection, ethical concerns and trans-differentiation to other lineages forms a major challenge in embryonic stem cell based therapies. Bone marrow MSC on the other hand can be differentiated into cardiomyocytes if a suitable microenvironment is provided. Their differentiation and expansion potential has added extra benefits to the MSC for regenerative and tissue engineering applications. Still for the effective homing of MSC, appropriate scaffolds with favorable characteristics are necessary. Such scaffolds should favor the differentiation of MSCs into adequate number of cardiomyocytes and promote vascularization to meet the high metabolic demand of the myocardial tissue (Sreerekha et al., 2013).

The gene expression analysis of MSC grown on thew present PMFSA-PEGDA and PMFSA-DEGDMA hydrogels confirmed their differentiation to cardiomyocytes. This indicates that the cellular microenvironment provided by the PMFSA based hydrogels favored the differentiation of MSCs into myogenic cells. This is due to the favourable characteristics of the materials like amphiphilicity, porosity, water content, protein adsorption and compatibility. So the MSC approaches the scaffolds for attachment, spreading and differentiation by acquiring the metabolites and signals from the surrounding medium. These results are promising for the application of these hydrgel scaffolds for stem cell based cardiac regeneration and tissue engineering. However, more validations, especially in the biological aspects of the differentiated MSC on PMFSA based hydrogels, are needed to extrapolate this approach to clinical arena for MI management.

Chapter 6
SUMMARY AND CONCLUSIONS

12 Summary and conclusions

Tissue engineering of myocardium *in vitro* needs an appropriate hydrogel scaffold material. The performance of tissue engineered myocardial is largely influenced by the material parameters viz mechanical strength of hydrogel scaffold material, compatibility of degradation products of hydrogel scaffold material to the host tissue, interconnected pore architecture of hydrogel for supply of nutrients to cells, maintenance of cellular viability and differentiation and favoring cell integration. None of the hydrogel materials developed so far has met these stringent and diagonally opposite requirements. The major objective of the present investigation was design and development of biomechanically favourable and biodegradable hydrogel scaffolds using biosynthetic comacromers involving 1,2-propanediol, maleic anhydride, mannitol, sebacic acid and sodium alginate, which can elicit favourable long-term biological responses for the engineering of heart tissue. The other objectives include studies on protective effects of hydrogels against oxidative stress, cardiomyoblast growth and adhesion under hydrodynamic conditions, cell cycle analyses of cardiomyoblast progression, co-culture of cardiomyoblast and fibroblast and influence of hydrogels for differentiation of bone marrow MSC to cardiomyocyte.

By combining the biological polymer, alginate with structurally versatile synthetic unsaturated polyesters, the construction of a biosynthetic hydrogel scaffolds with a balanced physiochemical and biomechanical properties and a controlled degradation profile is achieved. Biosynthetic hydrgoel scaffolds were prepared with poly (propylene fumarate)-alginate (HPAS) and poly (mannitol fumarate-co-sebacate)-alginate (PMFSA) comcromers. Monomodal and bimodal network hydrogels were prepared by crosslinking the alginate segments with calcium ions and the unsaturated double bonds of the polyester macromer and crosslinker with different vinyl monomers, methyl methacrylate (MMA), N N' methylene bis acrylamide (NMBA), 2-hydroxy ethyl methacrylate (HEMA), n-butyl methacrylate (BMA), acrylic acid (AA), poly(ethylene glycol diacrylate) (PEGDA) and diethylene glycol dimethacrylate (DEGDMA).

A panel of biomodal hydrogel scaffolds was prepared from HPAS comcaromer. The hydrogels HPAS-MMA, HPAS-NMBA, HPAS-HEMA, HPAS-BMA and HPAS-AA were prepared by crosslnking HPAS comcaromer with calcium and vinyl monomer, methyl methacrylate (MMA), N N' methylene bis acrylamide (NMBA), 2-hydroxy ethyl methacrylate (HEMA), n-butyl methacrylate (BMA) and acrylic acid (AA) respectively. The above combination of reactants along with PEGDA has yielded another set of biomodal hydrogel scaffolds HPAS-PM, HPAS-PN, HPAS-PH, HPAS-PB and HPAS-PA. Similarly PMFSA-PEGDA, PMFSA-NMBA and PMFSA-DEGDMA biomodal hydrogel scaffolds were prepared by crosslnking PMFSA comcaromer with calcium and divinyl monomer poly(ethylene glycol diacrylate) (PEGDA), N N' methylene bis acrylamide (NMBA) and diethylene glycol dimethacrylate (DEGDMA).

ATR spectral analyses of freeze-dried hydrogels confirm the presence of PPF and alginate fractions on the surface of all HPAS based hydrogels and mannitol, fumarate and alginate fractions on the surface of PMFSA based hydrogels. Equilibrium water content (EWC) and swelling (%) of the hydrogels reveals that the introduction of PEGDA segments into the HPAS based hydrogels has imparted hydrophilicity and hold more water. PMFSA based hydrogels also exhibited appreciable water content and holding capacity, which can be attributed to the hydrophilic nature of mannitol and alginate segments. The dynamic water contact angles of present hydrogel scaffolds lies in the range of 40^{o}-60^{o} signifying their amphiphilic nature. The environmental scanning electron microscopy (ESEM) analyses revealed the presence of interconnecting pores. The average pore length of HPAS based hydrogels were found to be around 30-60 μm and that of PMFSA based hydrogels were 5-15 μm. These pores are favourable for easy migration, communication and acquiring the nutrition from the surrounding medium.

The studies on biostability of the HPAS and PMFSA based hydrogel scaffolds in physiological conditions reveal relatively fast degradation with HPAS-HEMA, HPAS-MMA, HPAS-BMA and HPAS-PH. The mechanical properties of the water-swollen HPAS and PMFSA based hydrogels showed tensile properties greater than that of native myocardium whih implies that it can compromise the loss of mechanical properties *in vivo* conditions. Moreover, these hydrogels have appreciable fatigue life in simulated biological conditions.

The DSC analyses of the hydrogels showed higher degree of non-freezing bound water content except in the case of HPAS-PA and HPAS-PM hydrogel. The high degree

of non-freezing bound water favors the micro-niche of the surviving cells in the hydrogel mainly by accomplishing the easy transportation of biomolecules.

The studies on hemocompatibility reveal the hemolytic potential within the acceptable range of 5%, no aggregation of RBCs, no platelet adhesion on the surface. These evaluations confirmed the hemocompatibility of our hydrogels.The studies on adsorption of proteins reveal more than 25% of plasma proteins on the surface of the hydrogels except HPAS-PH, HPAS-PB and HPAS-PM. The adsorbed albumin imparts excellent blood compatibility by providing a friendly niche to the invading cells due to its passivation effect. The studies on cytocompatibility and MTT assay of the present hydrogels showed cell viability of L929 fibroblasts greater than 85%. The studies on genotoxicity and Comet assay of the fast degrading hydrogels (HPAS-No, HPAS-BMA, HPAS-MMA, HPAS-HEMA and HPAS-PH) revealed DNA content in the head region more than 99% and in tail region less than 1%. This confirmed genetic integrity without altering the genome of the cells.

The evaluations of specific biological responses of these hydrogels for cardiac tissue engineering were carried out. These evaluations include long-term viability and infiltration of fibroblast cells on to the interstices of stable hydrogels, protective effects of selected hydrogels against ROS induced oxidative stress on fibroblasts and cardiomyoblasts, cell cycle anlyses of proghression of cardiomyoblasts, co-culture of fibroblasts and cardiomyoblasts, growth of cardiomyoblasts under hydrodynamic conditions and differentiation of bone marrow mesenchymal stem cells (MSC) to cardiac lineage.The studies on long-term viability and infiltration of L929 fibroblast

cells reveal more than 50% viability even after a period of 3 weeks especially PMFSA based hydrogels which is attributed to the cell friendly microenvironment in the hydrogel. Complex macro and micro sized interconnected unidirectional pores introduced by controlled cyclic stretching in morphologically modified (MM) hydrogels induce fibroblast infiltration of 288% with HPAS-PA after one month. These results revealed that the unidirectional porosity provided sufficient rooms for the cell survival by facilitating effective trafficking of nutrients.

The studies on scavenging effects of reactive oxygen species (ROS) using H9c2 cardiomyoblast cells reveal appreciable inherent scavenging capability with HPAS-AA, HPAS-PA, PMFSA-PEGDA and PMFSA-NMBA. The protective effects of these hydrogels may be mediated by the ROS induced crosslinking of available double bonds at the hydrogel-medium interface, prevention of intracellular migration by calcium-induced conformational changes and rigidity in phospholipids present in the surface membrane of cells and also by dilution of ROS by freezing free and non-freezing bound water.

The studies on the growth of H9c2 cardiomyoblast cells under hydrodynamic conditions reveal adherence and growth of cells as clusters onto the scaffolds with viability higher than 50% after 10 days. This indicates the effective communication among the cardiomyoblast cells to get crowded and to function as a single unit. The studies on co-culture of L929 fibroblast cells with H9c2 cardiomyoblast on the PMFSA based hydrogel scaffolds reveal increased viability of the cardiomyoblast cells with cell cycle-arrested fibroblast cells when compared with the scaffold less controls. This

showed that both the cell types grow independently by depending on the secreted molecules from the both.

The cell cycle analysis of H9c2 cells grown on contact with PMFSA based hydrogels showed the existence of 60% cells in the G0/G1 phase of the cell cycle. The cells are constantly progressing through all the phases of the cell cycle as in the case of control. The studies on differentiation of bone marrow mesenchymal stem cells (MSC) to cardiac lineage with PMFSA-PEGDA and PMFSA-DEGDMA hydrogels and gene expression analysis of cardiac specific biomarkers like GATA-4, NKX-2.5, MEF-2, Troponin C and Troponin-C confirm the differentiation of MSCs to cardiac lineage.

The present hydrogels were evaluated for their cardiac tissue engineering applications. The physiochemical and mechanical properties of the present hydrogels are encouraging for their desired applications. All the hydrogels were hemocompatible, cytocompatible and genocompatible. The long-term fibroblast cell viability and infiltration attained on the biostable hydrogel scaffolds from both HPAS and PMFSA system signified their applicability for cardiac tissue engineering. ROS scavenging responses, cell cycle progression, growth under hydrodynamic conditions and co-culture studies on the selected models of hydrogels from both HPAS and PMFSA based hydrogel system showed their ability to sustain cell growth under harsh conditions similar to that of infarct zone. The ability of PMFSA based hydrogels to promote differentiation of MSC to cardiac lineage pave way for their application in stem cell based regenerative therapies for MI management. Comparatively the HPAS-AA, HPAS-PA and PMFSA-PEGDA hydrogels are better candidate for cardiac tissue engineering.

6.1 Future prospects

Regeneration of myocardium can be accomplished by repopulation of the heart with new cardiomyocytes. However repopulating the hearts with new cardiomyocytes may have a beneficial effect, only if the new cells become structurally integrated within the heart and contribute to cardiac function. Induction of cell proliferation and cell cycle progression (i.e., expression of proteins involved with various aspects of cell cycle activity, DNA synthesis, presence of mitotic figures, increases in cell number, etc.) and terminal differentiation of donor fetal cardiomyocytes to form mature adult-like cells are essential for achiving the structural integration within the heart. However, the ultimate success of cardiac repair strategies will depend on the number of de novo cardiomyocytes generated and on their ability to form a functional syncytium with the preexisting myocardium. It is thus imperative that cell cycle activity, cardiomyogenic activity, and functional activity are essential events in the regenerative interventions.

The present HPAS-AA, HPAS-PA and PMFSA-PEGDA hydrogel scaffolds were proven to have inherent ROS scavenging responses, cell cycle progression, and growth under hydrodynamic conditions and sustaining the co-culture of cells and ability to promote differentiation of MSC to cardiac lineage. Therefore, these cardiomyocte-loaded hydrogel scaffolds are more promsing tissue engineered product, which can

integrate within the heart. Accordingly, the functional acivity of these tissue engineered product *in vivo* has to be determined so that cardiomyocte-loaded myocardial patch implant could emerge as clinically relevant implant for the treatment of cardiac diseases.

References

Abbate Antonio, Biondi-Zoccai Giuseppe GL, Bussani Rossana, Dobrina Aldo, Camilot Debora, Feroce Florinda, Rossiello Raffaele, Baldi Feliciano, Silvestri Furio, Biasucci Luigi M, Baldi Alfonso (2003) Increased myocardial apoptosis in patients with unfavorable left ventricular remodeling and early symptomatic post-infarction heart failure. *J. Am. Coll. Cardiol.* 41: 753–760.

Akhyari Payam, Fedak Paul WM, Weisel Richard D, Lee Tsu-Yee Joseph, Verma Subodh, Mickle Donald AG, Li Ren-Ke (2002) Mechanical stretch regimen enhances the formation of bioengineered autologous cardiac muscle grafts. *Circulation* 106: I137–142.

Akins RE, Schroedl NA, Gonda SR, Hartzell CR (1997) Neonatal rat heart cells cultured in simulated microgravity. *In Vitro Cell. Dev. Biol. Anim.* 33: 337–343.

Aldenhoff YBJ, Koole LH (2003) Platelet adhesion studies on dipyridamole coated polyurethane surfaces. *Eur. Cell. Mater.* 5: 61–67; discussion 67.

Alge Daniel L, Azagarsamy Malar A, Donohue Dillon F, Anseth Kristi S (2013) Synthetically tractable click hydrogels for three-dimensional cell culture formed using tetrazine-norbornene chemistry. *Biomacromolecules* 14: 949–953.

Anderl Jeff N, Robey Thomas E, Stayton Patrick S, Murry Charles E (2009) Retention and biodistribution of microspheres injected into ischemic myocardium. *J. Biomed. Mater. Res. A* 88: 704–710.

Annabi Nasim, Nichol Jason W, Zhong Xia, Ji Chengdong, Koshy Sandeep, Khademhosseini Ali, Dehghani Fariba (2010) Controlling the porosity and microarchitecture of hydrogels for tissue engineering. *Tissue Eng. Part B Rev.* 16: 371–383.

Badrossamay Mohammad Reza, McIlwee Holly Alice, Goss Josue A, Parker Kevin Kit (2010) Nanofiber Assembly by Rotary Jet-Spinning. *Nano Lett.* 10: 2257–2261.

Bahorun T, Soobrattee MA, Ramma VL, Aruoma OI (2006) Free radicals and antioxidants in cardiovascular health and disease. *Internet J. Med. Update* 1: 3–5.

Baker Erin L, Bonnecaze Roger T, Zaman Muhammad H (2009) Extracellular matrix stiffness and architecture govern intracellular rheology in cancer. *Biophys. J.* 97: 1013–1021.

Balakrishnan Biji, Jayakrishnan A (2005) Self-cross-linking biopolymers as injectable in situ forming biodegradable scaffolds. *Biomaterials* 26: 3941–3951.

Barash Yiftach, Dvir Tal, Tandeitnik Pini, Ruvinov Emil, Guterman Hugo, Cohen Smadar (2010) Electric field stimulation integrated into perfusion bioreactor for cardiac tissue engineering. *Tissue Eng. Part C Methods* 16: 1417–1426.

Barrett Devin G, Yousaf Muhammad N (2009) Design and Applications of Biodegradable Polyester Tissue Scaffolds Based on Endogenous Monomers Found in Human Metabolism. *Molecules* 14: 4022–4050.

Barsotti A, Di Napoli P, Di Girolamo E, Di Muzio M, Vitullo P, Dini FL, Gallina S, Modesti A (1994) [Role of interstitial myocardium in ischemia-reperfusion injury: experimental data and clinical implications]. *Cardiol. Rome Italy* 39: 381–388.

Baskurt Oguz K, Meiselman Herbert J (2007) Hemodynamic effects of red blood cell aggregation. *Indian J. Exp. Biol.* 45: 25–31.

Bel Alain, Planat-Bernard Valérie, Saito Atsuhiro, Bonnevie Lionel, Bellamy Valérie, Sabbah Laurent, Bellabas Linda, Brinon Benjamin, Vanneaux Valérie, Pradeau Pascal, Peyrard Séverine, Larghero Jérôme, Pouly Julia, Binder Patrice, Garcia Sylvie, Shimizu Tatsuya, Sawa Yoshiki, Okano Teruo, Bruneval Patrick, Desnos Michel, Hagège Albert A, Casteilla Louis, Pucéat Michel, Menasché Philippe (2010) Composite cell sheets: a further step toward safe and effective myocardial regeneration by cardiac progenitors derived from embryonic stem cells. *Circulation* 122: S118–123.

Beltrami Antonio P, Barlucchi Laura, Torella Daniele, Baker Mathue, Limana Federica, Chimenti Stefano, Kasahara Hideko, Rota Marcello, Musso Ezio, Urbanek Konrad, Leri Annarosa, Kajstura Jan, Nadal-Ginard Bernardo, Anversa Piero (2003) Adult cardiac stem cells are multipotent and support myocardial regeneration. *Cell* 114: 763–776.

Berry CL, Greenwald SE, Rivett JF (1975) Static mechanical properties of the developing and mature rat aorta. *Cardiovasc. Res.* 9: 669–678.

Bhana Bashir, Iyer Rohin K, Chen Wen Li Kelly, Zhao Ruogang, Sider Krista L, Likhitpanichkul Morakot, Simmons Craig A, Radisic Milica (2010) Influence of substrate stiffness on the phenotype of heart cells. *Biotechnol. Bioeng.* 105: 1148–1160.

Bian Weining, Bursac Nenad (2009) Engineered skeletal muscle tissue networks with controllable architecture. *Biomaterials* 30: 1401–1412.

Boffito Monica, Sartori Susanna, Ciardelli Gianluca (2014) Polymeric scaffolds for cardiac tissue engineering: requirements and fabrication technologies. *Polym. Int.* 63: 2–11.

Boublik Jan, Park Hyoungshin, Radisic Milica, Tognana Enrico, Chen Fen, Pei Ming, Vunjak-Novakovic Gordana, Freed Lisa E (2005) Mechanical properties and remodeling of hybrid cardiac constructs made from heart cells, fibrin, and biodegradable, elastomeric knitted fabric. *Tissue Eng.* 11: 1122–1132.

Branco Érika, Fioretto Emerson Ticona, Cabral Rosa, Palmera Carlos Alberto Sarmento, Gregores Guilherme Buzon, Stopiglia Angelo João, Maiorka Paulo César, Lemos Pedro Alves, Campos Carlos, Takimura Celso, Ramires José Antônio Franchini, Miglino Maria Angelica (2009) Myocardial homing after intrapericardial infusion of Bone Marrow Mononuclear Cells. *Arq. Bras. Cardiol.* 93: e50–e53.

Brown Melissa A, Iyer Rohin K, Radisic Milica (2008) Pulsatile perfusion bioreactor for cardiac tissue engineering. *Biotechnol. Prog.* 24: 907–920.

Bryant Stephanie J, Anseth Kristi S (2003) Controlling the spatial distribution of ECM components in degradable PEG hydrogels for tissue engineering cartilage. *J. Biomed. Mater. Res. A* 64: 70–79.

Bursac N, Papadaki M, Cohen RJ, Schoen FJ, Eisenberg SR, Carrier R, Vunjak-Novakovic G, Freed LE (1999) Cardiac muscle tissue engineering: toward an in vitro model for electrophysiological studies. *Am. J. Physiol.* 277: H433–444.

Bursac Nenad, Papadaki Maria, White John A, Eisenberg Solomon R, Vunjak-Novakovic Gordana, Freed Lisa E (2003) Cultivation in rotating bioreactors promotes maintenance of cardiac myocyte electrophysiology and molecular properties. *Tissue Eng.* 9: 1243–1253.

Carrier RL, Papadaki M, Rupnick M, Schoen FJ, Bursac N, Langer R, Freed LE, Vunjak-Novakovic G (1999) Cardiac tissue engineering: cell seeding, cultivation parameters, and tissue construct characterization. *Biotechnol. Bioeng.* 64: 580–589.

Cascone Maria Grazia, Lazzeri Luigi, Sparvoli Enzo, Scatena Manuele, Serino Lorenzo Pio, Danti Serena (2004) Morphological evaluation of bioartificial hydrogels as potential tissue engineering scaffolds. *J. Mater. Sci. Mater. Med.* 15: 1309–1313.

Chan BP, Leong KW (2008) Scaffolding in tissue engineering: general approaches and tissue-specific considerations. *Eur. Spine J.* 17: 467–479.

Chauvel-Lebret DJ, Auroy P, Tricot-Doleux S, Bonnaure-Mallet M (2001) Evaluation of the capacity of the SCGE assay to assess the genotoxicity of biomaterials. *Biomaterials* 22: 1795–1801.

Choi Yu Suk, Matsuda Ken, Dusting Gregory J, Morrison Wayne A, Dilley Rodney J (2010) Engineering cardiac tissue in vivo from human adipose-derived stem cells. *Biomaterials* 31: 2236–2242.

Chung Chiung-yin, Bien Harold, Sobie Eric A, Dasari Vikram, McKinnon David, Rosati Barbara, Entcheva Emilia (2011) Hypertrophic phenotype in cardiac cell assemblies solely by structural cues and ensuing self-organization. *FASEB J. Off. Publ. Fed. Am. Soc. Exp. Biol.* 25: 851–862.

Copland Ian B, Jolicoeur E Marc, Gillis Marc-Antoine, Cuerquis Jessica, Eliopoulos Nicoletta, Annabi Borhane, Calderone Angelo, Tanguay Jean-Francois, Ducharme Anique, Galipeau Jacques (2008) Coupling erythropoietin secretion to mesenchymal stromal cells enhances their regenerative properties. *Cardiovasc. Res.* 79: 405–415.

Cox Thomas R, Erler Janine T (2011) Remodeling and homeostasis of the extracellular matrix: implications for fibrotic diseases and cancer. *Dis. Model. Mech.* 4: 165–178.

Curtis Matthew W, Russell Brenda (2009) Cardiac Tissue Engineering. *J. Cardiovasc. Nurs.* 24: 87–92. doi:10.1097/01.JCN.0000343562.06614.49.

Dar Ayelet, Shachar Michal, Leor Jonathan, Cohen Smadar (2002) Optimization of cardiac cell seeding and distribution in 3D porous alginate scaffolds. *Biotechnol. Bioeng.* 80: 305–312.

DeQuach Jessica A, Mezzano Valeria, Miglani Amar, Lange Stephan, Keller Gordon M, Sheikh Farah, Christman Karen L (2010) Simple and High Yielding Method for Preparing Tissue Specific Extracellular Matrix Coatings for Cell Culture. *PLoS ONE* 5: e13039.

Dohmen Pascal M, Ozaki Shigeyuki, Verbeken Erik, Yperman Jessa, Flameng Willem, Konertz Wolfgang F (2002) Tissue engineering of an auto-xenograft pulmonary heart valve. *Asian Cardiovasc. Thorac. Ann.* 10: 25–30.

Di Donato M, Sabatier M, Dor V, Gensini GF, Toso A, Maioli M, Stanley AW, Athanasuleas C, Buckberg G (2001) Effects of the Dor procedure on left ventricular dimension and shape and geometric correlates of mitral regurgitation one year after surgery. *J. Thorac. Cardiovasc. Surg.* 121: 91–96.

Drury Jeanie L, Mooney David J (2003) Hydrogels for tissue engineering: scaffold design variables and applications. *Biomaterials* 24: 4337–4351.

Elbert Donald L (2011) Liquid-liquid two-phase systems for the production of porous hydrogels and hydrogel microspheres for biomedical applications: A tutorial review. *Acta Biomater.* 7: 31–56.

El-Sherbiny Ibrahim M, Yacoub Magdi H (2013) Hydrogel scaffolds for tissue engineering: Progress and challenges. *Glob. Cardiol. Sci. Pract.* 2013: 316–342.

Ely SW, Berne RM (1992) Protective effects of adenosine in myocardial ischemia. *Circulation* 85: 893–904.

Engelmayr George C, Cheng Mingyu, Bettinger Christopher J, Borenstein Jeffrey T, Langer Robert, Freed Lisa E (2008) Accordion-like honeycombs for tissue engineering of cardiac anisotropy. *Nat. Mater.* 7: 1003–1010.

Eschenhagen T, Fink C, Remmers U, Scholz H, Wattchow J, Weil J, Zimmermann W, Dohmen HH, Schäfer H, Bishopric N, Wakatsuki T, Elson EL (1997) Three-dimensional reconstitution of embryonic cardiomyocytes in a collagen matrix: a new heart muscle model system. *FASEB J. Off. Publ. Fed. Am. Soc. Exp. Biol.* 11: 683–694.

Fan Changjiang, Liao Liqiong, Zhang Chao, Liu Lijian (2013) A tough double network hydrogel for cartilage tissue engineering. *J. Mater. Chem. B* 1: 4251–4258.

Finosh GT, Jayabalan Muthu (2012) Regenerative therapy and tissue engineering for the treatment of end-stage cardiac failure: new developments and challenges. *Biomatter* 2: 1–14.

Forte Giancarlo, Pietronave Stefano, Nardone Giorgia, Zamperone Andrea, Magnani Eugenio, Pagliari Stefania, Pagliari Francesca, Giacinti Cristina, Nicoletti Carmine, Musaró Antonio, Rinaldi Mauro, Ribezzo Marco, Comoglio Chiara, Traversa Enrico, Okano Teruo, Minieri Marilena, Prat Maria, Di Nardo Paolo (2011) Human Cardiac Progenitor Cell Grafts as Unrestricted Source of Supernumerary Cardiac Cells in Healthy Murine Hearts. *STEM CELLS* 29: 2051–2061.

Frisman Ilya, Seliktar Dror, Bianco-Peled Havazelet (2012) Nanostructuring biosynthetic hydrogels for tissue engineering: a cellular and structural analysis. *Acta Biomater.* 8: 51–60.

Fujimoto Kazuro L, Guan Jianjun, Oshima Hideki, Sakai Tetsuro, Wagner William R (2007) In Vivo Evaluation of a Porous, Elastic, Biodegradable Patch for Reconstructive Cardiac Procedures. *Ann. Thorac. Surg.* 83: 648–654.

Fukuda Junji, Khademhosseini Ali, Yeo Yoon, Yang Xiaoyu, Yeh Judy, Eng George, Blumling James, Wang Chi-Fong, Kohane Daniel S, Langer Robert (2006) Micromolding of photocrosslinkable chitosan hydrogel for spheroid microarray and co-cultures. *Biomaterials* 27: 5259–5267.

Gayet JC, Fortier G (1995) Drug release from new bioartificial hydrogel. *Artif. Cells. Blood Substit. Immobil. Biotechnol.* 23: 605–611.

Geckil Hikmet, Xu Feng, Zhang Xiaohui, Moon SangJun, Demirci Utkan (2010) Engineering hydrogels as extracellular matrix mimics. *Nanomed.* 5: 469–484.

Gerecht Sharon, Townsend Seth A, Pressler Heather, Zhu Han, Nijst Christiaan LE, Bruggeman Joost P, Nichol Jason W, Langer Robert (2007) A porous photocurable elastomer for cell encapsulation and culture. *Biomaterials* 28: 4826–4835.

Gnanaprakasam Thankam Finosh, Muthu Jayabalan (2013a) Influence of plasma protein–hydrogel interaction moderated by absorption of water on long-term cell viability in amphiphilic biosynthetic hydrogels. *RSC Adv.* 3: 24509.

Gnanaprakasam Thankam Finosh, Muthu Jayabalan (2013b) Influence of plasma protein–hydrogel interaction moderated by absorption of water on long-term cell viability in amphiphilic biosynthetic hydrogels. *RSC Adv.* 3: 24509.

Gnanaprakasam Thankam Finosh, Muthu Jayabalan, Sankar Vandana, Kozhiparambil Gopal Raghu (2013) Growth and survival of cells in biosynthetic poly vinyl alcohol–alginate IPN hydrogels for cardiac applications. *Colloids Surf. B Biointerfaces* 107: 137–145.

Go Alan S, Mozaffarian Dariush, Roger Véronique L, Benjamin Emelia J, Berry Jarett D, Borden William B, Bravata Dawn M, Dai Shifan, Ford Earl S, Fox Caroline S, Franco Sheila, Fullerton Heather J, Gillespie Cathleen, Hailpern Susan M, Heit John A, Howard Virginia J, Huffman Mark D, Kissela Brett M, Kittner Steven J, Lackland Daniel T, Lichtman Judith H, Lisabeth Lynda D, Magid David, Marcus Gregory M, Marelli Ariane, Matchar David B, McGuire Darren K, Mohler Emile R, Moy Claudia S, Mussolino Michael E, Nichol Graham, Paynter Nina P, Schreiner Pamela J, Sorlie Paul D, Stein Joel, Turan Tanya N, Virani Salim S, Wong Nathan D, Woo Daniel, Turner Melanie B (2013) Heart Disease and Stroke Statistics—2013 Update A Report From the American Heart Association. *Circulation* 127: e6–e245.

Gonen-Wadmany Maya, Gepstein Lior, Seliktar Dror (2004) Controlling the cellular organization of tissue-engineered cardiac constructs. *Ann. N. Y. Acad. Sci.* 1015: 299–311.

Hago Eltjani-Eltahir, Li Xinsong (2013) Interpenetrating Polymer Network Hydrogels Based on Gelatin and PVA by Biocompatible Approaches: Synthesis and Characterization. *Adv. Mater. Sci. Eng.* 2013: 1–8.

Hanjaya-Putra Donny, Bose Vivek, Shen Yu-I, Yee Jane, Khetan Sudhir, Fox-Talbot Karen, Steenbergen Charles, Burdick Jason A, Gerecht Sharon (2011) Controlled activation of morphogenesis to generate a functional human microvasculature in a synthetic matrix. *Blood* 118: 804–815.

Von Harsdorf R, Li PF, Dietz R (1999) Signaling pathways in reactive oxygen species-induced cardiomyocyte apoptosis. *Circulation* 99: 2934–2941.

Hill Elliott, Boontheekul Tanyarut, Mooney David J (2006) Regulating activation of transplanted cells controls tissue regeneration. *Proc. Natl. Acad. Sci. U. S. A.* 103: 2494–2499.

Hoover-Plow Jane, Gong Y (2012) Challenges for heart disease stem cell therapy. *Vasc. Health Risk Manag.* 99.

Huang Guoyou, Wang Lin, Wang ShuQi, Han Yulong, Wu Jinhui, Zhang Qiancheng, Xu Feng, Lu Tian Jian (2012) Engineering three-dimensional cell mechanical microenvironment with hydrogels. *Biofabrication* 4: 042001.

Hussain Ali, Collins George, Yip Derek, Cho Cheul H (2013) Functional 3-D cardiac co-culture model using bioactive chitosan nanofiber scaffolds. *Biotechnol. Bioeng.* 110: 637–647.

Isaka Mitsuhiro, Nishibe Toshiya, Okuda Yasuhiro, Saito Masaru, Seno Takahiro, Yamashita Kazuto, Izumisawa Yasuharu, Kotani Tadao, Yasuda Keishu (2006)

Experimental study on stability of a high-porosity expanded polytetrafluoroethylene graft in dogs. *Ann. Thorac. Cardiovasc. Surg. Off. J. Assoc. Thorac. Cardiovasc. Surg. Asia* 12: 37–41.

Ishii Osamu, Shin Michael, Sueda Taijiro, Vacanti Joseph P (2005) In vitro tissue engineering of a cardiac graft using a degradable scaffold with an extracellular matrix-like topography. *J. Thorac. Cardiovasc. Surg.* 130: 1358–1363.

Jayabalan M, Shalumon KT, Mitha MK (2009) Injectable biomaterials for minimally invasive orthopedic treatments. *J. Mater. Sci. Mater. Med.* 20: 1379–1387.

Jayabalan M, Thomas V, Sreelatha PK (2000) Studies on poly(propylene fumarate-co-ethylene glycol) based bone cement. *Biomed. Mater. Eng.* 10: 57–71.

Jefferson Brian K, Topol Eric J (2005) Molecular mechanisms of myocardial infarction. *Curr. Probl. Cardiol.* 30: 333–374.

Jin Lee Hyeong, Kim Geun Hyung (2012) Cryogenically direct-plotted alginate scaffolds consisting of micro/nano-architecture for bone tissue regeneration. *RSC Adv.* 2: 7578.

Jongpaiboonkit Leenaporn, King William J, Lyons Gary E, Paguirigan Amy L, Warrick Jay W, Beebe David J, Murphy William L (2008) An adaptable hydrogel array format for 3-dimensional cell culture and analysis. *Biomaterials* 29: 3346–3356.

Kallukalam BC, Jayabalan M, Sankar V (2009) Studies on chemically crosslinkable carboxy terminated-poly(propylene fumarate-co-ethylene glycol)-acrylamide hydrogel as an injectable biomaterial. *Biomed. Mater. Bristol Engl.* 4: 015002.

Karageorgiou Vassilis, Kaplan David (2005) Porosity of 3D biomaterial scaffolds and osteogenesis. *Biomaterials* 26: 5474–5491.

Khademhosseini Ali, Langer Robert (2007) Microengineered hydrogels for tissue engineering. *Biomaterials* 28: 5087–5092.

Kim Jinku, Hefferan Theresa E, Yaszemski Michael J, Lu Lichun (2009) Potential of Hydrogels Based on Poly(Ethylene Glycol) and Sebacic Acid as Orthopedic Tissue Engineering Scaffolds. *Tissue Eng. Part A* 15: 2299–2307.

Kim Yong-Nyun, Koo Kyung Hee, Sung Jee Young, Yun Un-Jung, Kim Hyeryeong (2012) Anoikis Resistance: An Essential Prerequisite for Tumor Metastasis. *Int. J. Cell Biol.* 2012.

Kinugawa S, Tsutsui H, Hayashidani S, Ide T, Suematsu N, Satoh S, Utsumi H, Takeshita A (2000) Treatment with dimethylthiourea prevents left ventricular remodeling and failure after experimental myocardial infarction in mice: role of oxidative stress. *Circ. Res.* 87: 392–398.

Klimanskaya Irina, Rosenthal Nadia, Lanza Robert (2008) Derive and conquer: sourcing and differentiating stem cells for therapeutic applications. *Nat. Rev. Drug Discov.* 7: 131–142.

Klouda Leda, Hacker Michael C, Kretlow James D, Mikos Antonios G (2009) Cytocompatibility evaluation of amphiphilic, thermally responsive and chemically crosslinkable macromers for in situ forming hydrogels. *Biomaterials* 30: 4558–4566.

Kloxin April M, Tibbitt Mark W, Anseth Kristi S (2010) Synthesis of photodegradable hydrogels as dynamically tunable cell culture platforms. *Nat. Protoc.* 5: 1867–1887.

Kochupura Paul V, Azeloglu Evren U, Kelly Damon J, Doronin Sergey V, Badylak Stephen F, Krukenkamp Irvin B, Cohen Ira S, Gaudette Glenn R (2005) Tissue-Engineered Myocardial Patch Derived From Extracellular Matrix Provides Regional Mechanical Function. *Circulation* 112: I–144–I–149.

Kofidis Theo, Akhyari Payam, Wachsmann Björn, Boublik Jan, Mueller-Stahl Knut, Leyh Rainer, Fischer Stefan, Haverich A (2002) A novel bioartificial myocardial tissue and its prospective use in cardiac surgery. *Eur. J. Cardio-Thorac. Surg. Off. J. Eur. Assoc. Cardio-Thorac. Surg.* 22: 238–243.

Kolodney MS, Elson EL (1993) Correlation of myosin light chain phosphorylation with isometric contraction of fibroblasts. *J. Biol. Chem.* 268: 23850–23855.

Kong Yen P, Carrion Bita, Singh Rahul K, Putnam Andrew J (2013) Matrix identity and tractional forces influence indirect cardiac reprogramming. *Sci. Rep.* 3.

Langer R, Vacanti J (1993) Tissue engineering. *Science* 260: 920–926.

Leach Jennie B, Schmidt Christine E (2005) Characterization of protein release from photocrosslinkable hyaluronic acid-polyethylene glycol hydrogel tissue engineering scaffolds. *Biomaterials* 26: 125–135.

Lee Ka-Heng, Chow Yuh-Lit, Sharmili Vidyadaran, Abas Faridah, Alitheen Noorjahan Banu Mohamed, Shaari Khozirah, Israf Daud Ahmad, Lajis Nordin Haji, Syahida Ahmad (2012) BDMC33, A Curcumin Derivative Suppresses

Inflammatory Responses in Macrophage-Like Cellular System: Role of Inhibition in NF-κB and MAPK Signaling Pathways. *Int. J. Mol. Sci.* 13: 2985–3008.

Lee Wen-Fu, Chen Ying-Jou (2001) Studies on preparation and swelling properties of the N-isopropylacrylamide/chitosan semi-IPN and IPN hydrogels. *J. Appl. Polym. Sci.* 82: 2487–2496.

Lees Justin G, Lim Sue Anne, Croll Tristan, Williams Georgia, Lui Sylvia, Cooper-White Justin, McQuade Leon R, Mathiyalagan Bagyalakshmi, Tuch Bernard E (2007) Transplantation of 3D scaffolds seeded with human embryonic stem cells: biological features of surrogate tissue and teratoma-forming potential. *Regen. Med.* 2: 289–300.

Leor J, Aboulafia-Etzion S, Dar A, Shapiro L, Barbash IM, Battler A, Granot Y, Cohen S (2000) Bioengineered cardiac grafts: A new approach to repair the infarcted myocardium? *Circulation* 102: III56–61.

Leor Jonathan, Cohen Smadar (2004) Myocardial tissue engineering: creating a muscle patch for a wounded heart. *Ann. N. Y. Acad. Sci.* 1015: 312–319.

Lewis MR. (1920) Muscular contraction in tissue cultures. *Contrib Embryol Carnegie Inst* 9: 191–212.

Li RK, Jia ZQ, Weisel RD, Mickle DA, Choi A, Yau TM (1999) Survival and function of bioengineered cardiac grafts. *Circulation* 100: II63–69.

Li Ren-Ke, Yau Terrence M, Weisel Richard D, Mickle Donald AG, Sakai Tetsuro, Choi Angel, Jia Zhi-Qiang (2000) Construction of a bioengineered cardiac graft. *J. Thorac. Cardiovasc. Surg.* 119: 368–375.

Li Zhenqing, Guan Jianjun (2011) Hydrogels for Cardiac Tissue Engineering. *Polymers* 3: 740–761.

Loh Xian Jun, Li Jun (2007) Biodegradable thermosensitive copolymer hydrogels for drug delivery. *Expert Opin. Ther. Pat.* 17: 965–977.

Luo Qing, Song Guanbin, Song Yuanhui, Xu Baiyao, Qin Jian, Shi Yisong (2009) Indirect co-culture with tenocytes promotes proliferation and mRNA expression of tendon/ligament related genes in rat bone marrow mesenchymal stem cells. *Cytotechnology* 61: 1–10.

Madden Lauran R, Mortisen Derek J, Sussman Eric M, Dupras Sarah K, Fugate James A, Cuy Janet L, Hauch Kip D, Laflamme Michael A, Murry Charles E, Ratner Buddy D (2010) Proangiogenic scaffolds as functional templates for cardiac tissue engineering. *Proc. Natl. Acad. Sci.* 201006442.

.Mäkinen KK, Hämäläinen MM (1985) Metabolic effects in rats of high oral doses of galactitol, mannitol and xylitol. *J. Nutr.* 115: 890–899.

Mandal Biman B, Kundu Subhas C (2009) Cell proliferation and migration in silk fibroin 3D scaffolds. *Biomaterials* 30: 2956–2965.

Mano JF, Silva GA, Azevedo HS, Malafaya PB, Sousa RA, Silva SS, Boesel LF, Oliveira JM, Santos TC, Marques AP, Neves NM, Reis RL (2007) Natural origin

biodegradable systems in tissue engineering and regenerative medicine: present status and some moving trends. *J. R. Soc. Interface R. Soc.* 4: 999–1030.

Martens Timothy P, Godier Amandine FG, Parks Jonathan J, Wan Leo Q, Koeckert Michael S, Eng George M, Hudson Barry I, Sherman Warren, Vunjak-Novakovic Gordana (2009) Percutaneous cell delivery into the heart using hydrogels polymerizing in situ. *Cell Transplant.* 18: 297–304.

Masaki Hitoshi, Izutsu Yukiko, Yahagi Shoichi, Okano Yuri (2009) Reactive oxygen species in HaCaT keratinocytes after UVB irradiation are triggered by intracellular Ca(2+) levels. *J. Investig. Dermatol. Symp. Proc. Soc. Investig. Dermatol. Inc Eur. Soc. Dermatol. Res.* 14: 50–52.

Matsuura Katsuhisa, Nagai Toshio, Nishigaki Nobuhiro, Oyama Tomomi, Nishi Junichiro, Wada Hiroshi, Sano Masanori, Toko Haruhiro, Akazawa Hiroshi, Sato Toshiaki, Nakaya Haruaki, Kasanuki Hiroshi, Komuro Issei (2004) Adult cardiac Sca-1-positive cells differentiate into beating cardiomyocytes. *J. Biol. Chem.* 279: 11384–11391.

McDevitt Todd C, Palecek Sean P (2008) Innovation in the culture and derivation of pluripotent human stem cells. *Curr. Opin. Biotechnol.* 19: 527–533.

McDonald TF, Sachs HG, DeHaan RL (1972) Development of Sensitivity to Tetrodotoxin in Beating Chick Embryo Hearts, Single Cells, and Aggregates. *Science* 176: 1248–1250.

Mironov Vladimir, Boland Thomas, Trusk Thomas, Forgacs Gabor, Markwald Roger R (2003) Organ printing: computer-aided jet-based 3D tissue engineering. *Trends Biotechnol.* 21: 157–161.

Mironov Vladimir, Visconti Richard P, Kasyanov Vladimir, Forgacs Gabor, Drake Christopher J, Markwald Roger R (2009) Organ printing: Tissue spheroids as building blocks. *Biomaterials* 30: 2164–2174.

Mirsadraee Saeed, Wilcox Helen E, Korossis Sotiris A, Kearney John N, Watterson Kevin G, Fisher John, Ingham Eileen (2006) Development and characterization of an acellular human pericardial matrix for tissue engineering. *Tissue Eng.* 12: 763–773.

Miyagawa Shigeru, Sawa Yoshiki, Sakakida Satoru, Taketani Satoshi, Kondoh Haruhiko, Memon Imran Ahmed, Imanishi Yukiko, Shimizu Tatsuya, Okano Teruo, Matsuda Hikaru (2005) Tissue cardiomyoplasty using bioengineered contractile cardiomyocyte sheets to repair damaged myocardium: their integration with recipient myocardium. *Transplantation* 80: 1586–1595.

MOSCONA AA (1959) Tissues from dissociated cells. *Sci. Am.* 200: 132–134 passim.

Naito Hiroshi, Takewa Yoshiaki, Mizuno Toshihide, Ohya Shoji, Nakayama Yasuhide, Tatsumi Eisuke, Kitamura Soichiro, Takano Hisateru, Taniguchi Shigeki, Taenaka Yoshiyuki (2004) Three-dimensional cardiac tissue engineering using a thermoresponsive artificial extracellular matrix. *ASAIO J. Am. Soc. Artif. Intern. Organs 1992* 50: 344–348.

Nelson Devin M, Ma Zuwei, Fujimoto Kazuro L, Hashizume Ryotaro, Wagner William R (2011) Intra-myocardial biomaterial injection therapy in the treatment of heart failure: Materials, outcomes and challenges. *Acta Biomater.* 7: 1–15.

Nerem Robert M (2007) Cell-based therapies: from basic biology to replacement, repair, and regeneration. *Biomaterials* 28: 5074–5077.

Nirmala Chandrasekar, Puvanakrishnan Rengarajulu (1996) Protective role of curcumin against isoproterenol induced myocardial infarction in rats. *Mol. Cell. Biochem.* 159: 85–93.

Norotte Cyrille, Marga Francois S, Niklason Laura E, Forgacs Gabor (2009) Scaffold-free vascular tissue engineering using bioprinting. *Biomaterials* 30: 5910–5917.

Nygren Håkan (1996) Initial reactions of whole blood with hydrophilic and hydrophobic titanium surfaces. *Colloids Surf. B Biointerfaces* 6: 329–333.

Ogunro Sunday, Ogungbamigbe Olabisi, Salawu Afolabi, Idogun Sylvester (2012) Erythrocyte antioxidant enzymes and lipid peroxidation in patients with acute attack of Plasmodium falciparum. *Oxid. Antioxid. Med. Sci.* 1: 1.

Pal K, Banthia AK, Majumdar DK (2009) Polymeric Hydrogels: Characterization and Biomedical Applications. *Des. Monomers Polym.* 12: 197–220.

Papadaki M, Bursac N, Langer R, Merok J, Vunjak-Novakovic G, Freed LE (2001) Tissue engineering of functional cardiac muscle: molecular, structural, and electrophysiological studies. *Am. J. Physiol. Heart Circ. Physiol.* 280: H168–178.

Peng Zhiyuan, Shen Yongqiang (2011) Study on Biological Safety of Polyvinyl Alcohol/Collagen Hydrogel as Tissue Substitute (I). *Polym.-Plast. Technol. Eng.* 50: 245–250.

Perin Emerson C (2006) Stem Cell Therapy for Cardiovascular Disease. *Tex. Heart Inst. J.* 33: 204–208.

Pojda Zygmunt, Machaj Eugeniusz K, Ołdak Tomasz, Gajkowska Agnieszka, Jastrzewska Marzena (2005) Nonhematopoietic stem cells of fetal origin--how much of today's enthusiasm will pass the time test? *Folia Histochem. Cytobiol. Pol. Acad. Sci. Pol. Histochem. Cytochem. Soc.* 43: 209–212.

Pok Seokwon, Myers Jackson D, Madihally Sundararajan V, Jacot Jeffrey G (2013) A multilayered scaffold of a chitosan and gelatin hydrogel supported by a PCL core for cardiac tissue engineering. *Acta Biomater.* 9: 5630–5642.

Provenzano Paolo P, Inman David R, Eliceiri Kevin W, Trier Steven M, Keely Patricia J (2008) Contact Guidance Mediated Three-Dimensional Cell Migration is Regulated by Rho/ROCK-Dependent Matrix Reorganization. *Biophys. J.* 95: 5374–5384.

Radisic Milica, Park Hyoungshin, Shing Helen, Consi Thomas, Schoen Frederick J, Langer Robert, Freed Lisa E, Vunjak-Novakovic Gordana (2004) Functional assembly of engineered myocardium by electrical stimulation of cardiac myocytes cultured on scaffolds. *Proc. Natl. Acad. Sci. U. S. A.* 101: 18129–18134.

Ratner Buddy D, Hoffman Allan S, Schoen Frederick J, Lemons Jack E (2012) Biomaterials Science, Third Edition: An Introduction to Materials in Medicine 3 edition. Amsterdam ; Boston: Academic Press, November 8.

Ribble Deborah, Goldstein Nathaniel B, Norris David A, Shellman Yiqun G (2005) A simple technique for quantifying apoptosis in 96-well plates. *BMC Biotechnol.* 5: 12.

Rnjak-Kovacina Jelena, Wise Steven G, Li Zhe, Maitz Peter KM, Young Cara J, Wang Yiwei, Weiss Anthony S (2011) Tailoring the porosity and pore size of electrospun synthetic human elastin scaffolds for dermal tissue engineering. *Biomaterials* 32: 6729–6736.

Sailakshmi G, Mitra Tapas, Gnanamani A (2013) Engineering of chitosan and collagen macromolecules using sebacic acid for clinical applications. *Prog. Biomater.* 2: 1–12.

Sakai T, Li RK, Weisel RD, Mickle DA, Kim ET, Jia ZQ, Yau TM (2001) The fate of a tissue-engineered cardiac graft in the right ventricular outflow tract of the rat. *J. Thorac. Cardiovasc. Surg.* 121: 932–942.

Santos Celio XC, Anilkumar Narayana, Zhang Min, Brewer Alison C, Shah Ajay M (2011) Redox signaling in cardiac myocytes. *Free Radic. Biol. Med.* 50: 777–793.

Sawa Yoshiki (2010) [Myocardial regeneration for heart failure]. *Nihon Rinsho Jpn. J. Clin. Med.* 68: 719–725.

Serrano Maria Concepcion, Chung Eun Ji, Ameer Guillermo A (2010) Advances and Applications of Biodegradable Elastomers in Regenerative Medicine. *Adv. Funct. Mater.* 20: 192–208.

Severs Nicholas J (2000) The cardiac muscle cell. *BioEssays* 22: 188–199.

Shakya Akhilesh Kumar, Holmdahl Rikard, Nandakumar Kutty Selva, Kumar Ashok (2013) Polymeric cryogels are biocompatible, and their biodegradation is independent of oxidative radicals: Biocompatibility And Biodegradation Of Cryogels. *J. Biomed. Mater. Res. A*: n/a–n/a. doi:10.1002/jbm.a.35013.

Shapira Keren, Dikovsky Daniel, Habib Manhal, Gepstein Lior, Seliktar Dror (2008) Hydrogels for cardiac tissue regeneration. *Biomed. Mater. Eng.* 18: 309–314.

Shi Jiawei, Dong Nianguo, Sun Zongquan (2008) [Impact of immobilized RGD peptides on cell attachment of decellularized valve scaffolds]. *Sheng Wu Yi Xue Gong Cheng Xue Za Zhi J. Biomed. Eng. Shengwu Yixue Gongchengxue Zazhi* 25: 388–392.

Shimizu Tatsuya, Yamato Masayuki, Isoi Yuki, Akutsu Takumitsu, Setomaru Takeshi, Abe Kazuhiko, Kikuchi Akihiko, Umezu Mitsuo, Okano Teruo (2002) Fabrication of pulsatile cardiac tissue grafts using a novel 3-dimensional cell sheet manipulation technique and temperature-responsive cell culture surfaces. *Circ. Res.* 90: e40.

Shin Su Ryon, Jung Sung Mi, Zalabany Momen, Kim Keekyoung, Zorlutuna Pinar, Kim Sang Bok, Nikkhah Mehdi, Khabiry Masoud, Azize Mohamed, Kong Jing, Wan Kai-Tak, Palacios Tomas, Dokmeci Mehmet R, Bae Hojae, Tang Xiaowu

Shirley, Khademhosseini Ali (2013) Carbon-nanotube-embedded hydrogel sheets for engineering cardiac constructs and bioactuators. *ACS Nano* 7: 2369–2380.

Shrikant Ashok, Shete Sandip, Meghnad Hulke. (2012) Study of reduced glutathione in seminal plasma and spermatozoa nuclear chromatin decondensation test (ncdt) in human subjects with different fertility potential. Journal (Paginated). http://www.biomedscidirect.com/586

Shu Xiao Zheng, Ghosh Kaustabh, Liu Yanchun, Palumbo Fabio S, Luo Yi, Clark Richard A, Prestwich Glenn D (2004) Attachment and spreading of fibroblasts on an RGD peptide-modified injectable hyaluronan hydrogel. *J. Biomed. Mater. Res. A* 68: 365–375.

Simpson DG, Terracio L, Terracio M, Price RL, Turner DC, Borg TK (1994) Modulation of cardiac myocyte phenotype in vitro by the composition and orientation of the extracellular matrix. *J. Cell. Physiol.* 161: 89–105.

Smith Matthew J, White Kimber L Jr, Smith Donna C, Bowlin Gary L (2009) In vitro evaluations of innate and acquired immune responses to electrospun polydioxanone-elastin blends. *Biomaterials* 30: 149–159.

Song Hannah, Yoon Charles, Kattman Steven J, Dengler Jana, Massé Stéphane, Thavaratnam Thushaanthini, Gewarges Mena, Nanthakumar Kumaraswamy, Rubart Michael, Keller Gordon M, Radisic Milica, Zandstra Peter W (2010) Interrogating functional integration between injected pluripotent stem cell-

derived cells and surrogate cardiac tissue. *Proc. Natl. Acad. Sci. U. S. A.* 107: 3329–3334.

Sreerekha Perumcherry Raman, Menon Deepthy, Nair Shantikumar V, Chennazhi Krishna Prasad (2013) Fabrication of Electrospun Poly (Lactide-co-Glycolide)–Fibrin Multiscale Scaffold for Myocardial Regeneration *In Vitro*. *Tissue Eng. Part A* 19: 849–859.

Stock UA, Wiederschain D, Kilroy SM, Shum-Tim D, Khalil PN, Vacanti JP, Mayer JE Jr, Moses MA (2001) Dynamics of extracellular matrix production and turnover in tissue engineered cardiovascular structures. *J. Cell. Biochem.* 81: 220–228.

Sultana Naznin, Khan Tareef Hayat (2012) Factorial Study of Compressive Mechanical Properties and Primary In Vitro Osteoblast Response of PHBV/PLLA Scaffolds. *J. Nanomater.* 2012: 1–8.

Sun Jinchen, Tan Huaping (2013) Alginate-Based Biomaterials for Regenerative Medicine Applications. *Materials* 6: 1285–1309.

Suuronen Erik J, Zhang Pingchuan, Kuraitis Drew, Cao Xudong, Melhuish Angela, McKee Daniel, Li Fengfu, Mesana Thierry G, Veinot John P, Ruel Marc (2009) An acellular matrix-bound ligand enhances the mobilization, recruitment and therapeutic effects of circulating progenitor cells in a hindlimb ischemia model. *FASEB J. Off. Publ. Fed. Am. Soc. Exp. Biol.* 23: 1447–1458.

Takahashi Kazutoshi, Tanabe Koji, Ohnuki Mari, Narita Megumi, Ichisaka Tomoko, Tomoda Kiichiro, Yamanaka Shinya (2007) Induction of pluripotent stem cells from adult human fibroblasts by defined factors. *Cell* 131: 861–872.

Tanaka Masaru, Motomura Tadahiro, Ishii Naoki, Shimura Kenichi, Onishi Makoto, Mochizuki Akira, Hatakeyama Tatsuko (2000) Cold crystallization of water in hydrated poly(2-methoxyethyl acrylate) (PMEA). *Polym. Int.* 49: 1709–1713.

Tandon Nina, Cannizzaro Christopher, Chao Pen-Hsiu Grace, Maidhof Robert, Marsano Anna, Au Hoi Ting Heidi, Radisic Milica, Vunjak-Novakovic Gordana (2009) Electrical stimulation systems for cardiac tissue engineering. *Nat. Protoc.* 4: 155–173.

Tao Ze-Wei, Mohamed Mohamed, Hogan Matthew, Gutierrez Laura, Birla Ravi K (2014) Optimizing a spontaneously contracting heart tissue patch with rat neonatal cardiac cells on fibrin gel. *J. Tissue Eng. Regen. Med.*

Teo Ailing, Mantalaris Athanasios, Lim Mayasari (2012) Hydrodynamics and bioprocess considerations in designing bioreactors for cardiac tissue engineering. *J. Regen. Med. Tissue Eng.* 1: 4.

Terracio L, Miller B, Borg TK (1988) Effects of cyclic mechanical stimulation of the cellular components of the heart: in vitro. *Vitro Cell. Dev. Biol. J. Tissue Cult. Assoc*. 24: 53–58.

Thankam Finosh G, Muthu Jayabalan (2013a) Biosynthetic alginate–polyester hydrogels with inherent free radical scavenging activity promote cellular response. *J. Bioact. Compat. Polym.* 28: 557–573.

Thankam Finosh Gnanaprakasam, Jayabalan Muthu (2013) Reactive oxygen species—Control and management using amphiphilic biosynthetic hydrogels for cardiac applications. *Adv. Biosci. Biotechnol.* 04: 1134–1146.

Thankam Finosh Gnanaprakasam, Muthu Jayabalan (2013b) Biosynthetic hydrogels-Studies on chemical and physical characteristics on long-term cellular response for tissue engineering: Biosynthetic Hydrogels. *J. Biomed. Mater. Res. A*: n/a–n/a. doi:10.1002/jbm.a.34895.

Thankam Finosh Gnanaprakasam, Muthu Jayabalan (2014a) Infiltration and sustenance of viability of cells by amphiphilic biosynthetic biodegradable hydrogels. *J. Mater. Sci. Mater. Med.*

Thankam Finosh Gnanaprakasam, Muthu Jayabalan (2014b) Influence of physical and mechanical properties of amphiphilic biosynthetic hydrogels on long-term cell viability. *J. Mech. Behav. Biomed. Mater.* 35: 111–122.

Thankam Finosh Gnanaprakasam, Muthu Jayabalan Alginate based hybrid copolymer hydrogels - Influence of pore morphology on cell-material interaction. *Carbohydr. Polym.* doi:10.1016/j.carbpol.2014.05.083. http://www.sciencedirect.com/science/article/pii/S014486171400561X.

Thevenot Paul, Hu Wenjing, Tang Liping (2008) Surface chemistry influences implant biocompatibility. *Curr. Top. Med. Chem.* 8: 270–280.

Tous Elena, Purcell Brendan, Ifkovits Jamie L, Burdick Jason A (2011) Injectable Acellular Hydrogels for Cardiac Repair. *J Cardiovasc. Transl. Res.* 4: 528–542.

Vandenburgh HH, Karlisch P, Farr L (1988) Maintenance of highly contractile tissue-cultured avian skeletal myotubes in collagen gel. *Vitro Cell. Dev. Biol. J. Tissue Cult. Assoc.* 24: 166–174.

Vasita Rajesh, Katti Dhirendra S (2012) Structural and functional characterization of proteins adsorbed on hydrophilized polylactide-co-glycolide microfibers. *Int. J. Nanomedicine* 7: 61–71.

Vunjak-Novakovic Gordana, Tandon Nina, Godier Amandine, Maidhof Robert, Marsano Anna, Martens Timothy P, Radisic Milica (2010) Challenges in Cardiac Tissue Engineering. *Tissue Eng. Part B Rev.* 16: 169–187.

Van Wachem PB, Hogt AH, Beugeling T, Feijen J, Bantjes A, Detmers JP, van Aken WG (1987) Adhesion of cultured human endothelial cells onto methacrylate polymers with varying surface wettability and charge. *Biomaterials* 8: 323–328.

Wang Jane, Bettinger Christopher J, Langer Robert S, Borenstein Jeffrey T (2010a) Biodegradable microfluidic scaffolds for tissue engineering from amino alcohol-based poly(ester amide) elastomers. *Organogenesis* 6: 212–216.

Wang Xin, Luo Hanqing, Guan Yanqing (2010b) [Application of poly (N-isopropylacrylamide) and its derivatives in tissue engineering]. *Sheng Wu Yi Xue Gong Cheng Xue Za Zhi J. Biomed. Eng. Shengwu Yixue Gongchengxue Zazhi* 27: 206–210.

Wei Jianhua, Igarashi Toshio, Okumori Naoto, Igarashi Takayasu, Maetani Takashi, Liu Baolin, Yoshinari Masao (2009) Influence of surface wettability on competitive protein adsorption and initial attachment of osteoblasts. *Biomed. Mater. Bristol Engl.* 4: 045002.

Weissman Irving L (2006) Medicine: Politic stem cells. *Nature* 439: 145–147.

Welzel Petra Birgit, Prokoph Silvana, Zieris Andrea, Grimmer Milauscha, Zschoche Stefan, Freudenberg Uwe, Werner Carsten (2011) Modulating Biofunctional starPEG Heparin Hydrogels by Varying Size and Ratio of the Constituents. *Polymers* 3: 602–620.

White HD, Norris RM, Brown MA, Brandt PW, Whitlock RM, Wild CJ (1987) Left ventricular end-systolic volume as the major determinant of survival after recovery from myocardial infarction. *Circulation* 76: 44–51.

Widziewicz Kamila, Kalka Joanna, Skonieczna Magdalena, Madej Pawel (2012) The Comet Assay for the Evaluation of Genotoxic Potential of Landfill Leachate. *Sci. World J.* 2012: 1–8.

Wielgosz AT (1995) What do we really know about secondary prevention after myocardial infarction? *Can. J. Cardiol.* 11 Suppl A: 31A–32A.

Yang S, Leong KF, Du Z, Chua CK (2001) The design of scaffolds for use in tissue engineering. Part I. Traditional factors. *Tissue Eng.* 7: 679–689.

Young Lawrence H, Renfu Yin, Russell Raymond, Hu Xiaoyue, Caplan Michael, Ren Jianming, Shulman Gerald I, Sinusas Albert J (1997) Low-Flow Ischemia Leads to Translocation of Canine Heart GLUT-4 and GLUT-1 Glucose Transporters to the Sarcolemma In Vivo. *Circulation* 95: 415–422.

Zammaretti Prisca, Jaconi Marisa (2004) Cardiac tissue engineering: regeneration of the wounded heart. *Curr. Opin. Biotechnol.* 15: 430–434.

Zhao Wen, Jin Xing, Cong Yang, Liu Yuying, Fu Jun (2013) Degradable natural polymer hydrogels for articular cartilage tissue engineering. *J. Chem. Technol. Biotechnol.* 88: 327–339.

Zimmermann Wolfram-Hubertus, Eschenhagen Thomas (2003) Cardiac tissue engineering for replacement therapy. *Heart Fail. Rev.* 8: 259–269.

Zimmermann Wolfram-Hubertus, Melnychenko Ivan, Eschenhagen Thomas (2004) Engineered heart tissue for regeneration of diseased hearts. *Biomaterials* 25: 1639–1647.

Zimmermann Wolfram-Hubertus, Melnychenko Ivan, Wasmeier Gerald, Didié Michael, Naito Hiroshi, Nixdorff Uwe, Hess Andreas, Budinsky Lubos, Brune Kay, Michaelis Bjela, Dhein Stefan, Schwoerer Alexander, Ehmke Heimo, Eschenhagen Thomas (2006) Engineered heart tissue grafts improve systolic and diastolic function in infarcted rat hearts. *Nat. Med.* 12: 452–458.

List of publications

[1] G. T. Finosh, M. Jayabalan, S.Vandana and K. G. Raghu. Hybrid alginate-polyester bimodal network hydrogel for tissue engineering - Influence of

structured water on long-term cellular growth. Colloids and Surfaces B: Biointerfaces. doi: 10.1016/j.colsurfb.2015.03.020.

[2] Remya Komeri, Finosh G T and Jayabalan Muthu. Influence of matrix and bulk behaviour of injectable hydrogel on the survival of encapsulated cardiac cells. RSC Adv., 2015, **5**, 31439-31449

[3] Finosh Gnanaprakasam Thankam, Muthu Jayabalan. Alginate based hybrid copolymer hydrogels - Influence of pore morphology on cell-material interaction. Carbohydrate Polymers. 2014, 112, (4) 235–244

[4] G.T. Finosh and M. Jayabalan. Infiltration and Sustenance of Viability of Cells by Amphiphilic Biosynthetic Biodegradable Hydrogels. *Journal* of Materials Science: *Materials in Medicine.* 2014, 25(8), 1953-65.

[5] G.T.Finosh and M. Jayabalan. Influence of physical and mechanical properties of amphiphilic biosynthetic hydrogels on long-term cell viability. Journal of Mechanical Behavior of Biomedical Materials. 2014, 35:111-22.

[6] G.T.Finosh and M. Jayabalan. Biosynthetic hydrogels – studies on chemical and physical characteristics on long term cellular response for tissue engineering. *Journal of Biomedical Materials Research* Part A. 102(7), 2014, 2238-47. *DOI: 10.1002/jbm.a.34895*

[7] G.T.Finosh and M. Jayabalan. Influence of plasma protein-hydrogel interaction moderated by absorption of water on long-term cell viability in amphiphilic biosynthetic hydrogels. RSC Advances. 2013,**3**, 24509-24520.

[8] Gnanaprakasam Thankam Finosh and Muthu Jayabalan. Biosynthetic alginate-polyester copolymer hydrogels with inherent free radical scavenging activity promote favorable cellular response. Journal of Bioactive and Compatible Polymers. 2013, 28(6):557-573.

[9] Finosh G T and Muthu Jayabalan. Reactive oxygen species – control and management using amphiphilic biosynthetic hydrogels for cardiac

applications. *Advances in Bioscience and Biotechnology*. 2013, 4, 1134-1146.

[10] M. Medha, G.T.Finosh and M. Jayabalan. Studies On Biodegradable Polymeric Nanocomposites based on Sheet Moulding Compound For Orthopedic Applications, Adv.Mater.Sci.Applications, 2013, 2(2), 73-87.

[11] Finosh Gnanaprakasam Thankam, Jayabalan Muthu, Vandana Sankar, Raghu Kozhiparambil Gopal. Growth and survival of cells in biosynthetic poly vinyl alcohol–alginate IPN hydrogels for cardiac applications. Colloids and Surfaces B: Biointerfaces 107 (2013) 137– 145.

[12] G.T. Finosh and Muthu Jayabalan. Regenerative therapy and tissue engineering for the treatment of end-stage cardiac failure-New developments and challenges. Biomatter 2:1, 1–14; 2012.

Conference proceedings

1. Finosh G T, Jayabalan M. Amphiphilic poly (sebacate-co-fumarate-co-manitol) – alginate copolymer hydrogel with better cell responses for tissue engineering. Materials in Medicine International Conference, Faenza, Italy, 8th to 11th October, 2013.
2. Finosh G T, Jayabalan M. Biosynthetic Copolymer Hydrogels as Carrier for Cardiac Tissue Engineering. FAPS-MACRO-2013, Indian Institute of Science, Bangalore, India, May 15-18, *2013.*
3. G.T.Finosh, M. Jayabalan, S.Vandana and K.G.Raghu. Novel Biosynthetic Hydrogel IPNS for Cardiac Tissue Engineering. 9th World Biomaterials Congress, Chengdu, China, 1-5 June, 2012.
4. G.T.Finosh and M. Jayabalan Studies on the Cell Response Modulated By Free Water in Biosynthetic Poly Vinyl Alcohol-Alginate Hydrogels. 9th World Biomaterials Congress, Chengdu, China, 1-5 June, 2012
5. G.T.Finosh, M. Jayabalan, and K.G.Raghu. Studies on Biosynthetic Hydrogels For Tissue Engineering - Effect of Free Water on Cell Penetration And Survival. 24th Kerala Science Congress conducted by *Kerala State Council for Science, Technology and Environment (KSCSTE)* held at Rubber Research Institute of India Kottayam on 2012-January 29th -31st.

Curriculum vitae

Education

PhD (01/2011 to 04/2015)	Biomaterials science at SCTIMST, Kerala, India. Advisor : Dr. M. Jayabalan Ph.D, D.Sc, FABMS
M.Sc (2005-2007)	Medical Biohemistry with **80%** and **2nd rank.** 2006-2009. School of Medical Education, Mahatma Gandhi University, Kottayam, Kerala, India.
B.Sc (2003-2006)	Biochemistry with **88.7%.** Kerala University, Kerala, India.

Home address

Gift Nest

Mulluvila P O

Neyyattinkara

Thiruvananthapuram - 695133

Phone: (+91) 471-2261981 (home)

E-mail: finoshgt@yahoo.co.in